Investigations into the role of histone H2A ubiquitination in chromatin

Laure Jeanine Monique Jason

Thesis Presented for the Degree of

DOCTOR OF PHILOSOPHY

In the Department of Biochemistry

UNIVERSITY OF CAPE TOWN

May 1999

Laure Jeanine Monique Jason

Department of Biochemistry
University of Cape Town
Private Bag
7701 Rondebosch
South Africa

May 1999

Investigations into the role of histone H2A ubiquitination in chromatin

Abstract

An *in vitro* system was used to determine the effect of histone H2A ubiquitination on linker histone binding to mononucleosomes. Hybrid octamers containing either H2A or ubiquitinated H2A (uH2A) were reconstituted onto random sequence 167 bp DNA. The affinity of the resultant nucleosome cores for linker histone H1 was determined from nucleoprotein gel shifts, protein analyses and thermal denaturation. Ubiquitinated H2A did not inhibit linker histone binding to nucleosome cores.

The effect of uH2A on nucleosome and chromatosome positioning on a 208 bp *Lytechinus variegatus* 5S rDNA fragment was investigated using a combination of micrococcal nuclease digestion and subsequent restriction enzyme digestion of the core particle or chromatosome DNA. Nucleosomes and chromatosomes containing uH2A were found to occupy the same positions on the template DNA as those containing H2A.

Chromatin folding of nucleosomal arrays containing either H2A or uH2A was analysed using a quantitative agarose gel electrophoresis system developed by Hansen and co-workers. The extent of folding of nucleosomal arrays containing uH2A was comparable to that of control nucleosomal arrays. A differential centrifugation assay was used to monitor the extent of divalent cation induced oligomerisation of reconstituted nucleosomal arrays. Nucleosomal arrays containing uH2A were found to oligomerise at a lower magnesium concentration than control arrays.

As a first step towards studying the effects of H2A ubiquitination in linker histone-bound nucleosomal arrays, a novel method for linker histone reconstitution onto long chromatin stripped of linker histones was developed. The fidelity of linker histone reconstitution was assayed by micrococcal nuclease digestion, thermal denaturation and determination of the orientation of neighbouring linker histone molecules in extended chromatin.

In a separate study, the relationship between the observed repeat length of chromatin and the rate of micrococcal nuclease digestion was investigated. The repeat length of the same starting chromatin preparation at equivalent extents of digestion was found to vary according to the rate of digestion.

Certificate of supervisors

In terms of paragraph eight of "General rules for the degree of doctor of philosophy (PhD)", we the supervisors of the candidate L.J.M Jason, certify that we approve of the incorporation into this thesis of material that has already been published or submitted for publication. We also approve of the use of scanned images.

Associate Professor G.G. Lindsey
Department of Biochemistry, University of Cape Town

Associate Professor W.F. Brandt
Department of Biochemistry, University of Cape Town

Dr. H.-G. Patterton
Department of Microbiology and Biochemistry, University of the Free State

Acknowledgements

I wish to thank,

My supervisors, Assoc. Professor G. Lindsey, Assoc. Professor W. Brandt and Dr H.-G. Patterton, for their advice and assistance.

Assoc. Professor W. Brandt for performing the protein sequencing.

Doctor Jerry Rodrigues for performing the amino acid analysis.

Patricia Thompson for her assistance with the repeat length determinations and her support in the laboratory.

Mohamed Jaffer for performing the electron microscopy.

Assoc. Professor Jeff Hansen and Pete Walker of the University of Texas Health Science Center for kindly providing details of the multigel electrophoresis apparatus.

Assoc. Professor Tim Dunne of the Mathematics Department for assistance with the statistical analyses.

My husband, Jón, for his infinite patience and continuous support.

Abbreviations

A_{230}	Absorbance at 230 nm, 1 cm path length
A_{260}	Absorbance at 260 nm, 1 cm path length
ATCC	American type culture collection
Bp	Base pairs
DNase	Deoxyribonuclease
EDTA	Ethylene diamine tetra-acetic acid
EEO	Electroendo-osmosis
EGTA	Ethyleneglycol-bis-(2-amino-ethyl ether) N, N' tetra-acetic acid
Min	Minutes
MNase	Micrococcal nuclease
NMR	Nuclear magnetic resonance
PAGE	Polyacrylamide gel electrophoresis
PMSF	Phenylmethylsulfonyl fluoride
Rpm	Revolutions per minute
SDS	Sodium dodecyl sulphate
TCA	Trichloroacetic acid
Tris	Tris (hydroxymethyl)-aminomethane
uH2A	Ubiquitinated histone H2A

Chemicals and Reagents

Product	Source
Acrylamide (> 99 %)	Merck
N,N'-methylene-*bis*-acrylamide	Fluka
Agarose (gold)	Seakem
Agarose (Type II A)	Sigma
Ammonium persulfate	Riedel-de Haën
Amido Black	Merck
α-Amylase (Type XII-A) (EC 3.2.1.1)	Sigma
Boric Acid	Merck
BioGel P60 (medium)	Bio-Rad
Citric acid	Merck
α-Chymotrypsin (Type VII) (EC 3.4.21.1)	Sigma
CM Sephadex C-25	Pharmacia
Coomassie blue	Research Organics
N,N-dimethylformamide	Burdick & Jackson
Dimethylsuberimidate	Merck
3,3'-Dithio-bis(Propionic Acid N-Hydroxysuccinimide Ester)	Sigma
Dodecyl sulfate sodium salt (SDS)	Merck
Ethidium bromide	Merck
Ethylenediaminetetraacetic acid (EDTA)	Merck
Ethyleneglycol-bis- (2-amino-ethyl ether) N, N' tetra-acetic acid (EGTA)	Sigma
D-Glucose	Merck
Glycerol	BDH
Glycine (ultrapure)	Research Organics
β-Mercaptoethanol	Merck
Magnesium chloride	BDH

Micrococcal nuclease (EC 3.1.31.1)	Sigma
Orcinol	Merck
Polygalacturonic acid (from oranges)	Sigma
Pectinase (from *Rhizopus* sp.)	Sigma
Phenylmethanesufonyl fluoride (PMSF)	Fluka
Photographic film for SDS gels	Ilford technical Pan
Photographic film for DNA gels	Ilford Pan F plus
Restriction enzymes	Boehringer Mannheim
Sephadex G100	Pharmacia
Sepharose 6B	Pharmacia
Silver Nitrate	Univar
Sodium azide	Merck
Spermidine	Sigma
Spermine	Sigma
Sucrose	Merck
SYBR Gold	Molecular probes
N,N,N',N'-tetramethylenediamine (TEMED)	Merck
Trichloroacetic acid	Merck
Tris-(hydroxymethyl)aminomethane (Tris) (ultrapure)	Research Organics
Trisodium citrate	Merck
Urea	Merck

TABLE OF CONTENTS

1.1 Introduction

Eukaryotic cells can modulate the packaging of their DNA into chromatin at various developmental and cell cycle stages by making use of histone subtypes and post-translational modifications. Post-translational histone modifications include ubiquitination, acetylation, phosphorylation, methylation, glycosylation and ADP ribosylation (see van Holde, 1989; Bradbury, 1992 and Davie, 1998 for reviews). These modifications occur in the flexible histone tail domains that are not constrained in the globular central histone fold. Numerous functions have been attributed to these modifications. A short introduction to ubiquitin and the ubiquitination enzymes is included to aid in the presentation of evidence pertaining to the role of histone ubiquitination in chromatin structure and function.

1.2 Ubiquitin

Ubiquitin is a small, mainly globular protein consisting of 76 amino acids found, as its name implies, in most living organisms. Ubiquitin has been found to be associated with numerous cellular processes, including protein degradation, DNA repair, cell cycle control, stress response, cellular differentiation, ribosome biogenesis, perioxisome biogenesis, viral infection, neural and muscular degeneration and transcription (reviewed by Rechsteiner, 1988; Finley & Chau, 1991; Jennissen, 1995).

1.2.3 Structure of ubiquitin

Initial sequencing studies of ubiquitin from various sources revealed the presence of only 74 amino acids (e.g. Schlesinger *et al.*, 1975; Schlesinger & Goldstein, 1975; Gavilanes *et al.*, 1982). The Gly-Gly sequence at the COOH-terminus missing from these studies is believed to have been lost due to *in vitro* proteolysis (Wilkinson & Audhya, 1981). Ubiquitin is highly conserved; its amino acid sequence is identical in all animals thus far examined and the sequences of yeast and oat ubiquitin differ from that of animals by three residues (Rechsteiner, 1988). The isoelectric point of ubiquitin has been found to be at pH 6.7 (Low *et al.*, 1979) reflecting its balanced content of 11 acidic and 11 basic residues. Ubiquitin is stable over a temperature range of 23 – 80 °C and a pH range of 1.18 - 8.48 (Lenkinski *et al.*, 1977) and

requires strong denaturing agents such as urea and guanidium chloride to reversibly denature it (Rechsteiner, 1988). This stability is conferred by high degrees of hydrogen bonding. This compact structure is also thought to be responsible for the resistance of ubiquitin to proteolytic digestion, an important asset for its role in protein degradation pathways. The crystal structure of human erythrocytic ubiquitin was initially determined to 2.8 Å resolution (Vijay-Kumar *et al.*, 1985) but later refined by the same group to 1.8 Å resolution (Vijay-Kumar *et al.*, 1987). From the crystal structure and the structure determined by two-dimensional proton NMR spectroscopy (Weber *et al.*, 1987), it was deduced that about 87 % of the polypeptide chain is involved in hydrogen-bonded secondary structures. Major secondary structural elements include a five-stranded mixed β-sheet that forms a concavity into which a 3.5 turn α-helix fits to form a hydrophobic core. Residues 56 to 59 form a short piece of 3_{10} helix. Seven reverse turns connect these structural elements. The four carboxyl terminal amino acids are not involved in hydrogen bonding and protrude from the main globular domain as an unstructured tail. It is through this tail that ubiquitin is covalently ligated to other proteins. Lysine 48 is the site of ubiquitin ligation involved in the formation of multi-ubiquitin adducts. This residue is found within a type III reverse turn in a highly twisted region of the protein.

1.3 Histone ubiquitination

Ubiquitinated H2A and H2B (uH2A and uH2B) are the most abundant ubiquitin conjugates in higher eukaryotes. uH2A was the first protein found to be post-translationally modified by covalent ligation to ubiquitin. It was originally identified as chromatin protein A24 (Orrick *et al.*, 1973). Clues as to its identity were provided by amino acid analysis (Goldknopf *et al.*, 1975) and peptide mapping (Goldknopf & Busch, 1975) which indicated the presence of H2A. Since the H2A moiety of the protein has an acetyl-blocked NH_2-terminus, the first 37 amino acids of A24 determined by sequence analysis corresponded to the sequence of the ubiquitin NH_2-terminal (Olson *et al.*, 1976; Hunt & Dayhoff, 1977). Ubiquitin is linked to the ε-amino group of lysine 119 of H2A by way of an isopeptide bond, forming a bifurcated structure. Lysine 119 is found at the beginning of the COOH terminal tail of uH2A in the trypsin accessible region of H2A (Böhm *et al.*, 1980). In the crystal structure of

the nucleosome determined to 2.8 Å (Luger *et al.*, 1997), this region is located on the face of the histone octamer. In eukaryotic cells, 5 to 15 % of the total H2A is post-translationally linked to ubiquitin. One or two uH2A molecules can replace H2A molecules in nucleosomes but the double modification is less frequently observed (Levinger & Varshavsky, 1980; Kleinshmidt & Martinson, 1981; Levinger *et al.*, 1981). Sequence variants of H2A (H2A.1, H2A.2, H2A.X and H2A.Z) can also be conjugated to ubiquitin (Rechsteiner, 1988).

Three years after the identification of ubiquitin in A24, ubiquitinated H2B was also found to occur naturally (West & Bonner, 1980). In this case the isopeptide bond linking ubiquitin and H2B is formed between the COOH-terminal glycine of ubiquitin and lysine 120 of H2B (Thorne *et al.*, 1987). This lysine residue lies within the histone fold region of H2B that is inaccessible to trypsin (Böhm *et al.*, 1982). The lysine residues to which ubiquitin is conjugated in H2A and H2B are highly conserved, suggesting an important function for this modification. About 1.5 % of eukaryotic cellular H2B is mono-ubiquitinated. A notable exception is *Physarum polycephalum*, where 6-7 % of both H2A and H2B are ubiquitinated in the growth plasmodial phase (Mueller *et al.*, 1985). Nucleosomes can be reconstituted with two molecules of uH2A or two molecules of uH2B (Kleinschmidt & Martinson, 1981; Davies & Lindsey, 1994) without obvious perturbation of the nucleosomal structure. Recently, ubiquitination of H3 was also reported to occur *in vivo* in elongating spermatids of rat testes (Chen *et al.*, 1998). The site of ubiquitination in H3 is presently unknown.

1.3.1 Polyubiquitination of histones

Polyubiquitinated species of histones H2A, H2B and H2A.Z have been detected in preparations of bovine thymus, chicken erythrocytes, *Tetrahymena* macronuclei and micronuclei, trout testis, trout liver and trout hepatocellular carcinoma (Nickel *et al.*, 1987; Davie *et al.*, 1987; Nickel *et al.*, 1989). Histone H2A has been determined to have the greatest level of polyubiquitination with tetra to hexa-ubiquitinated forms being observed (Davie *et al.*, 1987; Nickel *et al.*, 1989). The decreased accessibility of the COOH terminus of H2B may account for lower levels of polyubiquitination. Nickel and Davie (1989) have demonstrated that isopeptide bonds covalently link the

ubiquitin molecules in the ubiquitin chain of polyubiquitinated H2A. The authors proposed that lysine 6 is the main site of isopeptide bond formation in polyubiquitin chains since this residue is fully exposed on the surface of ubiquitin and readily acetylated. Four of the six lysine residues of ubiquitin (K6, K11, K29 and K48) may be involved in the formation of poylubiquitin chains (Pickart, 1997) although the main degradative signal of the ubiquitin mediated degradation pathway involves K48-linked polyubiquitin chains (Chau *et al.*, 1989; Finley *et al.*, 1994). It has been shown by *in vitro* ubiquitination, using reductively methylated ubiquitin, that core histones contain putative secondary ubiquitination sites (Haas *et al.*, 1988). These polyubiquitinated species were not observed *in vivo*. These sites must be sterically inaccessible to the ubiquitination enzymes when the histones are within the nucleosome. The same authors suggested that the direct polyubiquitination of histones could play a role in regulating their equilibrium positions for octamer assembly and/or their targeting for degradation.

1.3.2 Enzymes involved in histone ubiquitination

The levels of histone ubiquitination are determined by the activity of a family of ubiquitin conjugating enzymes (Haas & Bright, 1985), the activity of isopeptidases that release the ubiquitin moiety (Andersen *et al.*, 1981) and by the availability of free ubiquitin (Mimnaugh *et al.*, 1997). Two enzymes are thought to be involved in the conjugation of ubiquitin to histones. The first of these, E1, activates ubiquitin and is required for normal cell cycle progression (Cook & Chock, 1991a). Immuno-microscopic studies have shown that E1 is found in almost all compartments of the eukaryotic cell, including the nucleus (Cook & Chock, 1991b; Schwartz *et al.*, 1992). E1 has also been found to be associated with condensed chromosomes during mitosis (Cook & Chock, 1991a). Activation of ubiquitin involves the formation of an ubiquitin-E1 thiol ester via a ubiquitin adenylate intermediate. E1 transfers ubiquitin to the second enzyme in the pathway, E2, also resulting in the formation of a thiol ester intermediate. The subsequent ligation of ubiquitin to histones is thought to be mediated by E2 through a ligase independent reaction (Pickart & Rose, 1985). The conjugation of ubiquitin to many cytoplasmic proteins requires the additional action of an isopeptide ligase, E3 (Hershko *et al.*, 1986). A family of five E2 isoenzymes has

been isolated (Haas & Bright, 1988) which includes E2 $_{14\,kD}$, E2 $_{17\,kD}$, E2 $_{20\,kD}$, E2 $_{24\,kD}$ and E2 $_{32\,kD}$. No measurable rate of histone-ubiquitin ligation could be observed with either E2 $_{17\,kD}$ or E2 $_{24\,kD}$ alone or in combination with the other E2 isoenzymes (Haas *et al.*, 1988). Isoenzymes E2 $_{20\,kD}$ and E2 $_{32\,kD}$ have been shown by catalytic studies to be specific for free H2A and H2B. In *Saccharomyces cerevisiae*, the *RAD6/UBC2* and *CDC34/UBC3* genes are homologues of the E2 $_{20\,kD}$ and E2 $_{32\,kD}$ isoenzymes found in mammalian reticulocytes (Haas *et al.*, 1991). It is also of interest that a protein-tyrosine kinase has been reported to activate E2 $_{32\,kD}$ approximately 2.4-fold (Kong & Chock, 1992) providing a link to signaling systems. *Rad6* mutants are very sensitive to UV light, X-rays and chemical mutagens and it has therefore been suggested that the role of *RAD6/UBC2* could be to induce structural changes in chromatin through histone ubiquitination to provide access to DNA repair enzymes to the site of damage (Rechsteiner, 1988). However, no uH2A could be detected by immunoblotting in *Saccharomyces cerevisiae* and mutations engineered at the ubiquitination site of H2A did not affect yeast growth, sporulation or resistance to either UV radiation or heat stress (Swerdlow *et al.*, 1990). This would indicate that histones are not the *in vivo* substrates of Rad6p in yeast and that the effects of histone ubiquitination may only be of consequence in higher eukaryotes. The study of histone ubiquitination has been complicated by the multiplicity of substrates and lack of inhibitors of enzymes involved in ubiquitination and de-ubiquitination.

1.3.3 Histone ubiquitination and protein degradation

Ligation of ubiquitin chains to many short-lived proteins, such as P53 (Scheffner *et al.*, 1990; Ciechanover *et al.*, 1994) and cyclins A and B (Glotzer *et al.*, 1991; Hershko *et al.*, 1994), tags them for degradation by a large cytoplasmic 26S ATP-dependent complex, the 26S proteasome (Hough *et al.*, 1987). To complete the cycle, an isopeptidase releases intact ubiquitin from the proteolysed proteins (see Finley & Chau, 1991 and Jennissen, 1995 for reviews). Ubiquitin and ubiquitin conjugates can be recognised by a subunit of the 26S proteasome (Deveraux *et al.*, 1994). Multi-ubiquitinated substrates were reported to be bound by the 26S proteasome with a higher affinity than mono-ubiquitinated substrates and this may explain why the former are degraded at higher rates (Deveraux *et al.*, 1994).

Although *in vitro* studies have shown that histone-ubiquitin conjugates can be degraded in an ATP-dependent reaction in reticulocyte lysates (Mayer *et al.*, 1989; Haas *et al.*, 1990), two independent studies have shown that ubiquitination of histones does not tag them for degradation by the 26 S proteasome *in vivo* (Wu *et al.*, 1981; Seale, 1981). In L1210 cells, the half-life of the ubiquitin moiety of uH2A was found to be identical to that of free ubiquitin (~9 h) whilst no turnover of the core histones occurred in 24 h (Wu *et al.*, 1981). Changes in uH2A concentrations were later found to be affected by the rates of ubiquitin ligation (Matsumoto *et al.*, 1983; Ciechanover *et al.*, 1984) and/or isopeptidase activity (Andersen *et al.*, 1981). No *in vivo* study of the degradation of poly-ubiquitinated histones has been carried out to date, and it would be interesting to determine if polyubiquitination does tag histones for proteolysis.

1.3.4 Histone ubiquitination and the cell cycle

Histone ubiquitination has been suggested to alter chromatin structure by hindering chromatin condensation. The levels of uH2A and uH2B have been reported to vary during the cell cycle in a manner compatible with such a role. During the cell cycle of Chinese hamster cells, the ubiquitin moiety of uH2A was found to disappear during the G2-mitosis transition and reappear as the chromatin decondenses at the mitosis-G1 transition, regardless of protein synthesis (Matsui *et al.*, 1979). The absence of uH2A and uH2B in metaphase chromosomes was confirmed by Wu *et al.* (1981). In a more detailed study, Mueller *et al.* (1985) studied the appearance and disappearance of ubiquitinated histones during the cell cycle of *Physarum polycephalum*. This organism is well suited to cell cycle studies as all the nuclei in a macroplasmodium divide within 2 to 3 minutes of each other during the organism's 9 hour cell cycle. The authors report the strong presence of ubiquitinated histones at early prophase. The levels of uH2A and uH2B begin to decline at late prophase and decrease to non-detectable levels at metaphase. Ubiquitinated histones could be detected at anaphase, after which their levels rose to reach those of interphase cells. The rates of ubiquitin synthesis and conjugation were found to be minimal during metaphase when uH2A is absent from nucleosomes (Busch & Goldknopf, 1981). Additionally, the amount of isopeptidase associated with chromatin was reported to increase at mitosis (Matsui *et*

al., 1982). In another study, the ATP-dependant ligation of ^{125}I-ubiquitin to the histones of permeabilised mammalian cells was demonstrated to decrease strikingly in metaphase cells whereas the formation of other ubiquitin adducts was only slightly reduced (Raboy *et al.*, 1986). This decreased conjugation of ubiquitin to histones could possibly be the result of chromosome condensation altering the conformation of nucleosomes such that ubiquitination sites are more sensitive to isopeptidase activity and/or less available for ubiquitination. Whereas ubiquitination of histones does not target them for degradation, the situation is different for the mitotic cyclins that induce the metaphase to anaphase transition. The mitosis-specific degradation of cyclins is believed to occur by means of poly-ubiquitination and subsequent proteolysis by the 26S proteasome (Glotzer *et al.*, 1991). Cyclins contain a conserved sequence, the destruction box, that is proposed to contain the recognition site for the ubiquitin conjugating enzymes. It is interesting to note that a sequence similar to the cyclin destruction box exists upstream of H2A lysine 119 in *Tetrahymena* and vertebrates (Hunt, 1991). These proteins may thus share ubiquitin conjugating enzymes but no correlation between their states of ubiquitination has been investigated.

A number of studies have used cell cycle mutants to identify possible functions of histone ubiquitination. Studies of a mouse G_2 phase mutant cell line ts85 that has a temperature sensitive E1 ubiquitin activating enzyme, revealed that at the non-permissive temperature cell cycle arrest occurred near the S/G_2 boundary. Incubation at the non-permissive temperature also resulted in de-ubiquitination of uH2A in arrested cells, where the chromatin remained dispersed (Yasuda *et al.*, 1981; Finley *et al.*, 1984). A subsequent investigation showed that not all ubiquitin conjugation was inhibited at the non-permissive temperature (Deveraux *et al.*, 1990). These results indicate that ubiquitination of a subset of H2A and H2B and/or other proteins may be required for cell cycle progression from S to G_2 phase.

Incubation of tsBN2 hamster cells, another cell cycle mutant, at the non-permissive temperature, resulted in premature chromosome condensation in S and G_2 phases accompanied by the loss of uH2A and the phosphorylation of H1 and H3 (Bradbury, 1992 and references cited therein). This suggests that de-ubiquitination of uH2A and phosphorylation of H1 and H3 may be linked events in the process of chromatin

condensation. The mutant gene in tsBN2 cells encodes for *RCC1* (Ohtsubo *et al.*, 1989) which has recently been crystallized (Renault *et al.*, 1998) and functions as the guanine-nucleotide-exchange factor (GEF) for Ran, the nuclear Ras homologue (Klebe *et al.*, 1995). Other *RCC1* mutants have been found to affect mating, pre-messenger RNA processing, RNA transport and initiation of mitosis (Renault *et al.*, 1998 and references cited therein).

The involvement of histone ubiquitination in the cell cycle cannot be general since only a subset of histones are ubiquitinated prior to and after chromatin condensation. This is unlike phosphorylation of H1 and H3, where all these histones are modified prior to chromatin condensation (Bradbury, 1992). It is therefore likely that histone ubiquitination serves to label certain regions of the genome to interact with specific proteins or to be packaged in a special way in metaphase chromosomes.

1.3.5 Histone ubiquitination and spermatogenesis

A number of chromatin rearrangements occur during spermatogenesis. As spermatogenesis progresses, testis-specific histones are synthesized. In later stages, transition proteins displace nearly all the histones and these transition proteins are eventually replaced by protamines in condensed spermatids and spermatozoa (see Oliva & Dixon, 1991 for a review). The levels of ubiquitinated histones have been found to vary at different stages and to different extents during spermatogenesis in vertebrate species such as the rooster (Agell *et al.*, 1983), trout (Nickel *et al.*, 1987) and rat (Chen *et al.*, 1998). In the rooster, the levels of uH2A are at their highest just before the replacement of histones by protamine in late spermatids (Agell *et al.*, 1983). In mice, a homologue of the yeast E2 enzyme RAD6 called mHR6B is highly expressed in the nucleus of spermatids (Koken *et al.*, 1996). *RAD6* was the first ubiquitin-conjugating enzyme able to mono- and polyubiquitinated H2A and H2B *in vitro* (Jentsch *et al.*, 1987) leading to a proposed role in modulating chromatin structure. If this gene is inactivated by gene replacement, male mice are sterile. This effect was thought to be brought about by abnormalities in histone displacement during spermatogenesis (Roest *et al.*, 1996) but it was subsequently shown that the overall pattern of histone ubiquitination during spermatogenesis in HR6B knockout mice was not affected (Baarends *et al.*, 1999).

Histone ubiquitination cannot be a universal signal for histone displacement since the levels of uH2A do not change during trout spermatogenesis. The levels of trout uH2B however, were found to decrease and those of doubly ubiquitinated H2B to increase during germ cell maturation (Nickel *et al.*, 1987). In the rat, the levels of uH2A were found to decrease in elongating spermatids (Chen *et al.*, 1998). De-ubiquitination of rat H2A therefore occurs at an earlier stage in spermatogenesis than the rooster (Agell *et al.*, 1983). The study of rat spermatogenesis also reports the first identification of *in vivo* ubiquitinated H3. The levels of uH3 were highest in elongating spermatids and uH3 could thus play a role in histone displacement (Chen *et al.*, 1998). The mechanisms by which ubiquitinated histones operate during spermatogenesis have yet to be elucidated. It has been proposed that histone ubiquitination could facilitate histone displacement by decondensing chromatin so as to facilitate the access of proteins involved in histone removal or direct displacement by transition proteins (Chen *et al.*, 1998).

1.3.6 Cellular stress response and ubiquitinated histones

After heat shock treatment of cells, most genes are repressed but a few are induced. Ubiquitin is one of the stress proteins induced by heat-shock (Bond & Schlesinger, 1985). It has been shown that the levels of acetylated histones and uH2A are reduced following heat shock in a number of different cell lines (Parag *et al.*, 1987; Bond *et al.*, 1988; Davie & Murphy 1990; Fujimuro *et al.*, 1997; Mimnaugh *et al.*, 1997). Proteasome inhibitors also caused a depletion of ubiquitinated histones in human lymphocytes and tumour cells (Mimnaugh *et al.*, 1997). When cells were exposed to stressful conditions such as heat shock, noxious chemicals and proteasome inhibitors, the levels of free ubiquitin were found to decrease dramatically whilst ubiquitinated non-histone proteins were found to accumulate (Mimnaugh *et al.*, 1997). These treatments cause the ubiquitin-dependent 26S proteasome pathway to be overloaded or inhibited and therefore lead to the accumulation of ubiquitinated proteins destined for proteolysis. It has been proposed that under stressful conditions, ubiquitin released during the known rapid turnover of the ubiquitin moiety of uH2A and uH2B, is rapidly ligated to damaged proteins (Fujimuro *et al.*, 1997; Mimnaugh *et al.*, 1997). This would provide an additional source of ubiquitin to the stress induced expression

of ubiquitin genes. Interestingly, no free ubiquitin could be detected in the nuclear fraction of either control or experimental cells (Mimnaugh *et al.*, 1997) implying that ubiquitinated histones may serve as a store of nuclear ubiquitin.

1.3.7 Histone ubiquitination and transcription

Nucleosomal and higher order packaging of DNA pose a major obstacle to the transcriptional machinery (see van Holde, 1989 and Wolffe, 1995 for reviews). Actively transcribed and poised chromatin has been proposed to have an altered nucleosomal organisation since it has been reported to exhibit an increased overall sensitivity to both DNase I (Weintraub & Groudine, 1976; Izban & Luse, 1991) and MNase (Bellard *et al.*, 1980; Bloom & Anderson, 1978), an altered nucleosomal repeat length (Smith *et al.*, 1983) and nuclease hypersensitivity near the 5' end of transcribed genes (Elgin, 1988). Transcribed chromatin has also been shown to be deficient in histones H2A/H2B (Baer & Rhodes, 1983; Gonzalez *et al.*, 1987; Gonzalez & Palacián, 1989) and in linker histones (Kamakaka & Thomas, 1990; Postnikow *et al.*, 1991).

Histone modifications have long been thought to play a role in altering chromatin structure. A recent investigation into core histone acetylation has provided additional evidence for such a role, demonstrating that in the absence of linker histones, core histone acetylation disrupts higher-order chromatin folding (Tse *et al.*, 1998). Further studies should determine if core histone acetylation also affects the higher order folding of reconstituted nucleosomal arrays containing linker histones as earlier studies carried out on isolated chromatin fibres containing linker histones indicate that core histone acetylation has a negligible effect on the higher order structure of these fibres (McGhee *et al.*, 1983b; Dimitrov *et al.*, 1986).

There has been much debate as to the presence of ubiquitinated histones in actively transcribed chromatin.

1.3.7.1 Evidence for location of ubiquitinated histones in actively transcribed chromatin

A decrease in transcriptional activity during chicken erythropoiesis was found to be paralleled by a loss of nuclear ubiquitin and the conversion of uH2A to H2A (Goldknopf *et al.*, 1980). The amount of uH2A containing nucleosomes has been reported to decrease during myogenesis of chicken embryo muscles (Wunsch *et al.*, 1987). The authors suggested that this decrease might reflect the segregation of uH2A in actively transcribed chromatin, which also decreases during myogenesis. The transcriptionally poised *hsp 70* and *copia* genes present in soluble chromatin after MNase digestion of *Drosophila melanogaster* cells were found to be highly enriched in uH2A. The nucleosomes packaging the *hsp 70* genes were found to contain 50 % uH2A. In contrast, nucleosomes of the non-transcribed 1.688 satellite DNA in the same fraction contained only one uH2A per 25 nucleosomes (Levinger & Varshavsky, 1982). Upon heat shock and the ensuing transcriptional activation of *hsp 70* genes, the canonical nucleosomal structure was lost. Evidence suggested that the histones remain associated with the DNA via their N-terminal tails (Nacheva *et al.*, 1989), whilst the interactions between the DNA and the histone-fold domains were disrupted.

In another analysis of histones associated with transcribed genes, nucleosomes containing uH2A and di-ubiquitinated H2A were found to be preferentially located near the 5' end of the transcribed mouse dihydrofolate reductase gene (Barsoum & Varshavsky, 1985).

Transcriptional activation is often associated with perturbation of the canonical nucleosome structure in the promoter region. Since histone ubiquitination has little apparent effect on the nucleosomal structure (Kleinschmidt & Martinson, 1981; Davies & Lindsey, 1994), the modification may alter higher order chromatin folding to act as a recognition signal for target proteins that could disrupt chromatin and/or nucleosomal structure. There have been many suggestions as to the fate of nucleosomes during transcription (see van Holde *et al.*, 1992 for a review). The model favoured by these authors involves the progressive displacement of H2A-H2B dimers in the partial unfolding of a nucleosome as RNA polymerase transcribes the associated DNA. Transcriptional initiation is also believed to require chromatin remodeling. While the mode of action of chromatin remodeling complexes such as SWI/SNF, NURF, CHRAC, RSC (see Workman & Kingston, 1998 for a review),

RSF and FACT (LeRoy *et al.*, 1998) is still under investigation, the histone tails seem to play an important role in the remodeling process (see Luger & Richmond, 1998 for a review). The effect of histone modifications on the activity of these complexes remains to be investigated but there is already evidence that core histone acetylation may modulate the action of SWI/SNF (Pollard & Peterson, 1997; Recht & Osley, 1999). It has also been proposed that histone binding proteins such as nucleoplasmin (Chen *et al.*, 1994) which is associated with actively transcribed chromatin (Moreau *et al.*, 1986), could aid transcription factor binding by selective removal of H2A-H2B dimers, thereby disrupting nucleosomal structure. However, subsequent *in vitro* studies showed that nucleoplasmin did not facilitate the binding of transcription factor IIIA to a nucleosome bound target sequence (Howe *et al.*, 1998a). Ubiquitination of H2A and H2B has been found to weaken the interaction of H2A-H2B dimers with H3-H4 tetramers in chromatin (Li *et al.*, 1993). If transcriptional initiation and elongation do indeed necessitate the displacement of H2A-H2B dimers, ubiquitination of these histones may facilitate transcription by decreasing the energy required for dimer displacement.

Another approach to understanding the role of histone ubiquitination has involved quantitation of ubiquitinated histones in chromatin fractions enriched in transcriptionally active sequences. The low salt soluble chromatin fractions of bovine thymus, which are believed to be enriched in transcriptionally active sequences, were found to be enriched in mono- and poly-ubiquitinated H2A and H2B. uH2B was found to be enriched to the greatest extent amongst mono-ubiquitinated histones (Nickel *et al.*, 1989). A fraction from chicken erythrocyte nuclei, 50 times enriched in transcriptionally active β-globin gene sequences was enriched 1.5 times in uH2A and four times in uH2B (Ridsdale & Davie, 1987). The distribution of ubiquitinated histones was also examined in the transcriptionally active macronuclei and transcriptionally inactive micronuclei of *Tetrahymena thermophila* (Nickel *et al.*, 1989). There was some enrichment of uH2A and a substantial enrichment of uH2B in the macronuclei.

Inhibition of rRNA or heterogeneous nuclear RNA (hnRNA) synthesis has no effect on the levels of uH2A (Ericsson *et al.*, 1986; Davie & Murphy, 1990). Inhibition of rRNA transcription did not affect the levels of uH2B, but there was an almost total disappearance of uH2B upon inhibition of hnRNA transcription. The levels of uH2B

were found to be directly dependent on ongoing transcription (Davie & Murphy, 1990). The proposal that uH2B may keep the nucleosome in an open structure (Davie & Murphy, 1990) is challenged by *in vitro* reconstitutions of nucleosomes containing 2 uH2B molecules that indicate no conformational change (Davies & Lindsey, 1994).

1.3.7.2 Evidence against location of ubiquitinated histones in actively transcribed chromatin

Early studies in rat liver nuclei linked the disappearance of uH2A to increased transcription (Ballal *et al.*, 1974; Ballal *et al.*, 1975). In contrast with earlier results (Levinger & Varshavsky, 1982), Levinger (1985) demonstrated that *Drosophila* mononucleosomes containing non-transcribed 1.705 satellite DNA, showed some enrichment in uH2A. Huang *et al.* (1986) used a system similar to that of Levinger & Varshavsky (1982) to investigate the composition of nucleosomes packaging the transcribed immunoglobulin κ chain gene in mice. MNase treated chromatin was fractionated to enrich for the κ sequence. This sequence was present in both the S1 soluble fraction (5 % of total nuclear DNA) and the P insoluble fraction (15 % of total nuclear DNA). The levels of uH2A and uH2B were similar in both fractions. The S1 fraction was depleted in linker histone H1 and non-transcribed sequences, contained HMG proteins 14 and 17 and consisted almost exclusively of mononucleosome length fragments. Through two dimensional gel electrophoresis of S1 mononucleosomes and DNA hybridisation with corresponding probes, the authors showed that the nucleosomes co-migrating with the κ sequence shared the features of bulk nucleosomes in the S1 fraction described above, including the presence of uH2A and uH2B. The presence of ubiquitinated histones was however questioned, as removal of the ubiquitin moiety by isopeptidase treatment prior to electrophoresis should have increased the mobility of the mononucleosomes containing uH2A and uH2B to that of non-ubiquitinated nucleosomes. The bulk nucleosomes and nucleosomes containing a non-transcribed sequence did increase in mobility following isopeptidase treatment but the mononucleosomes containing the immunoglobulin κ sequence were unaffected (Huang *et al.*, 1986). This result therefore questions conclusions from similar experiments regarding the association of ubiquitinated histones with transcribed sequences.

Fractionation of myotube nuclei chromatin has revealed that uH2A was not enriched in transcriptionally active nor in inactive chromatin, but was associated with a nuclease sensitive fraction (Parlow *et al.*, 1990). This fraction was not depleted in H1. It must also be noted that the actively transcribed actin gene was probed with a DNA sequence complementary to the 3' end of the gene and may not reflect the composition of nucleosomes at the 5' end of the gene if one takes the microheterogeneity proposed by Levinger and Varshavsky (1982) into account. The authors suggested that uH2A is distributed amongst decondensed, salt soluble chromatin simply because there may be fewer constraints on the ubiquitination enzymes. Other investigators have not found enrichment of uH2A in core particles preferentially liberated by MNase digestion (Albright *et al.*, 1979). Another study that used DNase I sensitivity to characterise actively transcribed sequences also found random distribution of uH2A between fractions enriched in actively transcribed chromatin and those enriched in inactive sequences (Dawson *et al.*, 1991). In *Drosophila* polytene chromosomes, ubiquitin is mainly associated with the compact band regions rather than the more decondensed and destabilised interbands and puffs (Izquierdo, 1994). This observation is, however, not specific to ubiquitinated histones and may also reflect the distribution of other ubiquitinated proteins associated with the chromosomes. uH2A has, however, been observed in mice spermatocytes in the inactive sex body that contains the heterochromatic X and Y chromosomes (Baarends *et al.*, 1999).

The exact function and mechanism of action of histone ubiquitination is still unclear. uH2B would appear to be mainly involved with transcribed chromatin, whilst uH2A would appear to be involved in a more general decondensation of chromatin. It is unlikely that histone ubiquitination plays a general role in facilitating transcription since ubiquitinated histones have not been detected in all eukaryotic organisms (e.g. *Schizosaccharomyces pombe* and *Arabidopsis thaliana*) (Finley & Chau, 1991). The effect of histone ubiquitination is more likely to be mediated at specific sites. It is also possible that the mono-ubiquitinated histones are substrates for poly-ubiquitination that could tag them for degradation, but again, based on the evidence available, this would not be a general cellular occurrence.

2 Histone ubiquitination and linker histone binding at the nucleosome level

2.1 Introduction

Ubiquitinated histones have been associated with chromatin partially depleted of linker histones (Davie & Nickel, 1987) and transcriptionally active or poised sequences (Levinger & Varshavsky, 1982; Barsoum & Varshavsky, 1985; Davie & Murphy, 1990) (see section 1) that are thought to be have a reduced linker histone content or have altered association with linker histones (reviewed by Zlatanova & van Holde, 1992). On the other hand, there is evidence which suggests that histone ubiquitination does not interfere with linker histone binding. Two independent studies have shown that H1 can be cross-linked to uH2A *in vitro* (Nelson *et al.*, 1979) and *in vivo* (Bonner and Stedman, 1979). Moreover, in the cross-linking studies performed in mouse cells, the molar ratio of H1-uH2A to H1-H2A was the same as the molar ratio of uH2A to H2A (Bonner and Stedman, 1979). If ubiquitinated histones are associated with less tightly packaged chromatin as many reports indicate (see section 1), is it because these chromatin regions are more accessible to the ubiquitination enzymes or because ubiquitinated histones interfere with chromatin folding? Linker histones are required for the stabilisation of well defined chromatin fibres (Thoma *et al.*, 1979; Allan *et al.*, 1981; Carruthers *et al.*, 1998) and interference with the binding of linker histones could affect chromatin condensation or the stability of the folded structures. Under physiological conditions, the structure of most linker histones is comprised of three domains; a strongly basic unstructured NH_2-terminal tail, a nonpolar globular domain and another strongly basic unstructured tail at the COOH terminal (Hartman *et al.*, 1977). The three dimensional structure of the globular domain of histones H1 and H5 has been determined using two dimensional NMR (Cerf *et al.*, 1993; Clore *et al.*, 1987) and the structure of the globular domain of histone H5 was further resolved to 2.5 Å following the determination of its crystal structure (Ramakrishnan *et al.*, 1993). Interestingly, the three-helix bundle structure of the globular domain of histone H5 has been reported to resemble that of the bacterial CAP (catabolite gene activator protein) (Clore *et al.*, 1987; Ramakrishnan *et al.*, 1993) as well as that of the DNA-recognition motif of HNF-3, a *Drosophila* transcription factor (Clark *et al.*, 1993). This structural similarity led to a model in which the primary binding site of linker

histones to DNA is comprised of helix III of the globular domain binding to the major groove and binding of the β-hairpin to the adjacent minor groove (Ramakrishnan *et al.*, 1993; Cerf *et al.*, 1994). The position of the globular domain of a linker histone on the nucleosome is still controversial and may be variable. The earlier data indicated that the globular domain of linker histones bound on the dyad axis of the nucleosome thereby protecting 10 bp of DNA on both sides of the axis (Simpson, 1978; Allan *et al.*, 1980a; Staynov & Crane-Robinson, 1988; Pehrson, 1989). Later models support an asymmetric location for the globular domain of linker histones. The first of these models placed the globular domain of H5 about 68 bp from the dyad on the inside of the DNA superhelix where it faces the core histones and is in contact with H2A and H3 (Hayes & Wolffe, 1993; Hayes *et al.*, 1994; Ura *et al.*, 1995; Pruss *et al.*, 1996; Hayes, 1996). Another model proposed that the globular domain of linker histones binds on the outside of the nucleosome, making contact with adjacent DNA gyres at positions ±7 and ±1 of the DNA superhelix (Travers & Muyldermans, 1996). The latest model, derived from cross-linking studies of mutant H5 globular domains to random sequence linker histone depleted chromatosomes, indicated that the globular domain binds near the dyad axis making contacts with an outer and the central DNA gyre (Zhou *et al.*, 1998). These models and the evidence supporting them have recently been reviewed (Crane-Robinson, 1997 and Travers, 1999).

The COOH-terminal of H2A has been found to make contacts with the linker DNA in nucleosomes containing at least 167 bp of associated DNA (Davies & Lindsey, 1991; Usachenko *et al.*, 1994). In the case of core particles lacking linker DNA, the H2A COOH tail repositions to contact the DNA of the dyad axis (Usachenko *et al.*, 1994). The H2A COOH tail is therefore likely to have some influence on linker histone binding at the nucleosomal level since some DNA contact sites are shared. The crystal structure of the nucleosome (Luger *et al.*, 1997) indicates that the H2A COOH-terminal tail emerges from the nucleosome near one of the proposed asymmetric binding sites of the H5 globular domain (Hayes, 1996). It has been shown that the contacts between the H2A COOH-terminal tail and the linker DNA are altered slightly in the presence of linker histone (Lee & Hayes, 1998; Guschin *et al.*, 1998) indicating that the H2A tail domain is repositioned upon linker histone binding. Ubiquitination of H2A is a bulky modification that occurs at lysine 119 at the

beginning of the COOH-terminal tail (see section 1), and it is therefore of interest to investigate if nucleosomal uH2A affects linker histone binding.

A defined *in vitro* system using individually purified components was used to investigate the effects of histone ubiquitination on linker histone binding since it would be difficult to generate chromatin enriched in ubiquitinated histones due to the unavailability of inhibitors of the enzymes involved.

2.2 Results and Discussion

2.2.1 Purification of chicken erythrocyte histones

Hybrid octamers reconstituted from individual chicken erythrocyte histones and a histone from another species replacing one of the chicken histones have successfully been used in a number of studies (e.g. Lindsey *et al.*, 1991; Lindsey & Thompson, 1992; Davies & Lindsey, 1994). In order to purify individual core histones, total acid extracted chicken erythrocyte histones were chromatographed on a BioGel P60 column (Fig. 2.1). Fractions containing pure H2A and H4 were pooled respectively but the H2B-H3 fraction had to be resolved further.

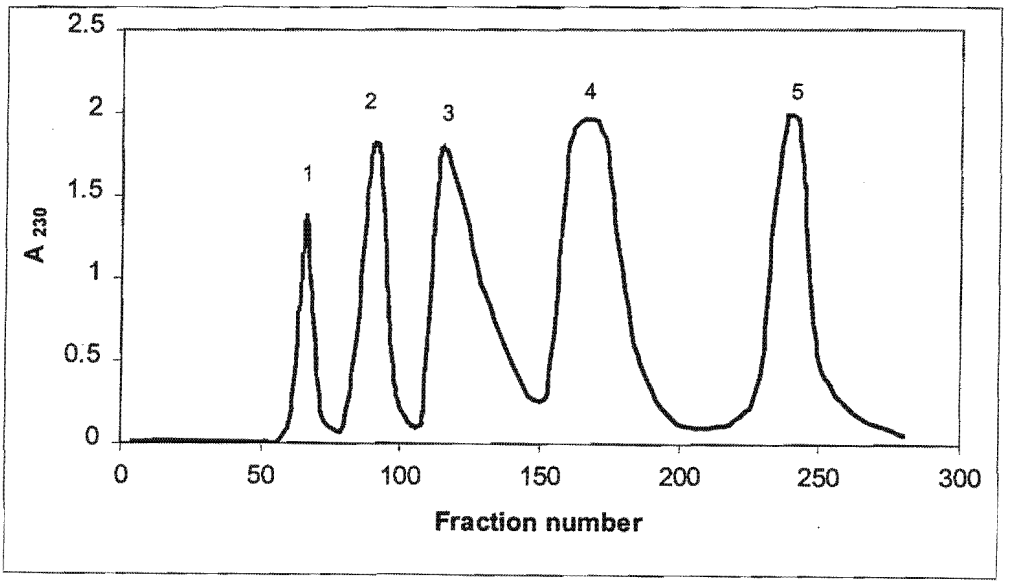

Figure 2.1. BioGel P60 chromatography of a total acid extract from chicken erythrocyte nuclei in 50 mM NaCl and 20 mM HCl. Peaks 1 to 5 contained histones H1s, H5, H2A, H2B & H3 and H4 respectively.

To separate histones H2B and H3, relevant BioGel P60 fractions containing these histones were pooled, concentrated and applied to a Sephadex G100 column in 50 mM NaCl and 20 mM HCl (Fig. 2.2).

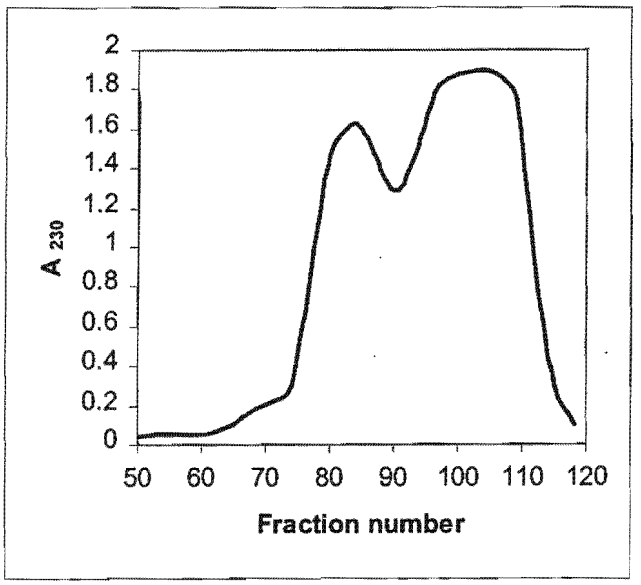

Figure 2.2. Sephadex G100 chromatography of the histone H2B-H3 fraction obtained after BioGel P60 chromatography of a total acid extract of chicken erythrocyte nuclei. The column buffer was 50 mM NaCl and 20 mM HCl (pH 1.7). Fractions 75 to 85 and 98 to 112 were pooled and contained pure H3 and pure H2B respectively, confirmed by SDS-PAGE.

2.2.2 Purification of ubiquitinated H2A

Calf thymus was used as a source of ubiquitinated H2A. Histones were acid extracted from thymus gland nuclei and chromatographed on a BioGel P60 column in 50 mM NaCl, 20 mM HCl. Ubiquitinated H2A eluted with the H2A-H3 peak. Under these conditions, the ubiquitin moiety of uH2A has little effect on the effective size and surface charge of uH2A as it remains fully folded whilst the histones are essentially in a random coil conformation (Thorne *et al.*, 1987). Fractions containing uH2A were pooled and applied to a Whatman CM 52 ion exchange column. The column buffer used contained 6 M urea to promote the unfolding of ubiquitin (Cary *et al.*, 1980). uH2A eluted with the leading edge of the salt gradient presumably as a consequence of its charge to mass ration being lower than that of H2A and H3. Fractions enriched

in uH2A were pooled and further resolved from contaminating H2A and H3 on a BioGel P60 column in 7 M urea and 2 mM Tris-HCl (pH 2.2) (Fig. 2.3).

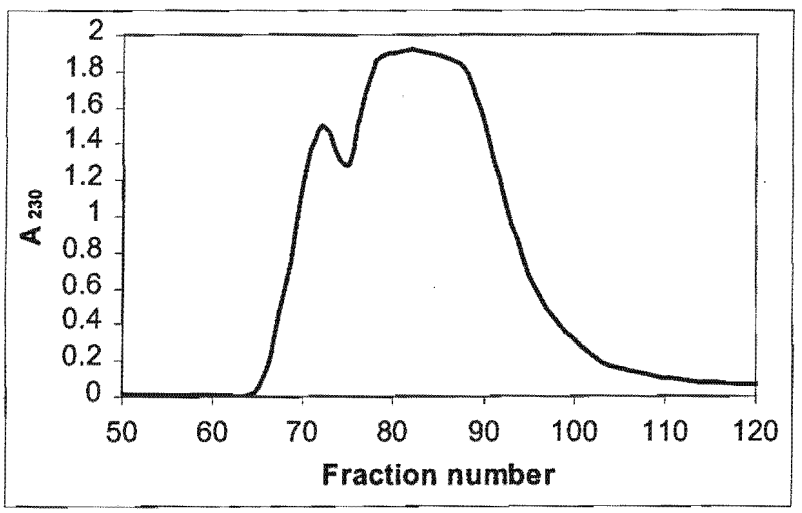

Figure 2.3. BioGel P60 chromatography of uH2A enriched fractions obtained from the Whatman CM 52 ion exchange chromatographic step. The column buffer was 7 M urea and 2 mM Tris-HCl (pH 2.2). Fractions 65 to 73, containing pure uH2A, were pooled, dialysed extensively against water, and stored at –20 °C.

Fractions containing pure uH2A were pooled and the identity of the purified uH2A was confirmed by SDS-PAGE using pure uH2A as a standard (Davies & Lindsey, 1994) (not shown) and amino acid analysis (Klapper, 1982). The results of the amino acid analysis are shown in Table 2.1. The results obtained correlated well with the values calculated from the amino acid content of calf H2A and ubiquitin.

Table 2.1

The amino acid composition of purified calf uH2A determined by amino acid analysis compared to the calculated values for the ubiquitin-calf H2A conjugate.

Amino Acid	Moles Calculated	Moles Found
D	16	15.50 (16)
T	11	10.67 (11)
S	8	8.60 (9)
E	23	22.84 (23)
P	8	Not included in analysis
G	19	18.78 (19)
A	20	21.20 (21)
C	0	0
V	12	12.00
M	1	1.06 (1)
I	13	12.00
L	25	23.78 (24)
Y	4	3.91 (4)
F	3	3.30 (3)
W	0	0
H	4	5.25 (5)
K	21	21.60 (21)
R	16	15.72 (16)

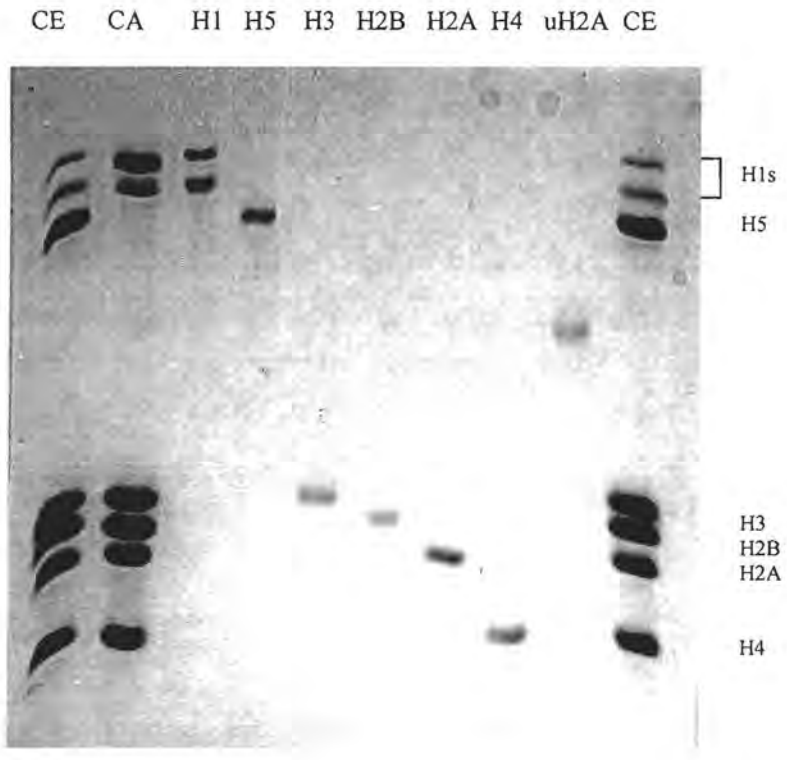

Figure 2.4. SDS-PAGE of the purified chicken erythrocyte histones and calf uH2A. The standards are total acid extracts from nuclei of calf thymus (CA) and chicken erythrocytes (CE).

2.2.3 Purification of linker histones

Chicken erythrocyte nuclei were used as a source of linker histones. Although linker histones exposed to acidic conditions have been used by several authors in reassociation studies (Nelson *et al.*, 1979; Biard-Roche *et al.*, 1982; Kaplan *et al.*, 1984; Russo *et al.*, 1995), it has been shown that acid extracted linker histones undergo irreversible conformational changes (Brand *et al.*, 1981). The method of Garcia-Ramirez *et al.* (1990) was therefore used to extract linker histones under non-denaturing conditions. This method uses the anionic resin CM Sephadex C-25 to remove linker histones from chromatin. The elution profile of linker histones extracted from chicken erythrocyte chromatin is shown in Fig. 2.5.

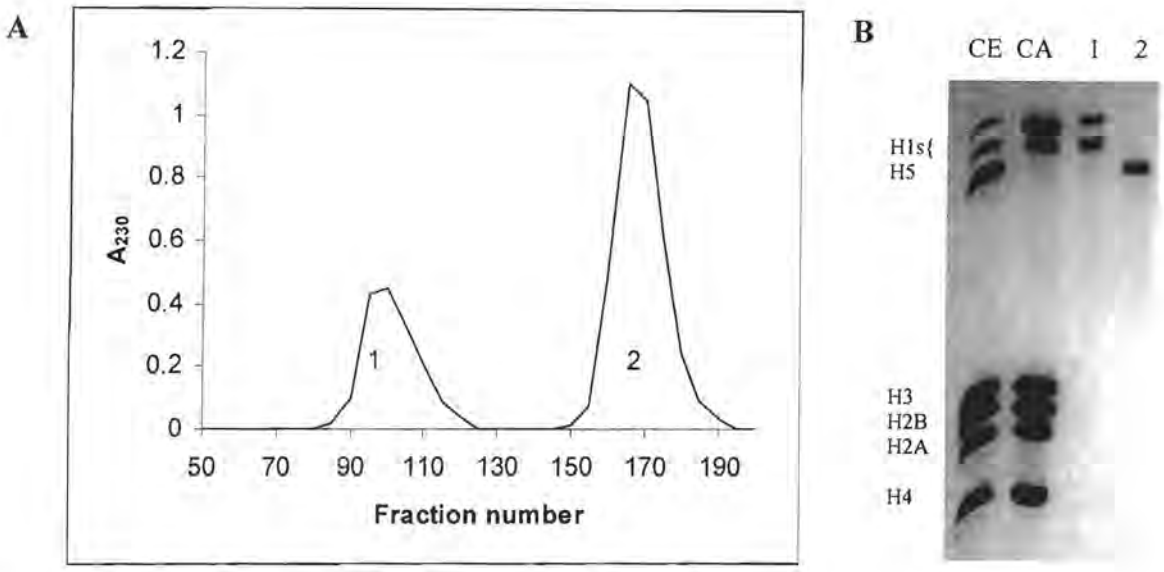

Figure 2.5. Purification of chicken erythrocyte linker histones. (**A**) CM Sephadex C-25 elution profile of the material extracted from chicken erythrocyte chromatin using CM Sephadex C-25 (see section 8). Bound linker histones were eluted with a linear gradient from 0.35 M to 1.3 M NaCl in 10 mM Tris-HCl (pH 8.8). (**B**) SDS-PAGE analysis of peaks 1 and 2. The standards used are total acid extracts of nuclei from chicken erythrocytes (CE) or calf thymus (CA). Linker histones were stored in 10 mM NaCl, 0.1 mM EDTA and 10 mM Tris-HCl (pH 7.4) in 50 % (v/v) glycerol at –20 °C.

2.2.4 Reconstitution of histone octamers

Stoichiometric amounts of acid extracted chicken erythrocyte H2B, H3, H4 together with either calf H2A or uH2A were reconstituted by salt dialysis (Tatchell & van Holde, 1977; Lindsey *et al.*, 1983; Davies & Lindsey, 1994) to form control and uH2A hybrid octamers respectively. Octamers were purified from other reconstitution products by gel exclusion chromatography on a Sepharose 6B column (Fig. 2.6). The uH2A octamers had the same elution profile as control octamers.

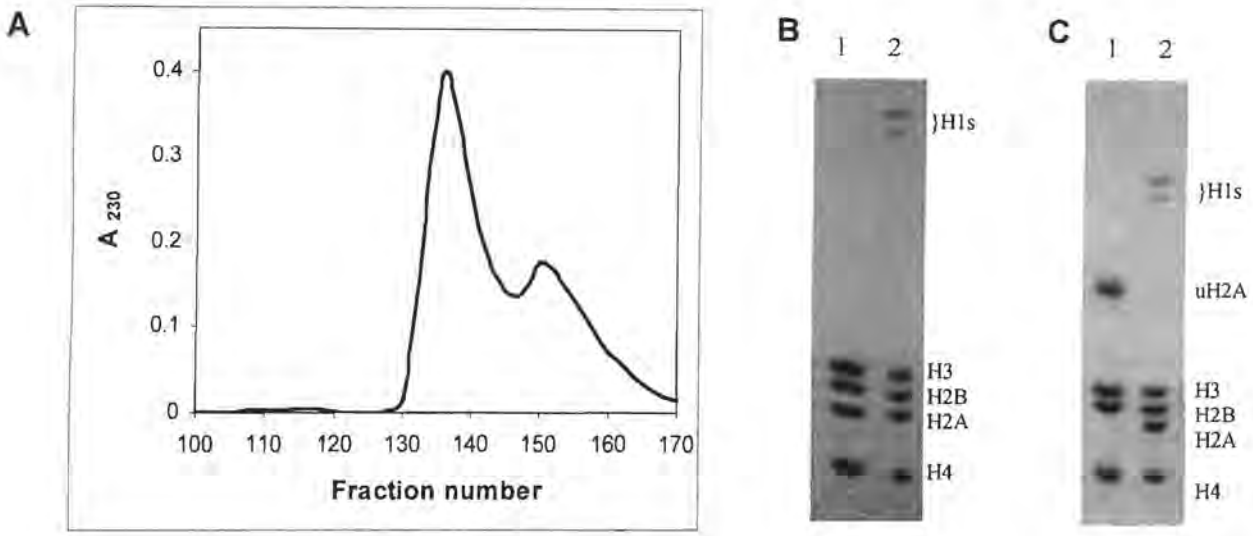

Figure 2.6. Purification of reconstituted octamers. (**A**) Sepharose 6B chromatography of the products of hybrid octamer reconstitution using chicken erythrocyte histones H2B, H3 and H4 and calf thymus uH2A. The column buffer was 2 M NaCl and 10 mM Tris-HCl (pH 7.4). Fractions 131 to 137 from the first elution peak containing pure octamers were pooled. (**B**) and (**C**) SDS-PAGE analysis of reconstituted control and uH2A hybrid octamers respectively (lanes 1). A total acid extract of calf thymus nuclei is included as a standard in lanes 2.

The histone content of the octamers was quantified by densitometric analysis of Coomassie stained SDS gels. The ratio of the core histones in the reconstituted octamers was the same as that of the standard total acid extracted histones used as standards on the same gel. The integrity of the octamers was further confirmed by dimethyl suberimidate cross-linking (von Holt *et al.*, 1989). Cross-linking was only performed on control octamers since the elution volume of uH2A hybrid octamers was the same as that of the control octamers, suggesting a likely similarity in shape and size of these two complexes. Moreover, quantities of the uH2A hybrid octamers were limited owing to the lengthy purification procedure of uH2A. The octameric cross-links were formed within 1 minute with dimer, tetramer and hexamer intermediates also being observed (Fig. 2.7 lane 4). After 10 minutes, insoluble complexes were formed thereby reducing the amount of material visible on the gel.

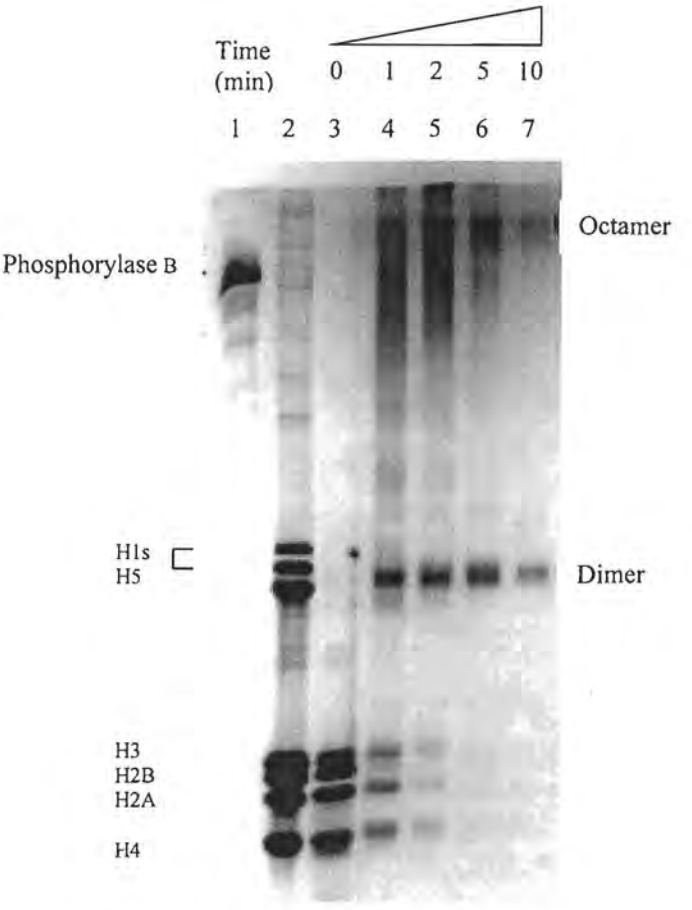

Figure 2.7. SDS-PAGE of reconstituted control histone octamers after cross-linking with dimethyl suberimidate in 2 M NaCl and 50 mM borate (pH 9). The cross-linking reaction was quenched after 0, 1, 2, 5 and 10 min by the addition of glycine to 50 mM and samples were dialysed against 50 mM glycine (pH 8) prior to application to the gel. The standards in lanes 1 and 2 are phosphorylase B (97 000 daltons) and a total acid extract of chicken erythrocyte nuclei respectively.

2.2.5 Purification of random sequence 167 bp DNA

It was decided to study linker histone binding to control and uH2A hybrid nucleosomes by analysing the protein content and gel retardation properties of the reconstitution products. Large quantities of material are required to perform protein based analyses of linker histone reconstitutions. The template DNA used in this study was therefore isolated from 167 bp random sequence nucleosome cores from chicken erythrocyte chromatin stripped of linker histones (Lindsey & Thompson, 1989). Long chicken erythrocyte chromatin stripped of histone H1 and H5 was digested with MNase under appropriate conditions, and 167 bp nucleosome cores were isolated by size-exclusion chromatography (Fig. 2.8). The length of the DNA associated with the nucleosome cores was monitored by 6 % non-denaturing PAGE and fractions containing 167 bp nucleosome cores were pooled and the DNA was purified by phenol extraction (Fig. 2.8). This method allows for the reproducible production of milligram quantities of random sequence, defined length DNA.

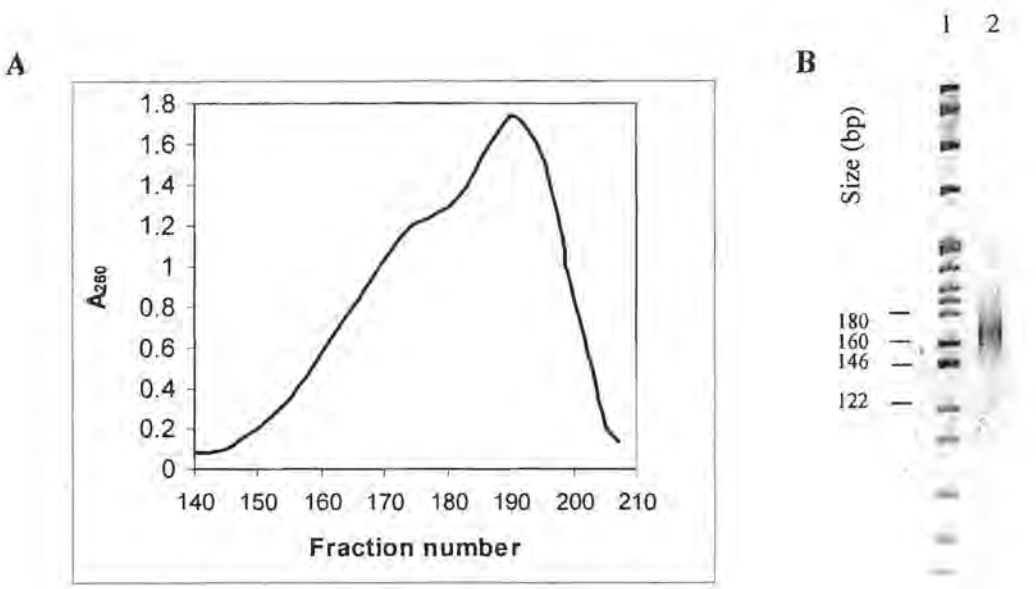

Figure 2.8. Isolation of 167 bp nucleosome cores. (A) Sepharose 6B chromatography of the MNase digestion products of long chicken erythrocyte chromatin stripped of linker histones digested under conditions to maximise the yield of 167 bp nucleosome cores. The column buffer was 0.3 M NaCl, 0.1 mM EDTA and 10 mM Tris-HCL (pH 7.4). Fractions 189 to 199 were pooled and contained pure 167 bp cores as judged by 6 % non-denaturing PAGE **(B)** (lane 2). The standard in lane 1 is a *Hpa* II digest of pBR322. The gel was stained with ethidium bromide.

2.2.6 Nucleosome reconstitution

Control and uH2A hybrid octamers were reconstituted onto 167 bp DNA by dialysis from high to low salt (Tatchell & van Holde, 1977). The extent of trial reconstitutions was monitored on agarose nucleoprotein gels (Fig. 2.9).

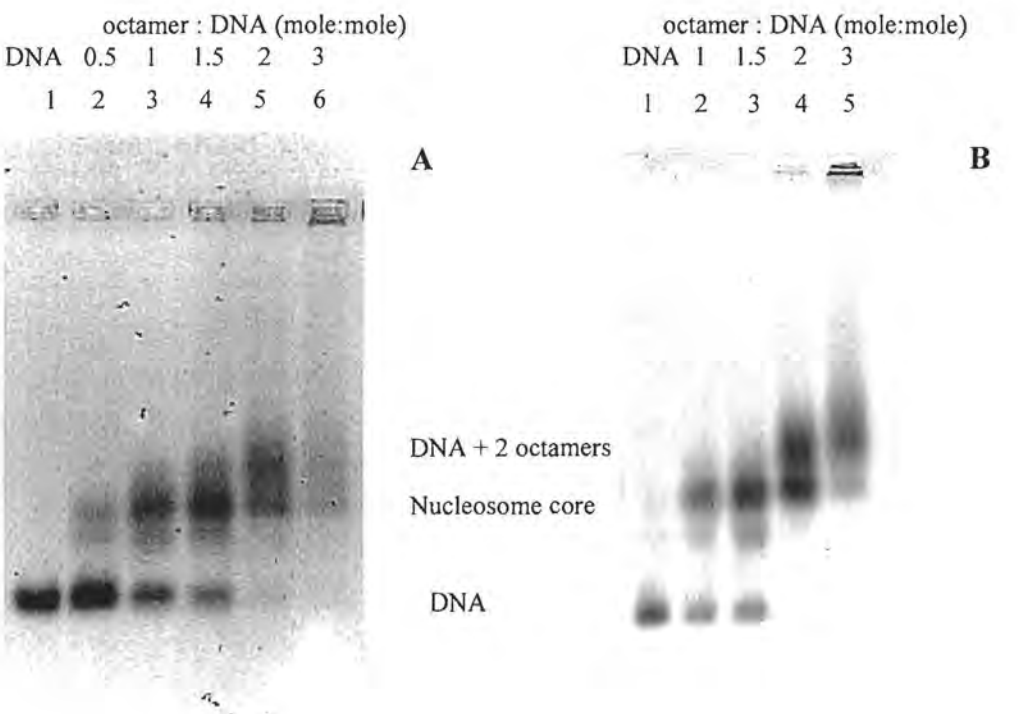

Figure 2.9. Reconstitution of purified random sequence 167 bp DNA with (A) control and (B) uH2A hybrid histone octamers. Reconstitutions were carried out at octamer to DNA molar ratios of 0.5, 1, 1.5, 2 and 3 and complexes were resolved by 0.7 % (w/v) agarose gel electrophoresis in 0.5 × TBE. Gels were stained with ethidium bromide.

For control and uH2A hybrid octamers, bulk reconstitutions of 25 µg of 167 bp DNA using an octamer to DNA molar ratio of 1.5:1 yielded mainly nucleosomes together with a small amount of free DNA and a complex of lower mobility that presumably had two octamers bound. Centrifugation of the reconstitution mixtures through linear 5-20 % (w/v) sucrose gradients allowed for the purification of nucleosomes from the other reconstitution products (Fig. 2.10 A). The purified control nucleosomes exhibited the same mobility as native 167 bp nucleosome cores depleted of linker histones on an agarose nucleoprotein gel (Fig. 2.10 B). uH2A hybrid nucleosomes had reduced mobilities compared to that of control nucleosomes, as previously observed (Kleinschmidt & Martinson, 1981; Levinger & Varshavsky, 1982; Barsoum & Varshavsky, 1985) and semi-ubiquitinated nucleosome containing one molecule of H2A and one molecule of uH2A exhibited intermediate mobilities (Fig. 2.10 C).

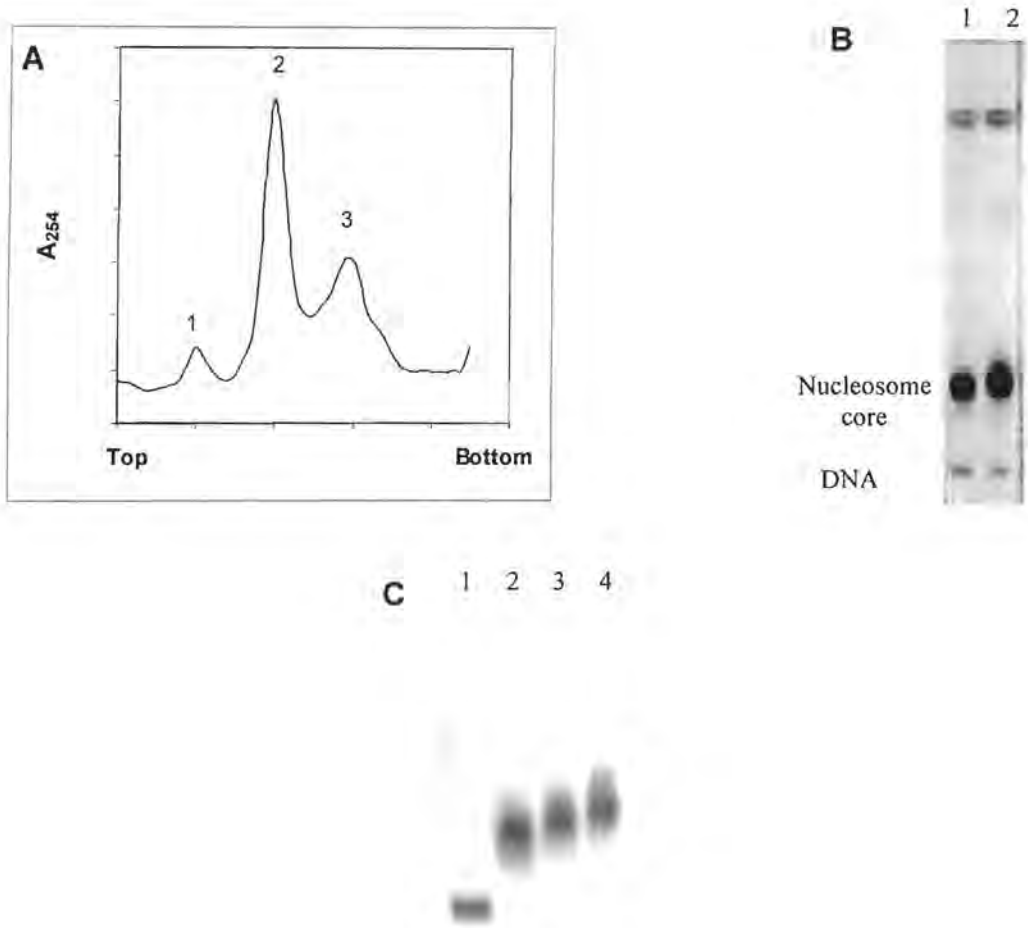

Figure 2.10. Purification of reconstituted nucleosome cores. (**A**) Fractionation profile of a 5–20 % (w/v) sucrose gradient in 10 mM NaCl, 0.2 mM EDTA and 10 mM Tris-HCl (pH 7.4) of the products formed following reconstitution of control octamers onto 167 bp DNA at a 1.5:1 molar ratio. The numbered peaks contained free 167 bp DNA (peak 1), 167 bp nucleosome cores (peak 2) and nucleosome cores with an additional octamer bound (peak 3), respectively. The position of the nucleosome cores in the gradient was the same as that observed for native 167 bp nucleosome cores and reconstituted uH2A hybrid nucleosome cores. (**B**) 0.7 % (w/v) agarose nucleoprotein gel of 167 bp nucleosome cores isolated from long stripped chicken erythrocyte chromatin (lane 1) and 167 bp DNA reconstituted with control octamers (lane 2). (**C**) 0.7 % (w/v) agarose nucleoprotein gel of 167 bp DNA (lane 1) reconstituted with control, semi-ubiquitinated and uH2A hybrid octamers (lanes 2-4). The reconstituted nucleosomes contained one octamer per DNA molecule. Gels were stained with ethidium bromide.

2.2.7 Linker histone reconstitution

2.2.7.1 Direct addition in low salt buffer

Numerous studies have made use of direct addition of linker histones to nucleosomes in low salt buffer to analyse linker histone binding (e.g. Hayes & Wolffe, 1993; Ura *et al.*, 1994; Hayes, 1996; An *et al.*, 1998). It must be noted that the nucleosomal DNA used in those studies was of defined sequence and in the order of 230 bp in size. Control and uH2A hybrid nucleosome cores, reconstituted onto 167 bp of random sequence DNA were incubated with increasing amounts of purified chicken erythrocyte histone H1 in 50 mM NaCl, 1 mM EDTA and 10 mM Tris-HCl (pH 7.4) for 90 minutes at 4 °C. The samples were then applied to 5–20 % (w/v) sucrose gradients in the same buffer to separate the chromatosomes from unbound linker histones. The chromatosome peaks were collected and the histones were precipitated by addition of ice cold trichloroacetic acid to 13 % (v/v). Ovalbumin was used as a carrier protein to minimise losses during precipitation. The samples were analysed by SDS-PAGE and the degree of linker histone reassociation was monitored by densitometric analysis of the gels. Under these conditions, binding of linker histones to reconstituted nucleosome cores was limited and never exceeded 20 % of the linker histone content of a total acid extract of calf thymus nuclei (Fig. 2.11). Aggregation occurred at a molar input ratio of 1.6 histone H1 per nucleosome core. Analysis of the reconstitution products on agarose nucleoprotein gels showed that there was no clear separation of nucleosomes from the linker histone bound complexes. As the amount of linker histone was increased, nucleosomal complexes exhibited a gradual decrease in mobility (not shown). Previous studies have indicated clear separation between nucleosomes and chromatosomes on similar nucleoprotein gels (e.g. Hayes & Wolffe, 1993; Ura *et al.*, 1994; An *et al.*, 1998). These results implied that the correct interaction between linker histones and the 167 bp nucleosome cores was not established. This linker histone reconstitution protocol was therefore deemed unsuitable for use with reconstituted 167 bp nucleosome cores.

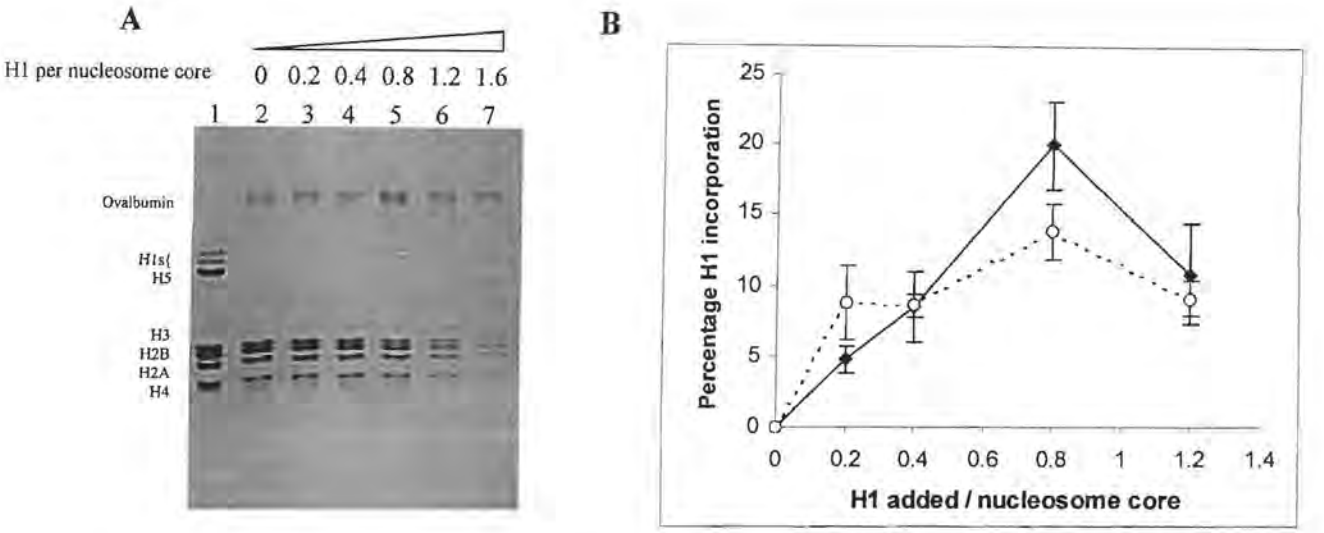

Figure 2.11. Analysis of the relationship between input ratio of linker histone H1 and that found in chromatosomes reconstituted by direct addition of H1. Control (**A**) and uH2A hybrid (not shown) 167 bp nucleosome cores were reconstituted at a molar input ratio of 0, 0.2, 0.4, 0.8, 1.20 and 1.6 H1 per nucleosome core (lanes 2-7). Chromatosomes were purified by sucrose density gradient centrifugation and their histone content was analysed by SDS-PAGE. (**B**) Gels were scanned and the quantity of H1 associated with each sample was determined by comparison with a total acid extract of calf thymus nuclei of similar intensity on the same gel. The solid line represents control 167 bp cores and the dashed line represents uH2A hybrid 167 bp cores. The data shown represent the average of 2 experiments. The ratio of H2A to H2B and H3 was used as an internal standard and in all cases this ratio never deviated more than 5 % compared to that of the standard calf thymus histones.

2.2.7.2 Salt dialysis reconstitution

The failure of linker histone reconstitution by direct addition was possibly due to the octamers adopting an equilibrium position on the 167 bp DNA that was unfavourable to successfully form chromatosomes. Since the histone octamer alone is known to protect 167 bp of DNA from MNase digestion (Weischet *et al.*, 1979; Lindsey & Thompson, 1989; Pruss & Wolffe, 1993), it is likely that the availability of thermodynamically favourable octamer positions will be restricted on such a short, although random sequence, DNA fragment. It has previously been shown that octamer position can affect linker histone binding (Hamiche *et al.*, 1996). Another commonly used linker histone reconstitution technique involves addition of the linker histones to nucleosomes or chromatin at elevated salt concentrations (0.5 to 0.6 M NaCl) and subsequent dialysis into low salt buffer. At the high salt concentrations, the cationic charges of linker histones are shielded and ionic interactions with the chromatin DNA are disrupted. If unfavourable octamer positions were inhibiting correct linker histone binding, this reconstitution protocol should allow repositioning of the octamer since it is known that octamers are mobile on DNA (Pennings *et al.*, 1991), especially at higher salt concentrations (Spadafora *et al.*, 1979). Purified control and uH2A hybrid 167 bp nucleosome cores at a final concentration of 60 µg core DNA per ml were incubated for one hour with increasing amounts of chicken erythrocyte histone H1 in 0.55 M NaCl, 1 mM EDTA and 10 mM Tris-HCl (pH 7.4) at 4 °C. The salt concentration was lowered by dialysis and the samples were applied to 5–20 % (w/v) sucrose gradients in 10 mM NaCl, 1 mM EDTA and 10 mM Tris-HCl (pH 7.4) to separate the chromatosomes from unbound linker histones. The histone content of the chromatosome peaks was analysed as before (section 2.2.7.1). These results (Fig. 2.12) show that uH2A does not prevent linker histone binding to 167 bp nucleosome cores in agreement with previous results (Nelson *et al.*, 1979; Bonner & Stedman, 1979) and that linker histone binding is slightly favoured in the presence of uH2A. The H1 content of uH2A hybrid and control 167 bp cores reached the levels found in a total acid extract of calf thymus at a molar input ratio of 1 and 1.3 histone H1 per 167 bp nucleosome core DNA respectively. A t-test for independent samples with 95 % confidence was performed at each histone H1 input ratio for the results shown in Fig. 2.12 using Satistica (Statsoft) software. The results indicated that there was no

statistical difference between control and uH2A hybrid nucleosome cores except at a molar input ratio of 1.2 histone H1 per nucleosome core. Further analysis was performed by fitting the data to a common intercept, using the standard deviations as weights. The results, shown in Table 2.2, indicate that there was no statistically significant difference in between the two slopes shown in Fig. 2.12.

Table 2.2. Statistical analysis of the data presented in Fig. 2.12.

Slope difference	Standard error	t- stat	P-value	Lower 95%	Upper 95%
37.91	22.41	1.69	0.12920	-13.77	89.60

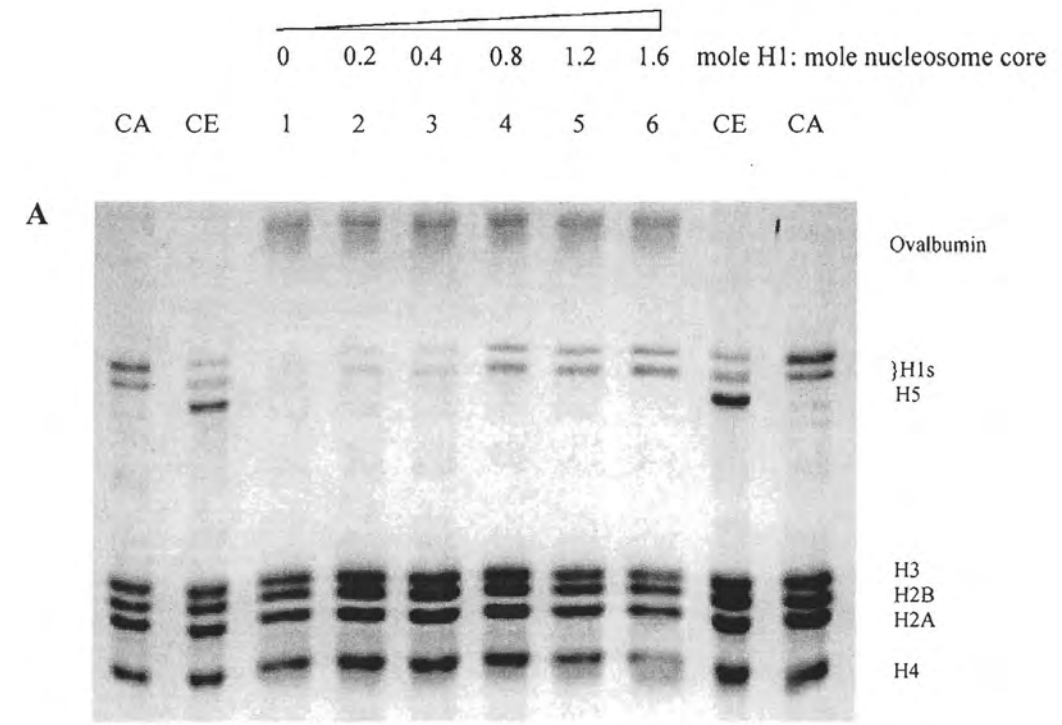
0 0.2 0.4 0.8 1.2 1.6 mole H1: mole nucleosome core
CA CE 1 2 3 4 5 6 CE CA
A
Ovalbumin
}H1s
H5
H3
H2B
H2A
H4

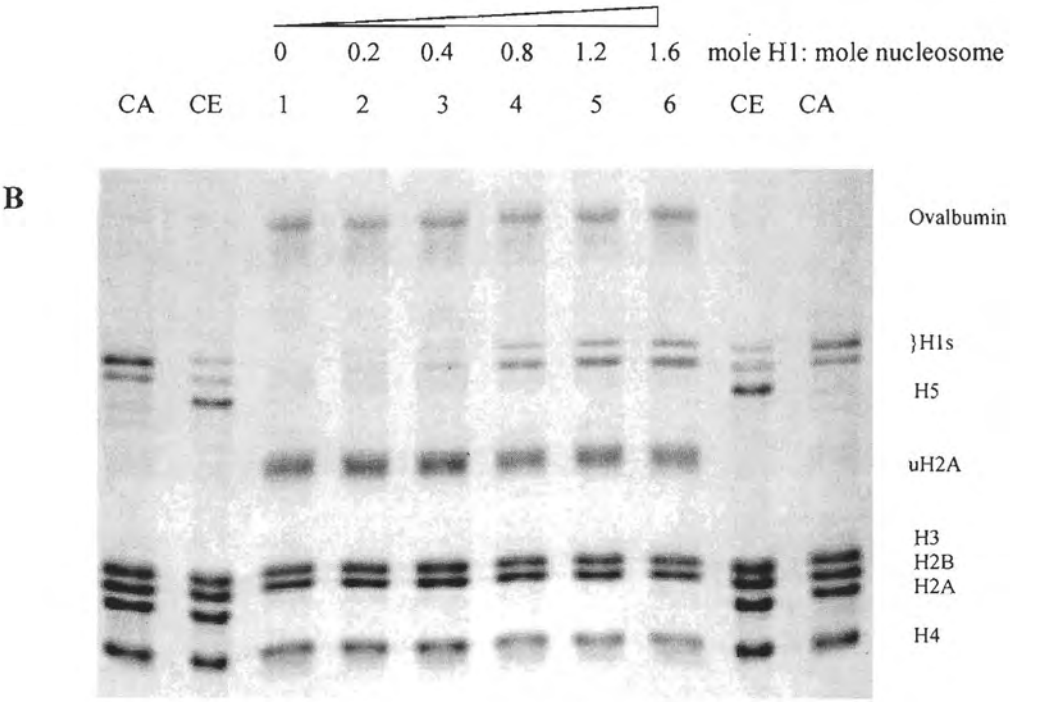
0 0.2 0.4 0.8 1.2 1.6 mole H1: mole nucleosome
CA CE 1 2 3 4 5 6 CE CA
B
Ovalbumin
}H1s
H5
uH2A
H3
H2B
H2A
H4

C

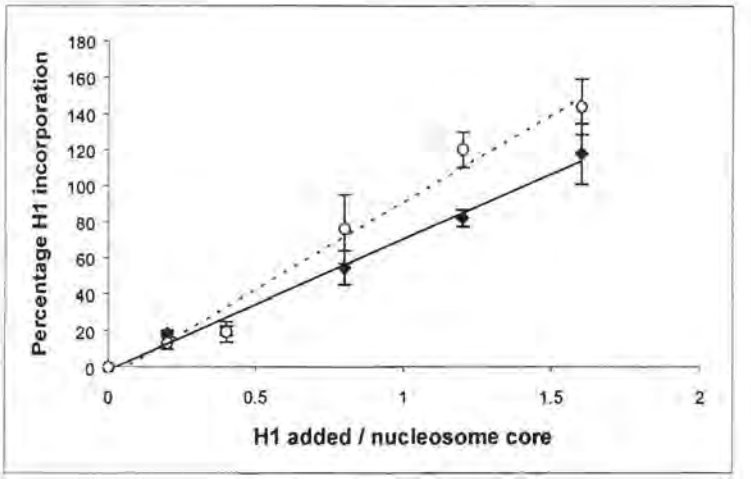

Figure 2.12. Analysis of the relationship between input ratio of linker histone H1 and that found in chromatosomes reconstituted by salt dialysis. SDS-PAGE of (**A**) control and (**B**) uH2A hybrid 167 bp nucleosome cores reconstituted at a molar input ratio of 0, 0.2, 0.4, 0.8, 1.2 and 1.6 histone H1 per nucleosome core (lanes 1 to 6). The standards were total acid extracts of nuclei from chicken erythrocytes (CE) or calf thymus (CA). Ovalbumin was used as a protein carrier and was added to the samples just before precipitation. (**C**) Gels were scanned and the quantity of H1 associated with each sample was determined by comparison with a total acid extract of calf thymus of similar intensity on the same gel. The data were fitted to lines representing the least squares. The solid line represents control 167 bp cores and the dashed line represents uH2A hybrid 167 bp nucleosome cores. The data shown represent the average of 4 experiments. R^2 values were determined to be 0.981 and 0.989 for uH2A hybrid and control nucleosome cores. The ratio of H2A to H2B and H3 was used as an internal standard and in all cases this ratio never deviated more than 5 % compared to that of the standard calf thymus histones.

Gel retardation assays were also used to monitor the reassociation of H1 to control and uH2A hybrid 167 bp nucleosome cores by salt dialysis (Fig. 2.13). The reconstitutions were performed at final concentration of 60 μg core DNA per ml. From Fig. 2.13 it can be seen that, in agreement with Fig. 2.12, uH2A hybrid chromatosomes were formed at slightly lower histone H1 concentrations than those required to form control chromatosomes.

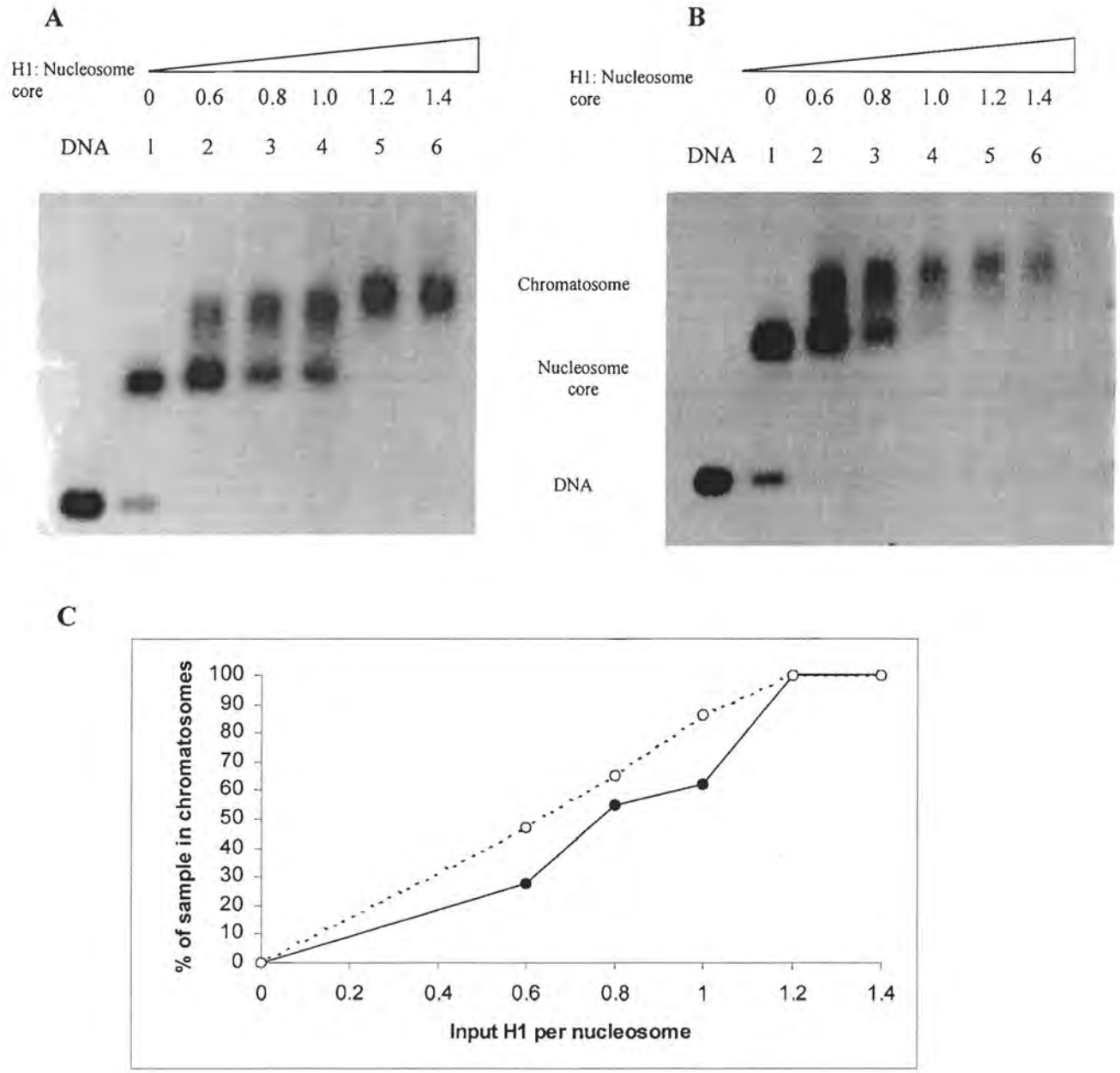

Figure 2.13. Nucleoprotein gel retardation assays of linker histone binding to 167 bp nucleosome cores. (**A**) Control and (**B**) uH2A hybrid 167 bp nucleosome cores were reconstituted at a molar input ratio of 0, 0.6, 0.8, 1.0, 1.2 and 1.4 histone H1 per nucleosome core (lanes 1-6) by salt dialysis and analysed on 0.7 % (w/v) agarose gels in 0.5 × TBE. DNA represents free 167 bp DNA. Gels were stained with ethidium bromide. (**C**) Gel negatives were scanned and bands were integrated using ImageQuant software to determine the percentage of chromatosomes at each linker histone input ratio. The solid line represents control 167 bp cores and the dashed line represents uH2A hybrid 167 bp cores.

2.2.7.3 Thermal denaturation

Control and uH2A hybrid 167 bp cores were reconstituted with H1 by salt dialysis at an input ratio of 1.2 moles chicken erythrocyte histone H1 per mole nucleosome core. The reconstitution products and 167 bp cores were purified through 5-20 % (w/v) sucrose gradients in 10 mM NaCl, 0.2 mM EDTA and 10 mM Tris-HCl (pH 7.4). The samples were degassed and analysed by thermal denaturation (Fig. 2.14). Under the conditions used, all samples exhibited a triphasic hyperchromicity curve. The first two transitions are thought be associated with the melting of the DNA associated with the ends of the nucleosome core, whilst protein denaturation and melting of the DNA more tightly associated with core histones represent the main transition (Cowman & Fasman, 1980; van Holde, 1989). In 167 bp control and uH2A hybrid nucleosome cores, the first transition occurred at 69 °C and 68 °C and represented 13 % (21 bp) and 15 % (25 bp) of the DNA respectively. This could reflect a slightly decreased interaction of histone tails with the ends of the nucleosome core DNA in the presence of uH2A. This decrease in protein-DNA interaction is more subtle than that caused by core histone acetylation, where a decrease of 3 °C in the T_m of the first transition was observed (Ausió & van Holde, 1986). In the presence of linker histones, the first transition decreased in magnitude and shifted to approximately 70 °C for both control and uH2A hybrid chromatosomes. This decrease in magnitude of the first transition was slightly more pronounced for the uH2A hybrid chromatosomes than for control chromatosomes. The association of linker histones with the ends of the core DNA would be expected to stabilise this DNA, correlating with the observed increase in the T_m value of the first transition of 1 °C and 2 °C for control and uH2A hybrid chromatosomes respectively. The second and third transitions of both samples occurred at 79 °C and 83.8 °C respectively, indicating that the presence of uH2A did not lead to large scale disruption of octamer-DNA interactions in good agreement with previous observations (Kleinschmidt & Martinson, 1981; Davies & Lindsey, 1994).

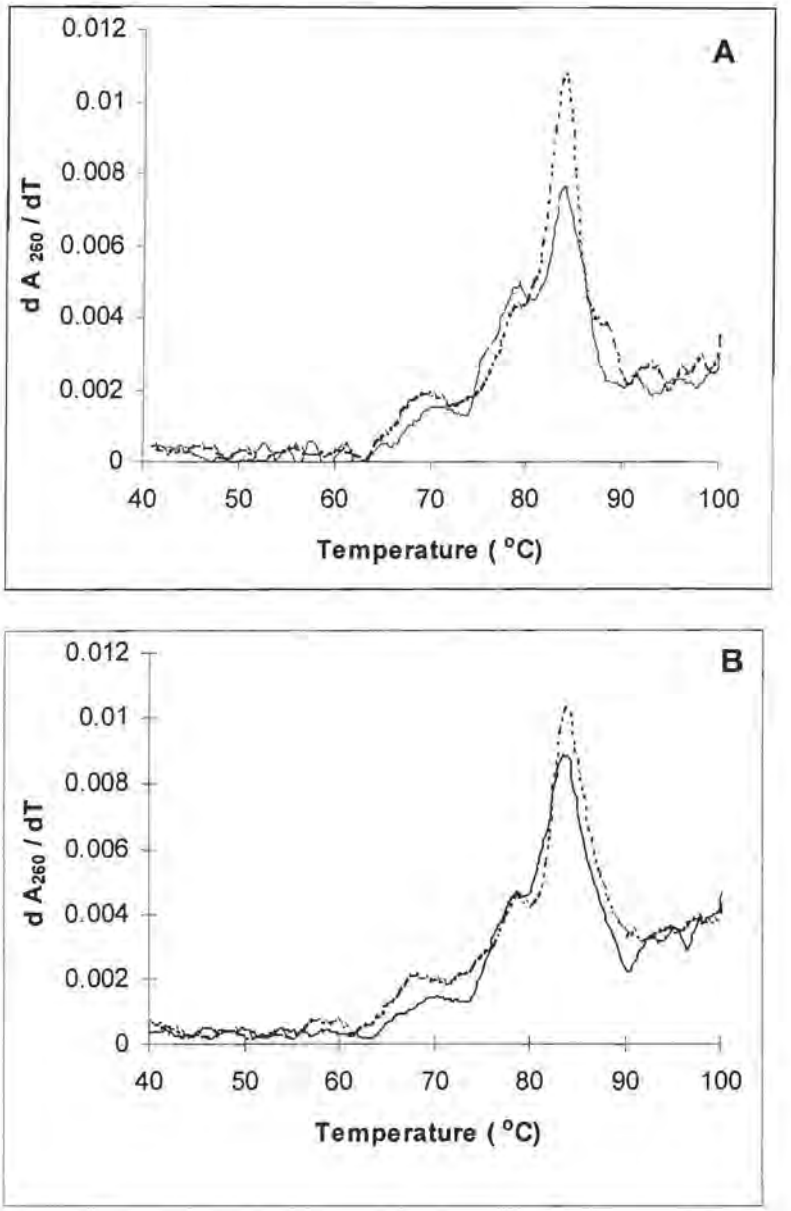

Figure 2.14. Thermal denaturation profile of control (A) and uH2A hybrid (B) 167 bp nucleosome cores (dashed lines) and chromatosomes (solid lines). Denaturation was carried out at 50 μg DNA/ml in 12 % (w/v) sucrose, 10 mM NaCl, 0.2 mM EDTA and 10 mM Tris-HCl (pH 7.4). The first derivatives of the A_{260} versus temperature profiles are shown.

These results suggested that ubiquitination of uH2A had little effect on the structure and molecular contacts of 167 bp nucleosome cores. Linker histone binding was not inhibited by the presence of the ubiquitin moiety but rather was slightly favoured at the nucleosome level (see also section 3).

Further studies will be required to determine if this situation is also reflected in long chromatin as the core histone tails are essential and are the main determinants for the proper folding of chromatin fibres (Allan *et al.*, 1982; Garcia-Ramirez *et al.*, 1992; Tse & Hansen, 1997). The conformation of chromatin fibers could be altered by nucleosomal uH2A and thus influence linker histone binding. Such conformational parameters would, however, not be evident at the nucleosomal level. As a first step towards such studies, a novel methodology was developed to reconstitute linker histone H5 onto long chromatin (see section 5).

3 The effect of histone H2A ubiquitination on nucleosome positioning

3.1 Introduction

Flexibility and bending of template DNA are important parameters that determine the ability of a particular DNA sequence to generate translationally and rotationally positioned nucleosomes in dialysis reconstitutions. Nucleosome positioning, of which there are numerous examples both *in vivo* and *in vitro*, can affect cellular processes such as transcription initiation by blocking or creating suitable DNA binding sites for regulatory DNA binding proteins (see Travers & Drew, 1997; Wolffe, 1994; Thoma, 1992 and Simpson, 1991 for reviews). A DNA segment from the sea urchin *Lytechinus variegatus* 5S rRNA gene was engineered in Robert Simpson's laboratory (Simpson & Stafford, 1983; Simpson *et al.*, 1985) and this template and 5S rDNA from *Xenopus* have become paradigms for studying nucleosome positioning *in vitro*. The *Lytechinus* DNA template was originally believed to contain a unique nucleosome positioning site (Simpson & Stafford, 1983) but subsequent investigations using restriction enzyme mapping established that nucleosomes are in equilibrium between a number of defined positions. These positions were found to be separated from each other by multiples of ~10 bp (Dong *et al.*, 1990; Meersseman *et al.*, 1991). Interestingly, the dominant position occupied by a nucleosome on this DNA template was observed to be different in numerous independent determinations. The variation reported in the literature is illustrated in Table 3.1.

Table 3.1. Previously reported dominant nucleosome positioning sites on the 5S rDNA *Lytechinus* sequence. The nucleosome positions are relative to the sequence shown in Fig. 3.1 below.

Main nucleosome position	5S rDNA fragment studied (mono/multimer)	Nucleosome reconstitution methodology	Reference
20 - 165	Monomer	Polyglutamate	Simpson & Stafford (1983)
20 - 165	Monomer	Exchange	Fitzgerald & Simpson (1985)
1 - 146	Multimer	Salt dialysis	Hansen *et al.* (1989)
1 - 146	Monomer & multimer	Salt dialysis	Dong *et al.* (1990)
6 – 153	Multimer	Salt dialysis	Meersseman *et al.* (1991)

In order to determine if the ubiquitination of H2A could have an effect on nucleosome positioning, the method of Hansen *et al.* (1989) was utilised to study nucleosome positioning on a 208 bp DNA template containing the *Lytechinus variegatus* 5S rRNA gene. This method has subsequently been widely used in the determination of nucleosome positions (e.g. Dong *et al.*, 1990; Meersseman *et al.*, 1991; Studitsky *et al.*, 1996; Sera & Wolffe, 1998). The template DNA sequence is shown in Fig. 3.1.

```
     0          10         20         30         40         50         60
CCGAGGAATTCCAACGAATAACTTCCAGGGATTTATAAGCCGATGACGTCATAACATCCCTGACCCTTT
Dra I  Alu I       80         90         100        110        120
↓AAATAG↓CTTAACTTTCATCAAGCAAGAGCCTACGACCATACCATGCTGAATATACCGGTTCTCGTCC
Sau3A I   140        150        160        170        180        190
↓GATCACCGAAGTCAAGCAGCATAGGGCTCGGTTAGTACTTGGATGGGAGACCGCCTGGGAATACGAAT
 200
TCC
```

Figure 3.1. Sequence of 208 bp DNA template containing a *Lytechinus variegatus* 5S rDNA gene segment used to reconstitute nucleosomes. The restriction sites of the enzymes used to determine nucleosome positioning are indicated. (Adapted from Simpson & Stafford, 1983; Simpson *et al.*, 1985).

3.2 Results and Discussion

3.2.1 Isolation of template DNA

DNA templates were prepared by digesting plasmid p5S 208-12 to completion with *Ava* I to produce 12 copies of the 208 bp template. The 208 bp template was purified from the rest of the plasmid by sucrose density centrifugation as outlined in the methods section.

Figure 3.2 illustrates a typical fractionation profile. Each gradient can accommodate up to 250 μg of plasmid before resolution is reduced. This technique also ensures that, unlike preparative agarose gel electrophoresis, the DNA is exposed to UV light for a minimum time thereby limiting the amount of UV-induced damage.

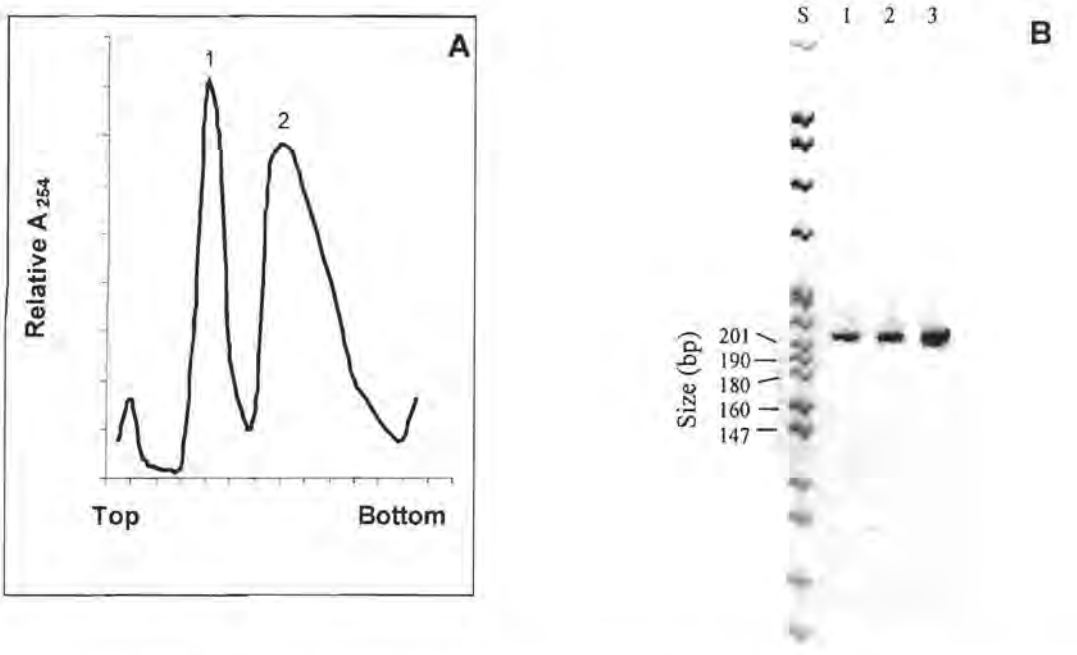

Figure 3.2. Purification of 208 bp 5S rDNA. (**A**) Fractionation profile of p5S 208-12 cut with *Ava* I applied to 5-12 % (w/v) sucrose gradient. Fractions across peak 1 were analysed by agarose gel electrophoresis and those containing pure 208 bp DNA were pooled. The top and bottom of the gradient are indicated. (**B**) 6 % non-denaturing PAGE of increasing loadings of pure 208 bp DNA fragment from peak 1 (lanes 1-3). The standard (S) is a *Hpa* II digest of pBR322.

3.2.2 Nucleosome positioning

Histone octamers were reconstituted onto template DNA by salt dialysis using an octamer to DNA ratio which resulted in the formation of ≤ 1 nucleosome per template. Nucleoprotein gel retardation assays were used to monitor the extent of reconstitution (not shown).

In order to determine the position of the octamer on the DNA, reconstituted nucleosomes were first digested with MNase to yield core particles. Depending on the position of the octamer on the template DNA, restriction sites will be present or absent since the template is 208 bp long and the core particle contains 147 bp (Noll & Kornberg, 1977). The core particle DNA is purified and cleaved with a specific restriction enzyme. The size of the resultant fragments pairs adding up to the original core particle DNA size allow one to determine the boundary positions of the core particle with respect to the restriction enzyme site in the known DNA sequence.

Positions are confirmed by performing the experiment with other restriction enzymes. The intensity of the DNA fragments indicates the prevalence of nucleosomes at a particular position.

Trial MNase digestions were performed to determine the optimal digestion time required to produce core particles. The kinetics of digestion of control and uH2A reconstitutes were comparable and in both cases digestion stops occurred at 158 bp and 151 bp, determined by comparing the length of DNA fragments of a *Hpa* II digest of pBR322. A typical digest is shown in Fig. 3.3.

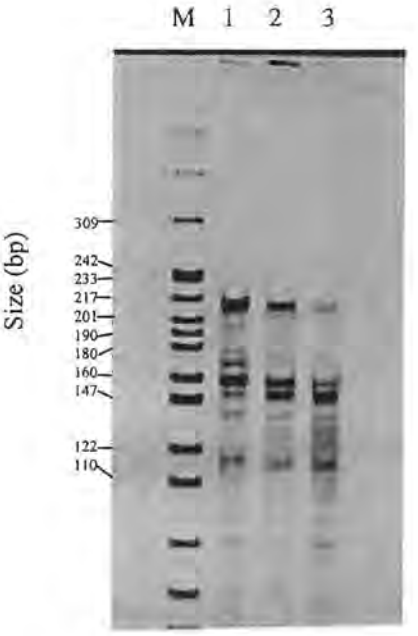

Figure 3.3. Trial MNase digest of uH2A hybrid nucleosomes reconstituted on 208 bp 5S rDNA. Reconstituted nucleosomes (3μg DNA content) were digested with 0.09 units MNase for 1(lane 1), 5 (lane 2) and 10 minutes (lane 3) at room temperature. Samples were phenol extracted and analysed on 6 % acrylamide non-denaturing gels. The marker (M) was a *Hpa* II digest of pBR322. The gel was stained with ethidium bromide.

The 151 bp band was taken to represent core particles. It has previously been reported that part of the *Lytechinus* 5S rDNA sequence exhibits aberrant migration on polyacrylamide gels relative to DNA fragments of pBR322, possibly due to a slight curvature of the 208 bp DNA fragment (Dong *et al.*, 1990). Naked 208 bp template DNA was digested with MNase as a control to account for any fragment that might arise due to the enzyme's sequence specificity. No bands of 157 bp or 151 bp were

visible (Figure 3.4). The main early digestion product of naked DNA was a 160 bp band.

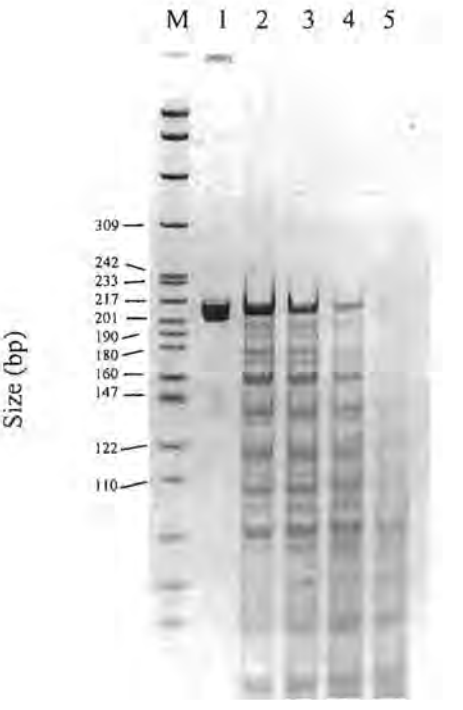

Figure 3.4. MNase digestion of naked 208 bp 5S rDNA. Three micrograms of template DNA were digested with 0.02 units of MNase at room temperature for 0 (lane 1), 15 (lane 2), 30 (lane 3), 60 (lane 4) and 120 seconds (lane 5). Samples were phenol extracted and analysed on 6 % acrylamide non-denaturing gels. The marker (M) was a *Hpa* II digest of pBR322.

Bulk MNase digestions of reconstituted control and uH2A hybrid nucleosomes were carried out under identical conditions to that of the trial digest and the deproteinated material was electrophoresed in several lanes of a 6 % polyacrylamide gel to ensure clear separation of bands. The 151 bp bands were excised and the DNA was extracted from the gel slices. Purified DNA was divided into aliquots and digested with the specified restriction enzymes. *Dra* I and *Alu* I were chosen as their restriction sites are found within previously reported nucleosome positions (see table 3.1) and should give rise to easily quantifiable bands. *Sau3A* I was used to represent the 3' end of the template. After overnight digestion with restriction enzymes, samples were phenol extracted, ethanol precipitated and electrophoresed through a non-denaturing 8 % acrylamide gel (Studitsky *et al.*, 1996; Sera & Wolffe, 1998) (Fig. 3.5).

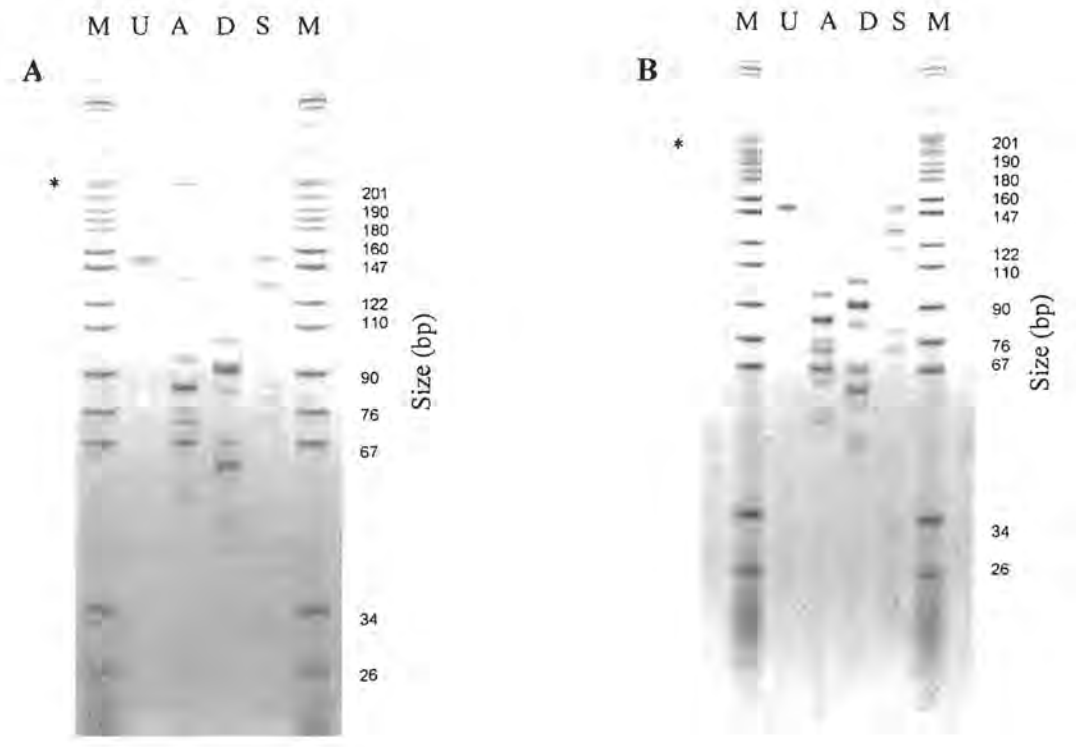

Figure 3.5. Determination of nucleosome positioning on the 208 bp 5S rDNA template. Eight percent polyacrylamide electrophoresis of restriction enzyme cleavage products of core particle DNA isolated after MNase digestion of nucleosomes containing either uH2A (**A**) or H2A (**B**). Lane M contains pBR322/ *Hpa* II size markers. Lane U contains undigested core particle DNA. Lanes A, D and S contain DNA fragments produced by digestion of core particle DNA with *Ava* I, *Dra* I and *Sau3A* I respectively. *A 232 bp fragment from plasmid pGBT9 lacking *Ava* I, *Dra* I and *Sau3A* I restriction sites was included as an internal control.

Band sizes in Fig. 3.5 were determined from a standard curve of log bp *versus* migration distance of the standard (pBR322/*Hpa* II). Pairs of fragments adding up to ~151 bp were determined from their calculated size and relative intensity. It is not possible to fully quantitate the distribution of positions since the extent of SYBR gold staining of DNA fragments is dependent on their size. The results obtained were essentially identical for control and uH2A hybrid nucleosomes (Table 3.2). Most nucleosomes (50 %) occupied the position 4 to 153 relative to the DNA template sequence shown in Fig. 3.1. Minor positions were also found at –3 to 145, 14 to 165 and 53 to 203.

Table 3.2. Control and uH2A nucleosome positions on 208 bp 5S rDNA template.

DNA restriction fragments from Figure 3.5 were sized and paired to add up to the length of the core particle (~151 bp). Positions were determined by comparison of fragment lengths to the position of the restriction sites (Fig.3.1).

Alu I					
Left Boundary	**Band size (bp)**	**Right Boundary**	**Band size (bp)**	**Position**	**Relative % of total ***
4	66	154	85	A	50
-3	74	145	76	B	25
14	55	165	96	C	19.5
56		203	134	D	3.5

Dra I					
Left Boundary	**Band size (bp)**	**Right Boundary**	**Band size (bp)**	**Position**	**Relative % of total ***
3	60	153	90	A	52
-4	67	147	84	B	23
17	46	166	103	C	20
57		204	141	D	4

*Sau3A*I					
Left Boundary	**Band size (bp)**	**Right Boundary**	**Band size (bp)**	**Position**	**Relative % of total ***
				Uncut	29
-1	131			A	25
-5	135			B	10
15	115	163	32	C	20
50	80	201	71	D	16

*Gels were scanned and the relative density of fragments was determined by integration.

These positions are in close agreement with previous reports (see Table 3.1). The rotational orientation is maintained between positions as the differences observed are multiples of 10 bp. The fact that, under these conditions, ubiquitination of H2A does not influence the positioning of nucleosomes on 208 bp 5S rDNA is perhaps not surprising since H2A is not believed to have a major role in nucleosome positioning (Dong *et al.*, 1990). The histone: DNA contacts of uH2A hybrid nucleosomes do not appear to be greatly disrupted on a macroscale as determined by DNase I digestion (Kleinschmidt & Martinson, 1981; Davies & Lindsey, 1994) and it is therefore unlikely that this modification would interfere with nucleosome positioning signals.

3.2.3 Chromatosome positioning

Linker histones have been shown to affect the distribution of nucleosome positions on 5S rDNA (Meersseman *et al.*, 1991, Sera & Wolffe, 1998). The COOH terminal domain of H2A (which contains the site of ubiquitination) is believed to interact with the linker DNA in linker histone-depleted chromatin and 167 bp nucleosome cores (Lindsey *et al.*, 1991; Davies & Lindsey, 1994; Usachenko *et al.*, 1994). Histone-histone cross-linking experiments have demonstrated the existence of contacts between the COOH tail of H2A and histone H1 (Boulikas *et al.*, 1980).
Chromatin regions enriched in ubiquitinated histones were reported to have decreased affinity for histone H1 (Davie & Nickel, 1987). Transcriptionally active chromatin regions are believed to have a lower linker histones content than inactive chromatin and have, in some cases, been found to be enriched in ubiquitinated H2A and/or H2B (Goldknopf *et al.*, 1980; Levinger & Varshavsky, 1982; Nickel *et al.*, 1989).
However, at the level of 167 bp nucleosome cores, ubiquitination of H2A does not impede linker histone binding (section 2). The effect of ubiquitination of H2A on the position of chromatosomes on 5S rDNA was therefore determined. The first step in this procedure was the reconstitution of nucleosomes together with the linker histone. Nucleoprotein gel retardation assays were used to determine the amount of linker histone required so that most of the nucleosomes would associate with a linker histone (Fig. 3.6). Chicken histone H1 was reconstituted with control and uH2A hybrid nucleosomes by direct addition at 50 mM NaCl (Hayes & Wolffe, 1993). Although this methodology was not suitable for reconstituting linker histones onto 167 bp nucleosome cores (section 2.2.7.1), direct addition of linker histones to 208 bp nucleosomes resulted in the formation of distinct chromatosome bands (Fig. 3.6). This suggests that the additional linker DNA plays a role during linker histone binding, perhaps by providing a favourable interaction site for the H2A C-terminal domain that would relocate it to a position that is less refractory to linker histone binding.

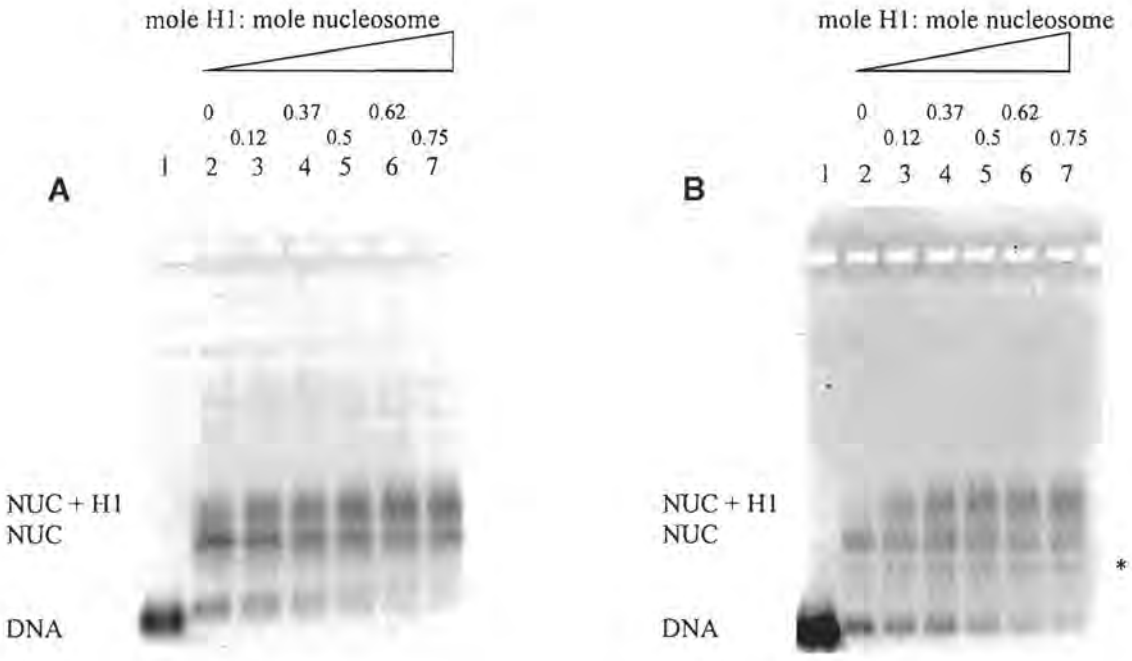

Figure 3.6. Nucleoprotein agarose gels of histone H1 reconstituted onto 208 bp control (A) or uH2A hybrid (B) nucleosomes. The positions of naked DNA (DNA), nucleosomes (NUC) and nucleosomes with bound H1 (NUC + H1) are indicated. Lane 1 contains 167 bp DNA. Lanes 2 to 7 represent nucleosomes reconstituted at molar input ratio of 0, 0.12, 0.37, 0.5, 0.62 and 0.75 histone H1 per nucleosome respectively. * This band co-migrated with H1-bound 208 bp DNA. Gels were stained with ethidium bromide.

In order to determine the affinity of the interaction between histone H1 and control and uH2A hybrid nucleosomes, the nucleoprotein gels were scanned and integrated, correcting for UV quenching. In all cases the starting material consisted of ~ 80 % nucleosomes and ~20 % free DNA. A proportion of the reconstituted nucleosomes had a mobility similar to that of H1-bound nucleosomes (Fig 3.6, lanes 2), presumably due to positional differences. The ratio (r) of nucleosomal material of slower electrophoretic mobility (a) to the bulk of nucleosomes (b) was determined for each gel in the absence of linker histones and assumed to remain constant. The amount of nucleosomes in any lane was calculated using this ratio and the main nucleosome band (nuc = b + rb). This ratio was also used to determine the amount of H1-bound nucleosomes (nuc + H1 = a – rb). The data were used to generate Hill plots (Fig. 3.7). Histone H1 was found to bind to control nucleosomes with a dissociation constant

(K_D) of 33 nM and to uH2A hybrid nucleosomes with a K_D of 21.8 nM. From these results, it can be deduced that under the experimental conditions used, uH2A nucleosomes have a 1.5 fold increased affinity for histone H1 compared to control nucleosomes.

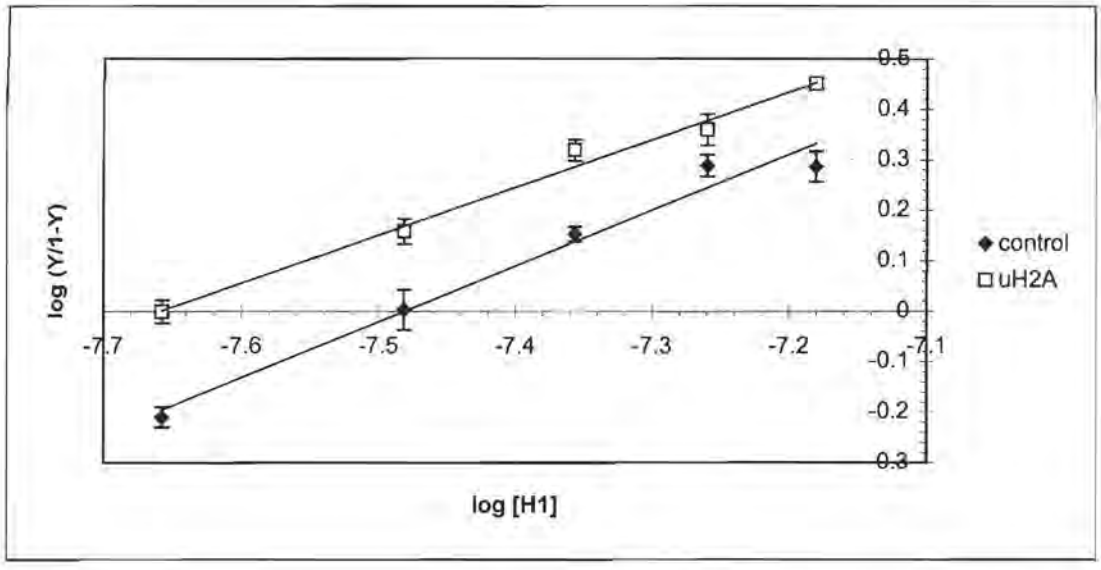

Figure 3.7. Hill plot of histone H1 binding to control and uH2A hybrid 208 bp nucleosomes. The fraction of H1 bound nucleosomes (Y) was determined by integration of nucleoprotein gel scans. The results are the average of 3 experiments. The concentration of H1 was determined using a molecular weight of 21782 g/mol (Sugarman *et al.*, 1983). R^2 values of the linear regression lines for uH2A and control nucleosomes were determined to be 0.988 and 0.976 respectively.

Statistical analysis (Table 3.2) performed by fitting the data sets in Fig 3.7 to a common slope, using the standard deviations as weights indicated that there was a statistically significant difference between the dissociation constants of control and uH2A hybrid nucleosomes.

Table 3.2. Statistical analysis of the data presented in Fig. 3.7.

Intercept difference	Standard error	t- stat	P-value	Lower 95%	Upper 95%
0.15	0.02	7.24	0.00017	0.10	0.20

In order to confirm linker histone binding, control and uH2A hybrid nucleosomes were reconstituted with 0.75 histone H1 per nucleosome and digested with MNase. Very definite pauses at 167 bp, characteristic of linker histone protection of DNA (Allan *et al.*, 1980a; Simpson, R.T., 1978) were observed in both cases from the trial digests (not shown). Although kinetic stops at 167 bp are observed in nucleosomes (Weischet *et al.*, 1979; Lindsey & Thompson, 1989; Pruss & Wolffe, 1993), comparison of trial digests of nucleosomes and chromatosomes demonstrated that 167 bp bands would no longer have been present in nucleosomes lacking linker histones at the optimal digestion time used to produce 167 bp bands from chromatosomes. This result and the gel retardation assays confirm histone H1 binding. Bulk digests were carried out on 10 μg of reconstituted material under conditions chosen to maximise the yield of 167 bp bands. These bands were excised and digested with restriction enzymes as described above. The results are shown in Fig. 3.8.

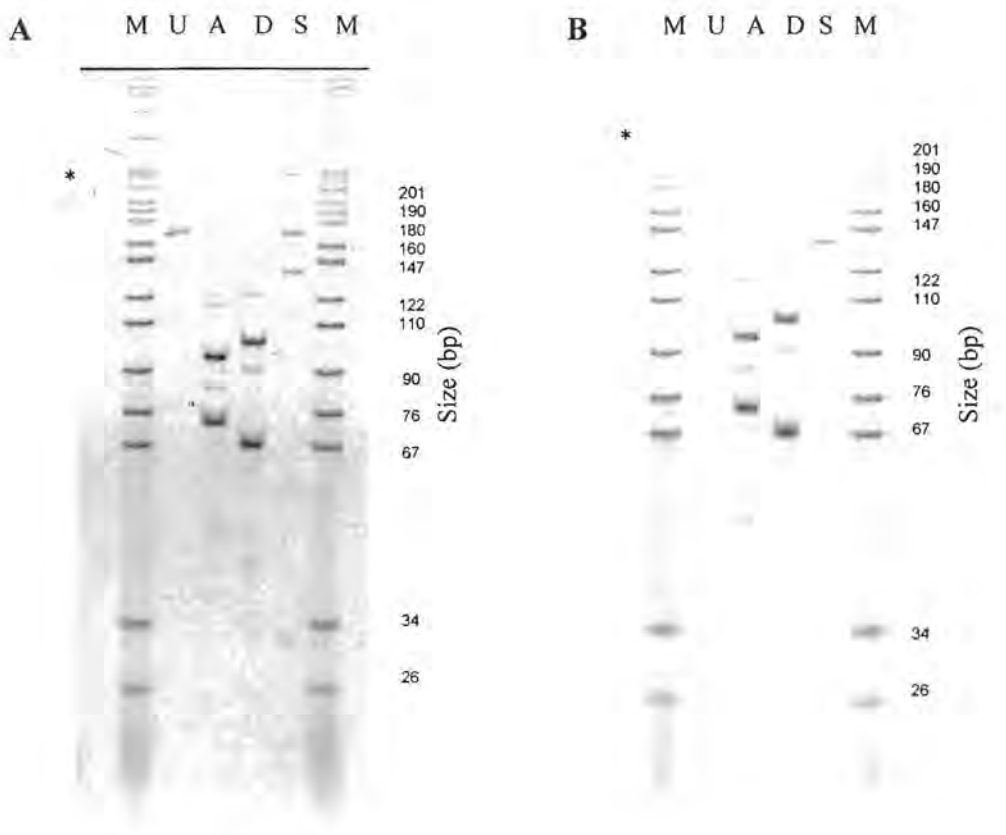

Figure 3.8. Determination of chromatosome positioning on the 208 bp 5S rDNA template. Eight percent polyacrylamide electrophoresis of restriction enzyme cleavage products of chromatosome DNA isolated after MNase digestion of chromatosomes containing either uH2A (**A**) or H2A (**B**). Lane M contains pBR322/ *Hpa* II size markers. Lane U contains undigested chromatosome 167 bp DNA. Lanes A, D and S contain DNA fragments produced by digestion of chromatosome DNA with *Ava* I, *Dra* I and *Sau3A* I respectively. *A 232 bp fragment from plasmid pGBT9 lacking *Ava* I, *Dra* I and *Sau3A* I restriction sites was included as an internal control.

Again the results were essentially identical for control and uH2A hybrid nucleosomes (Table 3.3). In the presence of histone H1, a dominant position (-4 to 163) was observed that is occupied by ~ 80 % of chromatosomes. This can be envisaged to correspond to a 10 bp protection of the DNA on either side of position A or a 20 bp protection downstream of position B (Table 3.2). This position and the shift from several translationally related positions, is in close agreement with a major position of chromatosomes on an 18-mer array of 208 template DNA (Meersseman *et al.*, 1991).

Table 3.3. Control and uH2A chromatosome positions on 208 bp 5S rDNA template.

DNA restriction fragments from Figure 3.8 were sized and paired to add up 167 bp. Positions were determined by comparison of fragment lengths to the position of the restriction sites (Fig. 3.1).

Alu I					
Left Boundary	**Band size (bp)**	**Right Boundary**	**Band size (bp)**	**Position**	**Relative % of total ***
-4	73	163	94	A'	85
1	68	155	86	B'$^{\phi}$	8
19	50	187	118	C'	6

Dra I					
Left Boundary	**Band size (bp)**	**Right Boundary**	**Band size (bp)**	**Position**	**Relative % of total ***
-4	67	165	102	A'	81
1	62	155	92	B'$^{\phi}$	11
19	44	186	123	C'	8

Sau3A I					
Left Boundary	**Band size (bp)**	**Right Boundary**	**Band size (bp)**	**Position**	**Relative % of total ***
				Uncut	44
-3	134	163	33	A'	55
16	115			C'	1

*Gels were scanned and the relative density of fragments was determined by integration. $^{\phi}$Position B' is probably the result of end trimming of position A' by MNase as slight quantities of contaminating 160 bp DNA are evident in the uncut lanes (U) of Fig. 3.8.

A 10 bp pattern of protection on either side of the nucleosome agrees with earlier data (Simpson, 1978; Allan *et al.*, 1980a; Staynov & Crane-Robinson, 1988; Pehrson, 1989). Under these conditions no evidence could be found for asymmetric protection of linker DNA as has been observed with *Xenopus* 5S rDNA (Hayes & Wolffe, 1993; Hayes *et al.*, 1994; Ura *et al.*, 1995). Interestingly this chromatosome position in *Xenopus* has recently been found to be susceptible to sequence specific artifacts and another major chromatosome position that involves protection of 20 bp on one side of the nucleosome has also been reported (Wong *et al.*, 1997; An *et al.*, 1998; Sera & Wolffe, 1998). If this type of protection were the case here, it implies that the incorporation of histone H1 has led to a shift in the equilibrium position of nucleosomes from position A to position B. Alternatively, since nucleosomes are more mobile in the absence of linker histones (Pennings *et al.*, 1994), it is possible that digestion with MNase could induce short range sliding of nucleosomes.

Since positions A and B are ~10 bp apart, the rotational setting of the DNA relative to the histone octamer would be unchanged.

A summary of nucleosome and chromatosome positions is shown in Fig. 3.9. uH2A hybrid nucleosomes occupy the same positions as control nucleosomes on a *Lytechinus* 5S rDNA 208 bp template in the presence and absence of histone H1. This further confirms that uH2A has little influence on the nucleosome structure (Kleinschmidt & Martinson, 1981; Davies & Lindsey, 1994) and that its effect, if any, is likely to influence higher order structure.

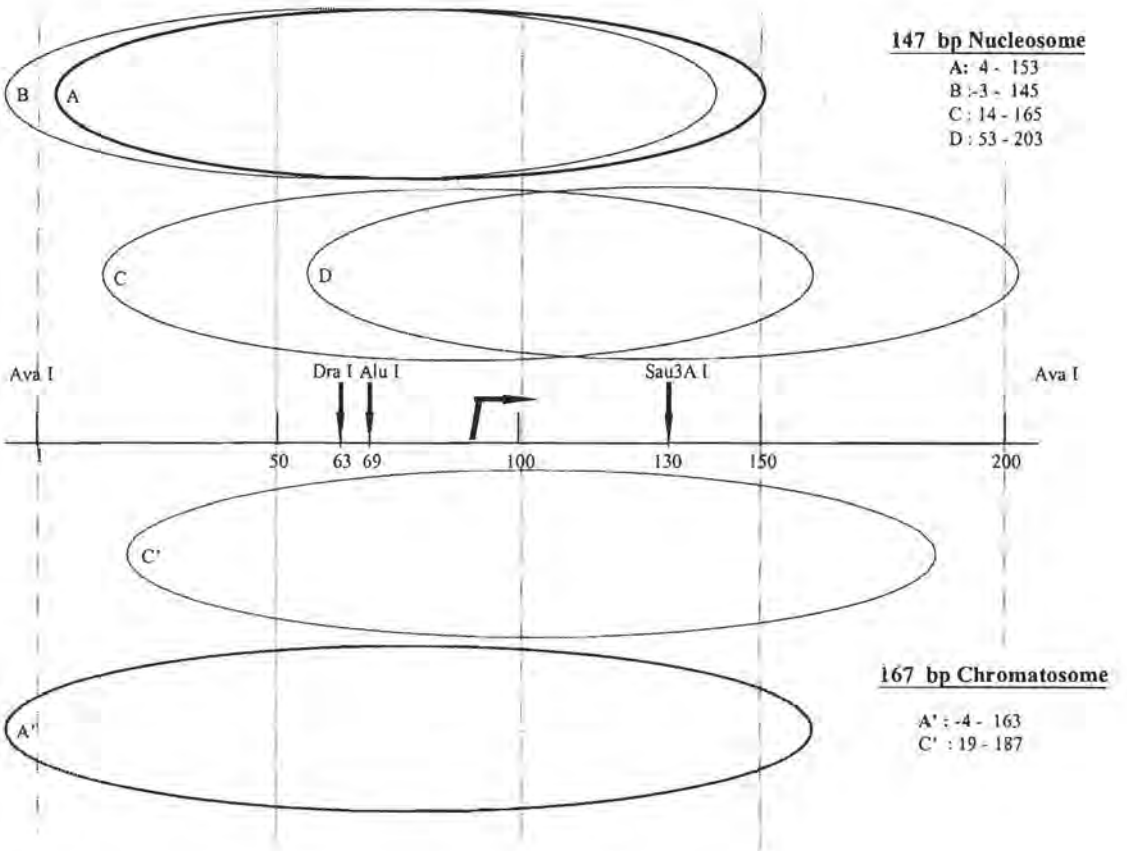

Figure 3.9. Summary of control and uH2A hybrid nucleosome and chromatosome positions on the 208 bp *Lytechinus* 5S rDNA fragment. Dominant positions are shown in bold.

From the results discussed above, it appears that under the conditions used here, the presence of two uH2A molecules in nucleosomes does not preclude linker histone binding, rather it appears to facilitate its association. These results are in agreement with cross-linking studies that determined that the proximity of H1 to H2A was unchanged by ubiquitination (Bonner & Stedman, 1979). The interaction between HMG 14 and 17 is also not inhibited by nucleosomal uH2A (Kleinschmidt & Martinson, 1981). The COOH terminal tail of H2A is known to contact the DNA at the ends of 167 bp nucleosome cores (Davies & Lindsey, 1991; Usachenko *et al.*, 1994) and it undergoes some displacement upon linker histone binding (Lee & Hayes, 1998; Guschin *et al.*, 1998). Since the site of ubiquitination of H2A (lys 119) is in the COOH terminal tail, it is possible that this modification leads to subtle repositioning of this domain so as to facilitate linker histone contacts with the linker DNA.

The situation *in vivo* may, however, be different since the ionic environment is different and higher order chromatin structures might influence the position of nucleosomes. As a first step towards understanding the effect of ubiquitinated H2A on higher order chromatin structures, the folding of nucleosomal arrays containing nucleosomal uH2A was investigated in the absence of linker histones (section 4).

4 Chromatin folding in the presence of ubiquitinated H2A

4.1 Introduction

Chromatin folding has been assayed by a variety of techniques including neutron, X-ray and light scattering, analytical centrifugation, electron microscopy and circular dichroism spectroscopy. Under very low non-physiological ionic conditions (0.2 mM EDTA, 1 mM triethanolamine chloride), nucleosomal arrays lacking linker histones were shown to form fibres resembling "beads on a string" while arrays containing linker histones displayed a zig-zag structure. Early electron microscopic studies indicated that at higher salt concentrations (0.2 mM EDTA, 5 mM triethanolamine chloride), native chromatin fibres form a flat ribbon approximately 25 nm wide with the nucleosomes in a more compact zig-zag structure (see van Holde, 1989 for a review). More recent observations obtained from scanning and cryoelectron microscope studies indicate that at 10 mM salt, chromatin fibres exist as irregular, helical, three dimensional structures (Leuba *et al.*, 1994; Bednar *et al.*, 1995). At higher salt concentrations which approach physiological ionic strength, irregular rod-like structures with a diameter of 30 nm are formed (see van Holde, 1989 and Wolffe, 1995 for reviews). The structure of condensed chromatin in 30 nm fibres has been a subject of controversy for over 20 years and is still hotly debated. Models for this structure range from a solenoidal arrangement of nucleosomes, originally proposed by Finch and Klug (1976), to a superbead structure (Franke *et al.*, 1976; Kiryanov *et al.*, 1976). Other models include a condensed zig-zag structure (Woodcock *et al.*, 1984) and models involving linker DNA traversing the fiber diameter (Staynov, 1983; Williams *et al.*, 1986). Each model and its subsequent variations have flaws in that their requirements do not always correlate with experimental data (van Holde, 1989). Whilst most modeling studies focussed on a regular arrangement of nucleosomes in folded chromatin fibres, others (e.g. Subirana *et al.*, 1985) proposed an irregular folding model. In nuclei, chromatin fibres are now generally believed to be irregular and models implicating a continuously regular structure do not account for observed structural variations (van Holde & Zlatanova, 1995). A recent review examines the proposed models for the 30 nm fibre (Ramakrishnan, 1997).

Folding of chromatin into 30 nm fibres represents not only a degree of DNA packaging but also an important level at which DNA accessibility can be influenced. This is of particular significance in the regulation of cellular process such as DNA replication and transcription where numerous protein factors must gain access to their cognate DNA sequences. It is believed that some post-translational histone modifications play a role in modulating chromatin structure. Histone acetylation has caused much excitement in this respect as some transcriptional activators possess histone acetyl transferase activity and some transcriptional repressors are histone deacetylases. The targeting of these activities to specific promoter regions correlates well with older observations that suggested that histone acetylation plays an important role in transcriptional regulation (see Davie, 1998; Razin, 1998; Struhl, 1998 & Wolffe, 1998 for reviews). Core histone acetylation was shown to reduce the number of negative DNA supercoils associated with a nucleosome core particle (Norton *et al.*, 1989). This observation has led to the proposal that the effects of core histone acetylation result from partial unraveling of DNA supercoils where the DNA enters and exits the nucleosome (Norton *et al.*, 1989; Garcia-Ramirez *et al.*, 1995). The ability of nucleosomal arrays to fold into higher order structures, in response to increasing concentrations of both monovalent (Garcia-Ramirez *et al.*, 1995) and divalent (Tse *et al.*, 1998) cations, has been shown to be disrupted by high levels of core histone acetylation. Interestingly, acetylated histone amino terminal tails maintain contacts with nucleosomal DNA, although these interactions are weakened at physiological ionic strengths (Mutskov *et al.*, 1998).

The effect of H2A ubiquitination on chromatin folding is, as for all its other proposed roles, unclear and subject to contradiction. Since ubiquitination is a comparatively bulky post-translational modification, many researchers have proposed that its function lies in hindering chromatin folding (e.g. Levinger & Varshavsky, 1982; Davie & Nickel, 1987). The experimental evidence does not, however, unanimously support this proposal. There have been several reports associating histone de-ubiquitination with chromatin condensation. The ubiquitin moiety of uH2A was reported to be released at mitosis in a Chinese hamster cell line (Matsui *et al.*, 1979). Similarly, it has been shown that the ubiquitin moiety of uH2A and uH2B is removed at a late stage in metaphase but is present at anaphase and early prophase in *Physarum*

polycephalum macroplasmodia (Mueller *et al.*, 1985). In *Physarum*, ubiquitination occurs in 7 % of H2A and 6 % of H2B in the growth plasmodial phase. The authors suggested that nucleosomal uH2A and uH2B serve to tag specific regions of the genome that are required by the cell to be available for activation. These regions are proposed to be the first to be decondensed after metaphase and ubiquitinated, but have to be de-ubiquitinated prior to packaging into metaphase chromosomes. The nucleosomal uH2A content decreases during chicken erythropoiesis (Goldknopf *et al.*, 1980) but, this situation is reversed during bullfrog erythrocyte maturation (Shimada *et al.*, 1981). Furthermore, in *Drosophila*, ubiquitin has been shown to be associated mainly with the compact structural domains of polytene chromosomes that form bands (Izquierdo, 1994). Thus not all compact chromatin structures are devoid of ubiquitinated histones. The cell cycle associated changes in the levels of ubiquitinated histones are unlikely to be the result of increased degradation since two independent studies have shown that mono-ubiquitination of histones does not tag them for *in vivo* degradation by the ubiquitin-26 S proteasome pathway (Wu *et al.*, 1981; Seale, 1981).

Histone ubiquitination could either hinder chromatin folding directly or modify the chromatin structure via differential interaction with accessory non-histone proteins or chromatin remodeling machinery. It is also not clear if the de-ubiquitination associated with nuclear processes that involve chromatin folding is a pre-requisite or a consequence of folding. Much of the evidence on the role of uH2A is indirect and in order to clarify the situation, a defined *in vitro* system has been used in this study to characterise chromatin folding in the presence of uH2A. Nucleosomal arrays lacking linker histones have been shown to fold moderately in physiological concentrations of monovalent salts but do not compact to form 30 nm fibers under these conditions (e.g. Hansen *et al.*, 1989; Garcia-Ramirez *et al.*, 1992). This folding is inhibited if H2A-H2B dimers are absent (Hansen & Wolffe, 1994) or if the histone tails, especially those of H3 and H4, are removed (Garcia-Ramirez *et al.*, 1992; Moore & Ausió, 1997). In contrast, nucleosomal arrays equilibrate between moderately folded and extensively folded structures in the presence of 2 mM $MgCl_2$ in the absence of linker histones (Schwarz & Hansen, 1994). Maximal folding of nucleosomal arrays in $MgCl_2$ is highly dependent on template saturation (Fletcher *et al.*, 1994b) and the presence of histone tails (Fletcher & Hansen, 1995; Moore & Ausió, 1997). In a separate process, nucleosomal arrays can form oligomers in the presence of Mg^{2+}.

This process is thought to be of biological relevance as it may form part of the interactions between chromatin segments that eventually lead to the formation of highly condensed metaphase chromosomes. Oligomerisation of reconstituted nucleosomal arrays has been extensively characterised (Schwarz *et al.*, 1996). The degree of saturation of nucleosomal arrays influences both the maximal proportion of arrays that will oligomerise and the concentration of Mg^{2+} at which 50 % oligomerisation is achieved. Oligomerisation of nucleosomal arrays can still occur even if these arrays are incapable of folding. Additionally, the histone tail domains, especially those of H3 and H4, are an absolute requirement for oligomerisation (Schwarz *et al.*, 1996; Tse & Hansen, 1997; Moore & Ausió, 1997). The effect of H2A ubiquitination on oligomerisation of nucleosomal arrays was therefore investigated.

A relatively new technique, analytical agarose gel electrophoresis, has helped elucidate some of the mechanisms involved in chromatin folding in the presence of $MgCl_2$ (Fletcher *et al.*, 1994b; Carruthers *et al.*, 1998) and core histone acetylation (Tse *et al.*, 1998). This technique was used to study the effect of histone H2A ubiquitination on chromatin folding in the absence of linker histones. For quantitative agarose gel electrophoresis, chromatin fragments of defined DNA sequence, length and nucleosome content are electrophoresed in several gels of varying agarose concentration in the same agarose frame (a multigel). The technique has been extensively described (Hansen *et al.*, 1997). Briefly, multigels of overlapping agarose percentages are used to cover the range from 0.2 to 3.0 % (w/v) agarose. The use of multigels diminishes the effects of temperature and current variation that are inevitable if multiple individual concentration agarose gels are used. The resultant migration distances of nucleosomal arrays or other particles of interest are used to generate Ferguson plots. Extrapolation of the linear region of the Ferguson plot (typically 0.3 to 1 % agarose) to zero percent agarose by linear regression, and conversion to mobility, gives μ'_o, the gel free mobility. The spherical bacteriophage T3, which has a radius of 30.1 nm, is used as an internal standard. The electro-osmotic contribution of the agarose in running buffer, μ_E, is determined by subtracting the $\mu'_o{}^{T3}$ in Seakem Gold agarose from $\mu'_o{}^{T3}$ in Sigma agarose. This determination is

based on the assumption that $\mu'_o{}^{T3}$ in Seakem Gold agarose is equal to $\mu_o{}^{T3}$ since Seakem Gold agarose has extremely low electro-osmosis (Fletcher *et al.*, 1994a,b).

The mobility of the particle to be measured, $\mu_o{}^x$, is determined by the use of equation (1) (Fletcher *et al.*, 1994a,b) using empirically determined values.

$$\mu_o{}^x = [(\mu'_o{}^x)(\mu_o{}^{T3} + \mu_E) / \mu'_o{}^{T3}] - \mu_E \qquad (1)$$

The relationship between μ obtained by electrophoresis in agarose gels and the effective radius of a spherical particle is described by equation (2):

$$\mu / \mu'_o = (1 - R / Pe)^2 \qquad (2)$$

Pe, the effective pore size of each gel is determined using equation (3):

$$Pe = 30.1 / [1 - (\mu^{T3} - \mu_o{}^{T3})^{1/2}] \qquad (3)$$

The effective radius of the particle of interest, Re^x, is determined at each pore size using equation (4):

$$Re^x = Pe \times [1 - (\mu^x - \mu_o{}^x)^{1/2}] \qquad (4)$$

These relationships were originally determined for rigid spherical particles (Griess *et al.*, 1989) but have been applied successfully to nucleosomal arrays (Fletcher *et al.*, 1994a,b; Tse *et al.*, 1998; Carruthers *et al.*, 1998). Nucleosomal arrays are believed to migrate through the agarose pores as rod-like objects. The Re values obtained can be used to determine the area of a sphere that would have the same surface area as the rod shaped particle (Griess *et al.*, 1990). This model has shown good correlation with expected values (Fletcher *et al.*, 1994b).

4.2 Results and Discussion

4.2.1 Reconstitution of saturated nucleosomal arrays

Nucleosomal arrays must be saturated with nucleosomes to ensure that they fold maximally in response to $MgCl_2$. The extent of folding decreases significantly as the number of nucleosomes per array decreases (Fletcher *et al.*, 1994b). The DNA template used (208-12) contains 12 tandem repeats of a segment from the *Lytechinus variegatus* 5S rRNA gene (Simpson *et al.*, 1985). Arrays are considered to be saturated when 12 nucleosomes are reconstituted since each repeat contains a 208 bp nucleosome positioning sequence.

To determine nucleosome loading, trial reconstitutions were performed with a fixed amount of DNA template and increasing molar ratios of octamers. Reconstitutes were digested with *Ava* I which has been shown to flank the principal nucleosome positioning site on this template (Dong *et al.*, 1990; Meersseman *et al.*, 1991). The digestion products were analysed on 0.7 % (w/v) agarose nucleoprotein gels in 0.5 × TBE (Fig. 4.1). This method has been used previously to quantitate nucleosomal loading and correlates well with the data obtained from analytical centrifugation (Hansen *et al.*, 1989; Tse & Hansen, 1997; Tse *et al.*, 1998). If a nucleosome occupies a 208 repeat in a position that does not prevent *Ava* I digestion, it should be represented as a mononucleosome on a nucleoprotein gel. Subsaturated arrays give rise to the additional formation of 208 bp DNA monomers from the nucleosome free regions of the array. Nucleosomes are not uniquely positioned on 208-12 DNA and some minor positions block the restriction site and result in the formation of oligomers of slower migration (Meersseman *et al.*, 1991). From Fig. 4.1 it can be seen that as the octamer: DNA ratio was increased the amount of free 208 bp DNA decreased and the intensity of the mononucleosome band increased. Saturated arrays were obtained using an octamer: DNA ratio of 1.3 (Fig. 4.1 lane 4) as evidenced by the absence of 208 bp DNA. Digestion of subsaturated arrays gave rise to the appearance of mononucleosomes and 208 bp monomeric DNA, indicating that digestion of the arrays was complete under these conditions. Moreover, the digestion

conditions used resulted in the complete digestion of an equivalent amount of free 208-12 DNA template (Fig. 4.1 lane 1). Supersaturated arrays (Fig. 4.1 lanes 5 and 6) were not digested by *Ava I* as nucleosomes are likely to be close-packed and therefore block *Ava I* digestion sites. Supersaturated arrays are smeared in nucleoprotein gels, indicative of aggregation (not shown).

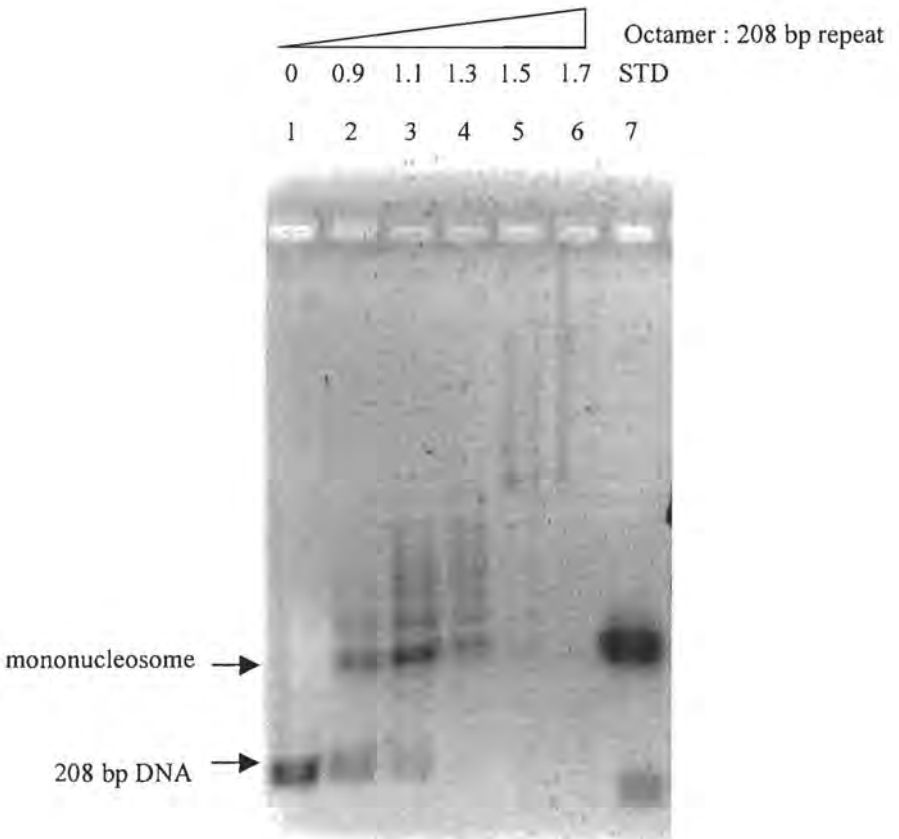

Figure 4.1. Quantitation of the number of nucleosome cores reconstituted onto 208-12 template DNA. 0.7 % (w/v) agarose nucleoprotein gel in 0.5 × TBE of *Ava I* digestion products of trial reconstitutions of control octamers onto 208-12 template DNA. The molar ratios of octamers to 208 bp DNA repeat were: lane 1 (0:1), lane 2 (0.9:1), lane 3 (1.1:1), lane 4 (1.3:1), lane 5 (1.5:1), lane 6 (1.7:1). 167 bp nucleosome cores were included as a standard in lane 7.

The nucleoprotein gel shown in Fig. 4.1 was scanned and the proportion of nucleosomes to free DNA determined by integration of the appropriate bands. The values obtained for nucleosomes were multiplied by 2.5 to compensate for the ethidium bromide quenching caused by octamer binding (McMurray & van Holde, 1986).

Table 4.1: Distribution of *Ava I* digestion products of reconstituted 208-12 nucleosomal arrays. Distribution was determined by integration analysis of *Ava I* digestion products of 208-12 DNA templates reconstituted with octamers at the specified octamer to 208 bp DNA repeat ratios as shown in Fig. 4.1. Gel negatives were scanned and analysed using ImageQuant software.

	Molar ratio of octamers: 208 bp DNA repeat		
Percentage of sample in	0.9 : 1	1.1 : 1	1.3 : 1
Oligomers	32	53	67
Mononucleosomes	42	38	32
208 bp DNA	26	9	1

In order to generate saturated arrays an input ratio of 1.2 octamers per DNA repeat was used. However, as seen in Fig. 4.1, it is very difficult to achieve 100 % saturation without generating supersaturated arrays. In previous studies, arrays were defined as saturated when 50 to 70 % of the templates contained 12 nucleosomes and the remainder contained 10 to 11 nucleosomes (Schwarz & Hansen, 1994; Tse & Hansen, 1997).

To analyse the effects of histone H2A ubiquitination on chromatin folding, it is important to ensure that the uH2A nucleosomal arrays are saturated to the same degree as the control nucleosomal arrays. Hybrid octamers containing uH2A were reconstituted onto the 208-12 DNA template at the same molar ratio used to achieve saturation of control nucleosomal arrays. The nucleoprotein gel of the *Ava I* digestion products is shown in Fig. 4.2. The quantitation of densitometric scans of control and uH2A hybrid reconstitutions indicated that the ratio of mononucleosomes to total reconstituted species were 45 % and 42 % respectively. These values indicated that

the reconstitution of the template DNA with identical molar ratios of control and uH2A hybrid octamers resulted in comparable levels of nucleosome core loading.

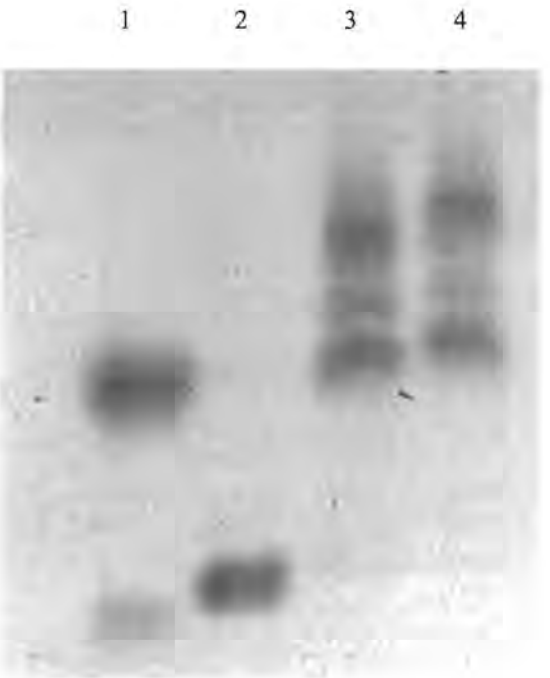

Figure 4.2. Comparison of saturated control and uH2A 208-12 nucleosomal arrays. Nucleoprotein gel of control (lane 3) and uH2A hybrid (lane 4) nucleosomal arrays following *Ava I* digestion. Lane 1: 167 bp nucleosome cores isolated from chicken erythrocyte chromatin stripped of linker histones; lane 2: 208 bp DNA produced by *Ava I* digestion of naked 208-12 template DNA.

uH2A nucleosomes display reduced migration on nucleoprotein gels when compared to control nucleosomes in accordance with the results obtained for random sequence 167 bp cores (see section 2) and previous observations (Levinger & Varshavsky, 1982). Integration analysis of nucleoprotein gels (e.g. Fig. 4.2) indicated that approximately 55 % and 58 % of the *Ava I* digestion products of control and uH2A hybrid nucleosomal arrays respectively were in the form of oligonucleosomes. A previous analysis of *Ava I* and *Eco* RI digestion products of saturated 208-12 nucleosomal arrays yielded approximately 50 % of the digested material in the form of nucleosome dimers, trimers and tetramers (Hansen *et al.*, 1989).
Micrococcal nuclease digestion of saturated control and uH2A nucleosomal arrays gave rise to the production of a well defined ladder at intermediate stages of digestion

(not shown). There was no significant difference in the rate of digestion of the two arrays and extensive digestion produced mononucleosomes in both cases.
The protein content of aliquots of saturated control and uH2A nucleosomal arrays was analysed by silver staining after SDS-PAGE (Fig. 4.3). These results indicated that the histones were not degraded during reconstitution, and that no H2A was present in uH2A nucleosomal arrays.

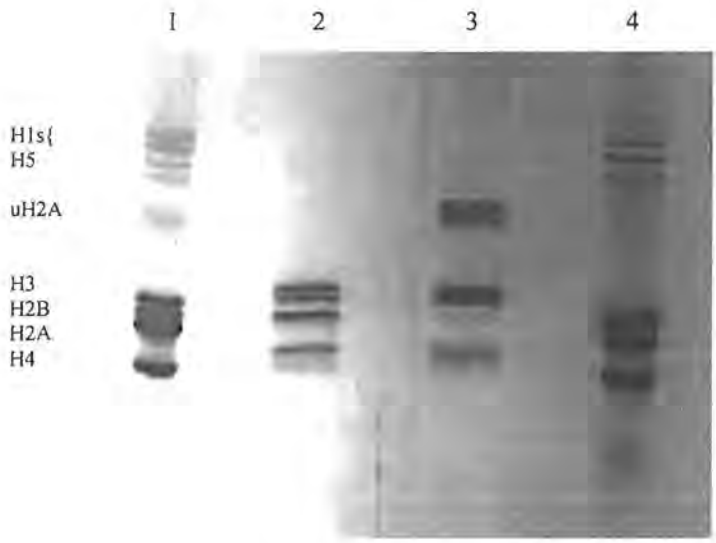

Figure 4.3. SDS-PAGE analysis of the histone content of saturated control and uH2A nucleosomal arrays. Lane 1: total acid extract calf thymus histones; lane 2: control nucleosomal arrays; lane 3: uH2A nucleosomal arrays; lane 4: total acid extract chicken erythrocyte histones.

4.2.2 Quantitative agarose gel electrophoresis

4.2.2.1 Determination of μ_E, the electro-osmotic contribution of the agarose matrix

Bacteriophage T3 was electrophoresed in multigels with running gels cast in either Sigma agarose or Seakem Gold agarose in E buffer (40 mM Tris-HCl (pH 7.8) and 0.25 mM EDTA) and E buffer containing $MgCl_2$ at a final concentration of 2 mM (E + Mg). Agarose concentrations ranged from 0.2 to 3.0 % (w/v) agarose.
The integrity of purified bacteriophage T3 was confirmed by electron microscopy (Fig. 4.4). The phages, including the small tail, were intact in all fields examined.

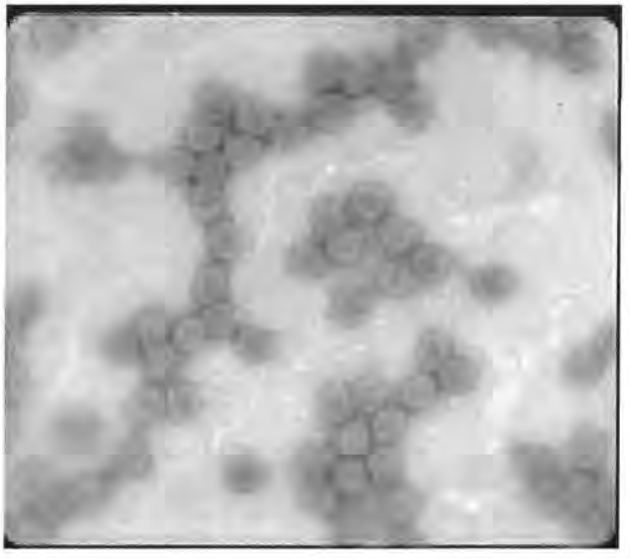

Figure 4.4. Electron microscopy of purified bacteriophage T3. The magnification was 80 000 times.

The data from the multigels were represented as Ferguson plots of which representative gels and plots are shown in Figs. 4.5 and 4.6. As expected for a spherical particle, the plots were convex as described previously (Fletcher *et al.*, 1994a,b). The gel free migrations were determined by linear regressions of the linear region of the Ferguson plots and converted to mobilities (Table 4.2). R^2 values ranged from 0.975 to 0.994. μ_o^{T3} and $\mu'_o{}^{T3}$ represent the gel free mobility of bacteriophage T3 in Seakem Gold agarose and Sigma agarose respectively. These values were used to calculate μ_E, the electro-osmotic contribution of Sigma agarose (Table 4.2).

Table 4.2: Determination of the μ of electro-osmotically driven buffer in Sigma agarose in the presence or absence of Mg^{2+}.

Buffer	μ_o^{T3} ($cm^2.V^{-1}.s^{-1}$)	$\mu'_o{}^{T3}$ ($cm^2.V^{-1}.s^{-1}$)	μ_E ($cm^2.V^{-1}.s^{-1}$)
E	-8.9×10^{-5}	-6.16×10^{-5}	2.68×10^{-5}
E + Mg	-6.25×10^{-5}	-4.34×10^{-5}	1.91×10^{-5}

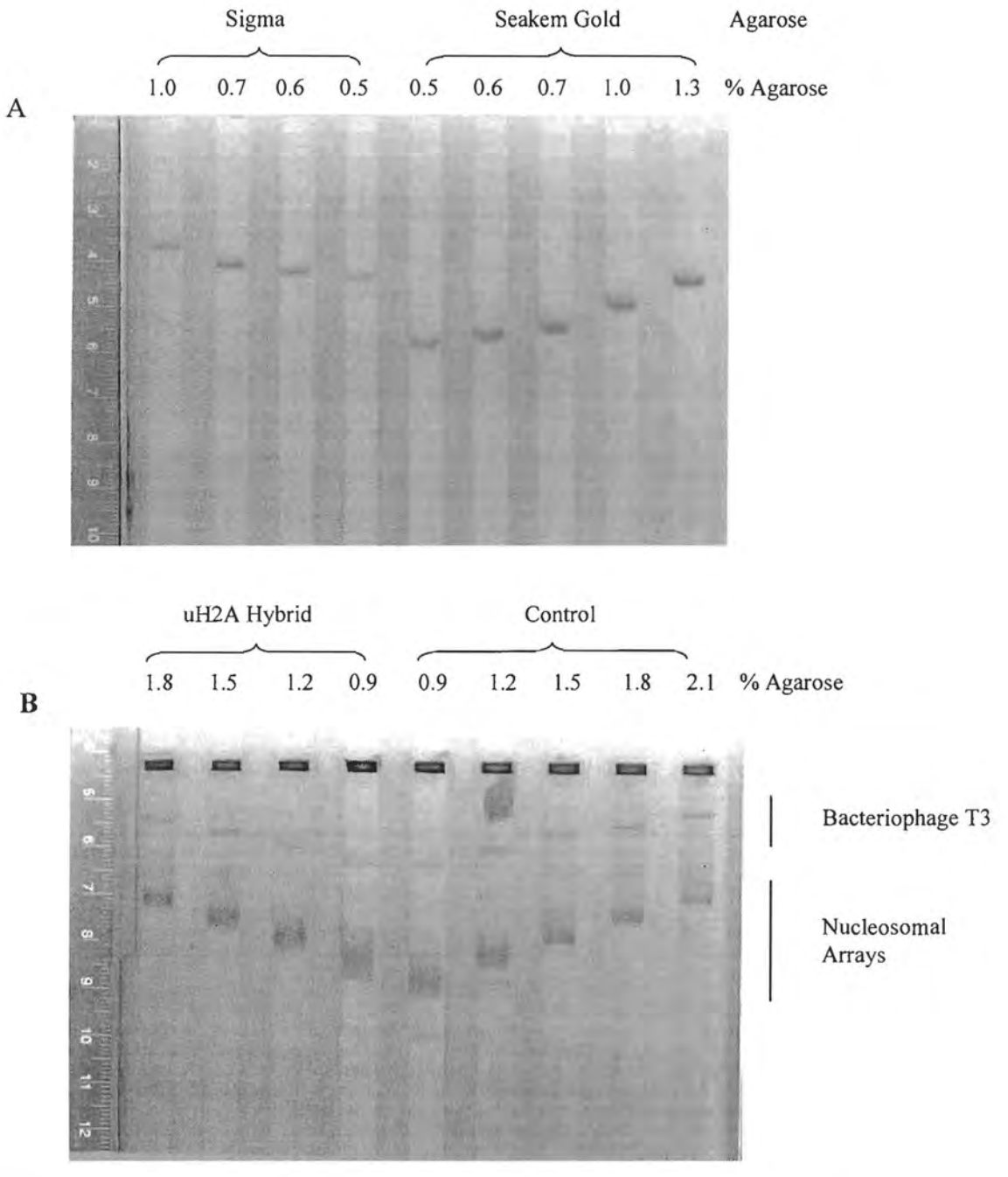

Figure 4.5. Representative multigels used to generate Ferguson plots. (A) Electrophoresis of bacteriophage T3 in the specified percentages of either Sigma or Seakem Gold agarose (see section 8). Data from this and other multigels were used to calculate μ_E. **(B)** Electrophoresis of saturated uH2A hybrid and control 208-12 nucleosomal arrays. Bacteriophage T3 was used as an internal standard. Electrophoresis was performed in E buffer containing 2 mM $MgCl_2$. Gels were stained with ethidium bromide. The wells in (B) were stained with a DNA-ethidium bromide solution after electrophoresis to facillitate migration distance measurements.

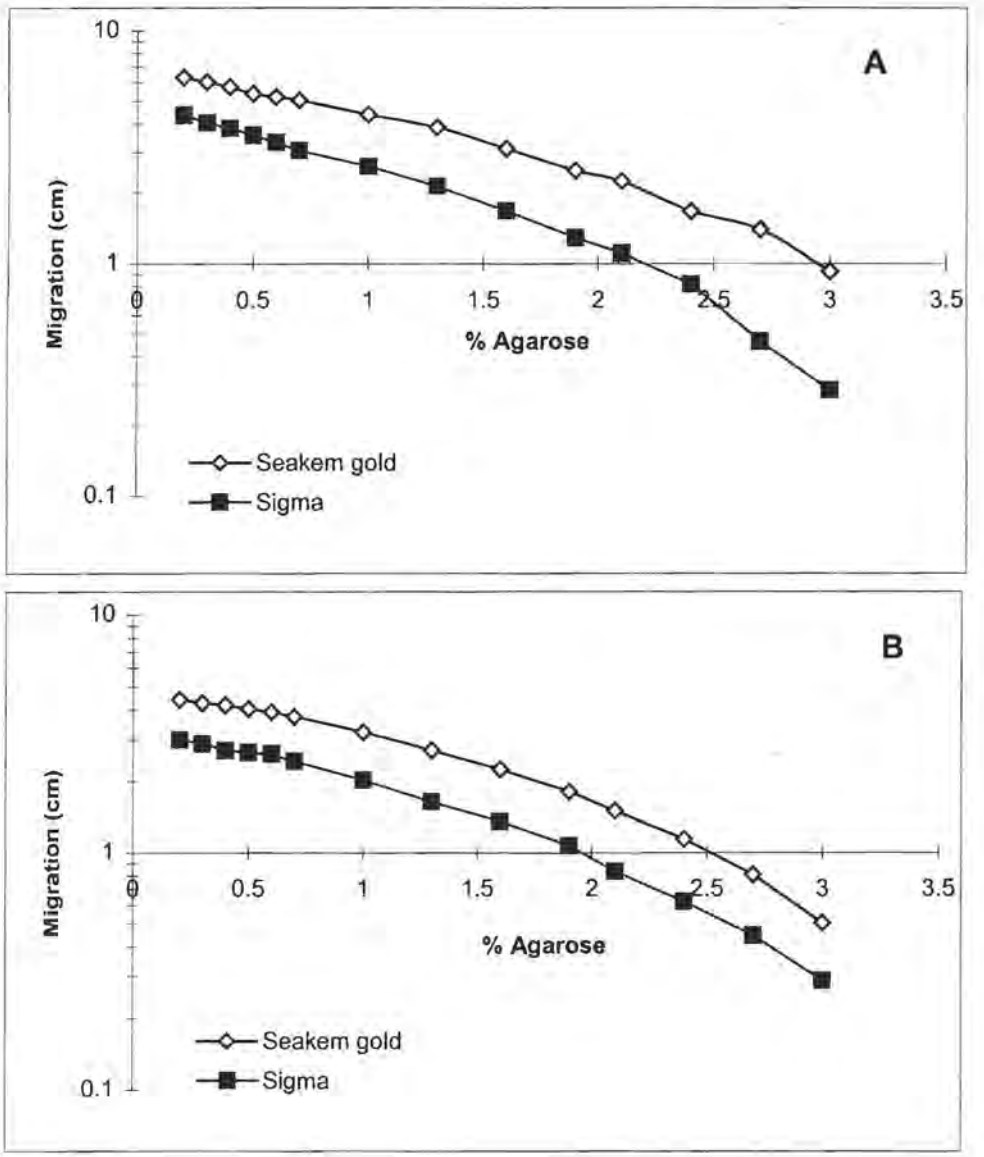

Figure 4.6. Ferguson plots of bacteriophage T3 in Sigma and Seakem Gold agarose. Plots were generated from data obtained from multigels of overlapping agarose concentrations. Electrophoresis was performed in **(A)** E buffer alone and **(B)** in E buffer containing 2 mM $MgCl_2$.

4.2.2.2 Determination of gel-free mobility (μ_o) in E buffer

Template DNA and reconstituted nucleosomal arrays were electrophoresed in agarose multigels ranging in concentration from 0.2 to 3.0 % (w/v). The Ferguson plot of 208-12 DNA (Fig. 4.7) was linear and that of saturated control nucleosomal arrays (Fig.4.8) was convex, as previously observed (Fletcher *et al.*, 1994a,b).

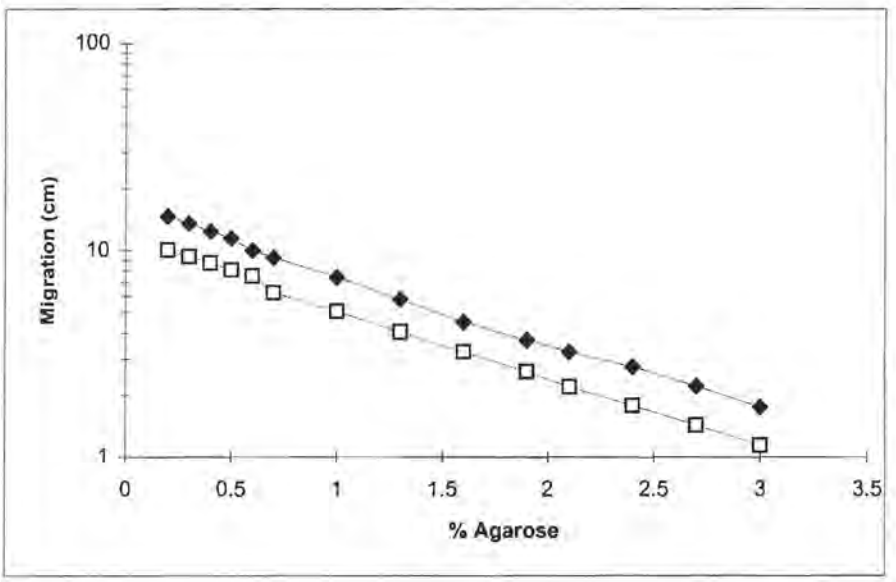

Figure 4.7. Ferguson plots of 208-12 DNA template in E buffer (♦) and E buffer containing 2 mM $MgCl_2$ (□).

The μ_o of naked 208-12 DNA in E buffer was determined to be -2.44 ± 0.03 $\times 10^{-4}$ $cm^2.V^{-1}.s^{-1}$. This value is in good agreement with previously reported values for this DNA of –2.42 ± 0.02 $\times 10^{-4}$ $cm^2.V^{-1}.s^{-1}$ and -2.45 ± 0.04 $\times 10^{-4}$ $cm^2.V^{-1}.s^{-1}$. (Fletcher *et al.*, 1994a,b).

The Ferguson plot of saturated uH2A hybrid nucleosomal arrays in E buffer (Fig.4.8) was also convex but consistently displayed slower migration than that of control nucleosomal arrays. The slower migration of the uH2A hybrid nucleosomal arrays appears to be due to differences in μ_o since Fig. 4.10 indicates that the shape of control and uH2A hybrid nucleosomal arrays must be very similar.

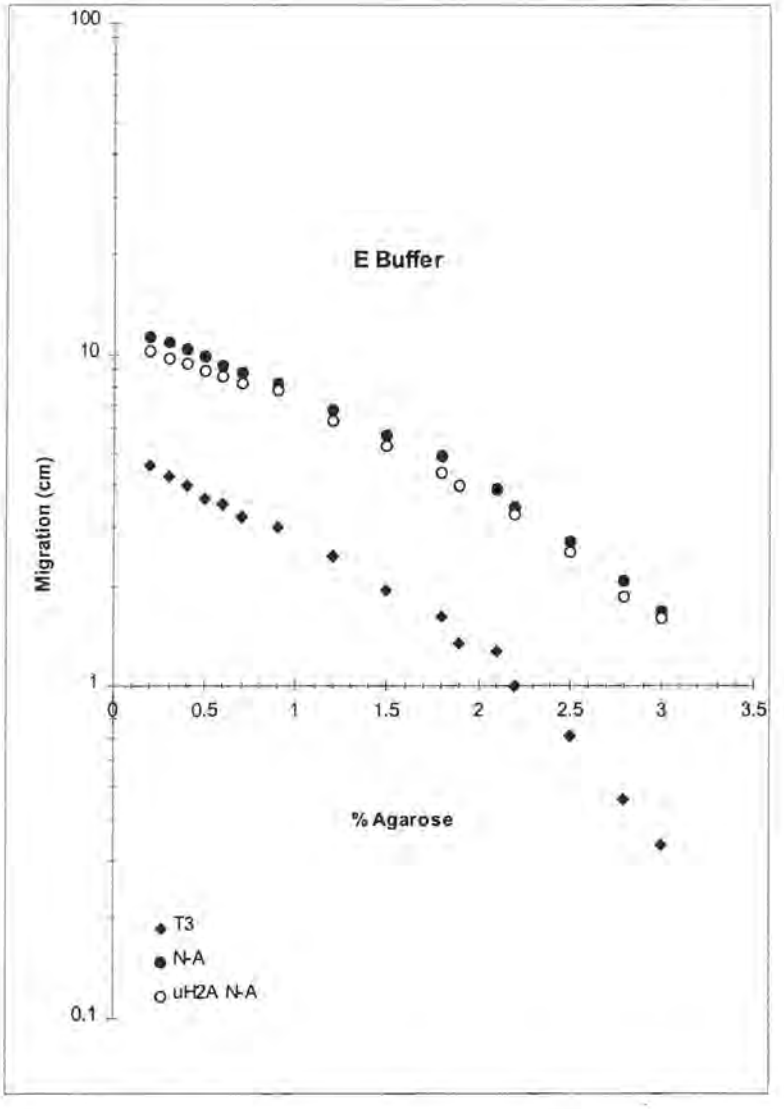

Figure 4.8. Ferguson plots of bacteriophage T3, saturated control and uH2A hybrid nucleosomal arrays (N-A) in E buffer.

The value of μ_o for saturated control nucleosomal arrays containing mock-reconstituted octamers was calculated to be $-1.88 \pm 0.04 \times 10^{-4}$ $cm^2.V^{-1}.s^{-1}$. Previously reported μ_o values of saturated nucleosomal arrays reconstituted on the same DNA template range from $-1.92 \pm 0.02 \times 10^{-4}$ $cm^2.V^{-1}.s^{-1}$ DNA (Fletcher *et al.*, 1994a,b; Tse *et al.*, 1998) to $-1.82 \pm 0.04 \times 10^{-4}$ $cm^2.V^{-1}.s^{-1}$ (Carruthers *et al.*, 1998). The value of μ_o obtained in this study is further confirmation that the control nucleosomal arrays were saturated. The μ_o of uH2A hybrid nucleosomal arrays was found to be $-1.69 \pm 0.02 \times 10^{-4}$ $cm^2.V^{-1}.s^{-1}$. The presence of uH2A therefore results in a 10 % decrease in the magnitude of μ_o.

The μ_o is a measure of the average electrical surface charge density of a macromolecule (Hansen *et al.*, 1997). This reduction in μ_o corresponds to either an increase of 25 to 30 positive charges per octamer (Fletcher *et al.*, 1994 a,b) or to the shielding of an equivalent number of negative charges per octamer or a combination of both effects. The secondary structure of ubiquitin, which contains 11 acidic and 11 basic residues at pH 7.0, indicated that ubiquitin has a hydrophobic, a basic and an acidic face (Rechsteiner, 1988). Even if all the basic amino acids were exposed to the solvent, 2 molecules of ubiquitin could only contribute 22 positive charges per uH2A hybrid octamer. The crystal structure of ubiquitin revealed that not all the basic residues of ubiquitin are exposed. Only three of the seven lysine residues form no intra-molecular contacts, and are fully exposed on the surface of the molecule (Vijay-Kumar *et al.*, 1987). It is therefore likely that the decrease in μ_o is mediated by a combination of the mechanisms mentioned above.

4.2.2.3 Determination of μ_o in E buffer containing 2 mM $MgCl_2$

In the presence of Mg^{2+}, the mobility of the template DNA was decreased by approximately 30 % to -1.73 ± 0.04 $cm^2.V^{-1}.s^{-1}$ (Fig. 4.6). This reduction in mobility, due to charge neutralisation, is 5 % greater than reported previously (Fletcher *et al.*, 1994b). Saturated nucleosomal arrays can fold extensively in the presence of 2 mM $MgCl_2$ (Hansen & Wolffe, 1992; Fletcher *et al.*, 1994b). Under these conditions, an equilibrium exists between a moderately folded state and an extensively folded state that is analogous to a 30 nm fiber. This folding process is inherently dependent on the core histone amino terminal tails, especially those of histones H3 and H4. In 2 mM $MgCl_2$, the decrease in the μ_o of nucleosomal arrays is due in part to the neutralization of the charge of the phosphodiester backbone of the DNA by Mg^{2+}. The mobility of control nucleosomal arrays decreased by 45 % to $-1.052 \pm 0.02 \times 10^{-4}$ $cm^2.V^{-1}.s^{-1}$ in 2 mM $MgCl_2$ (Fig. 4.8). Since Mg^{2+} binding alone cannot account for the decrease in mobility (Fletcher *et al.*, 1994b), it has been proposed that accompanying structural changes relocate the core histone N-termini (Fletcher & Hansen, 1995).

The proposed release of core histone tails from binding sites on nucleosomal DNA would also be accompanied by an increase in Mg^{2+} uptake and hence a lower μ_o value (Fletcher & Hansen, 1995). The μ_o value of uH2A hybrid nucleosomal arrays in 2 mM $MgCl_2$ was calculated to be $-0.94 \pm 0.01 \times 10^{-4}$ $cm^2.V^{-1}.s^{-1}$. The μ_o value of these arrays was therefore 44 % lower in 2 mM $MgCl_2$ than in E buffer alone. This decrease was comparable to that observed for control arrays. The difference in the magnitude of μ_o between control and uH2A hybrid nucleosomal arrays was again approximately 10 %.

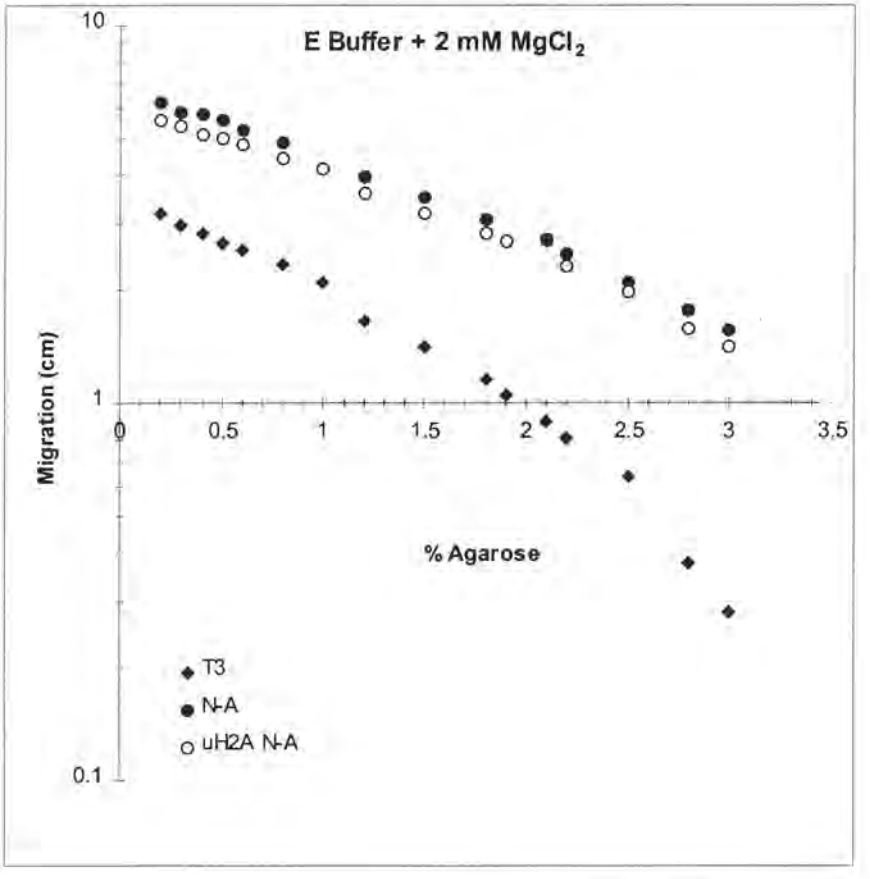

Figure 4.9. Ferguson plots of bacteriophage T3, saturated control and uH2A hybrid nucleosomal arrays (N-A) in E buffer containing 2mM $MgCl_2$.

These results suggest that under these experimental conditions, ubiquitination of histone H2A has a minimal effect on the folding of the nucleosomal arrays used.

4.2.2.4 Determination of Re values

The electrophoretic behaviour of macromolecules in varying agarose concentrations can yield information regarding their average shapes. The $(1\text{-}R / Pe)^2$ term of the equation $[\mu / \mu'_o = (1- R / Pe)^2]$ relates to the sieving of spherical molecules, of radius R, by the pores of the agarose gel (Griess *et al.*, 1989). For a spherical molecule, the value of the effective radius (Re) is equivalent to its macromolecular radius whilst for a rod shaped molecule the value of Re can be correlated to its surface area (Griess *et al.*, 1990; Fletcher *et al.*, 1994a,b). Flexible molecules such as DNA, which is expected to be in a random coil conformation in solution, have been shown to reptate during electrophoresis when the gel pore size approaches their effective radii (Fletcher *et al.*, 1994a and references cited therein). The 208-12 template DNA exhibited reptating behaviour in E buffer and E buffer containing 2 mM Mg^{2+} (Fig. 4.10 and Fig. 4.11).

The flexibility of a nucleosomal array is influenced by the extent of nucleosome free regions (Fletcher *et al.*, 1994a,b; Fletcher & Hansen, 1995). Subsaturated nucleosomal arrays do reptate at higher agarose concentrations as the nucleosome free regions impart flexibility to the array (Fletcher *et al.*, 1994a,b). Control experiments with subsaturated arrays (approximately 7 nucleosomes per array) displayed an increase in Re with increasing pore size in both E buffer and E buffer containing 2 mM $MgCl_2$ (not shown). Saturated trypsinised nucleosomal arrays have also been shown to reptate in E buffer (Fletcher & Hansen, 1995) and the authors attributed this increased flexibility to the increase in linker DNA resulting from the decreased DNA: histone contacts of the tailless octamers.

Saturated nucleosomal arrays do not reptate even in low salt conditions, but behave more like slightly flexible rod-like structures (Fletcher *et al.*, 1994a). Fig. 4.10 indicates that, in E buffer, the effective radii (Re) of both control and uH2A hybrid nucleosomal arrays remained essentially constant even at small pore size, further evidence that the arrays were saturated with nucleosome cores.

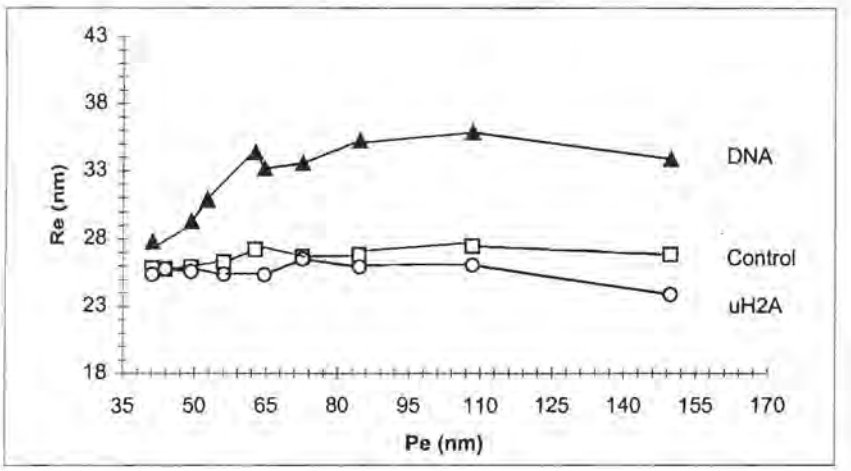

Figure 4.10.The pore size dependence of the Re of 208-12 template DNA and saturated control and uH2A nucleosomal arrays in E buffer. Results were obtained from multigels of overlapping agarose concentrations ranging from 0.9 to 3 % (w/v) agarose. Bacteriophage T3 was included as an internal standard in all gels.

The average Re in E buffer of saturated control and uH2A hybrid nucleosomal arrays at pore sizes ≥ 200 nm was 26.4 ± 3.8 nm and 25 ± 2.7 nm respectively. These values represent the mean ± standard error of 8 determinations. Previous estimates of Re values of saturated nucleosomal arrays under the same conditions ranged from 26 to 28 nm (Fletcher *et al.*, 1994a; Carruthers *et al.*, 1998). This result was intriguing, since the ubiquitin moiety of uH2A could be expected to increase the overall average radius of the nucleosomal array. This may indicate that the ubiquitin molecules are flexible due to their C-terminal tails, and that their spatial positions can be variable and undetectable by this methodology. No significant difference in the Re values of control and uH2A hybrid nucleosomal arrays was observed in E buffer, suggesting that, similarly to the nucleosomal level (see section 2), ubiquitination of H2A has little effect on the conformation of the nucleosome in an array at low ionic strength.

In the presence of 2 mM $MgCl_2$, saturated nucleosomal arrays condense and their effective radii decrease (Fletcher *et al.*, 1994b). If ubiquitination of H2A affects the Mg^{2+} induced compaction of nucleosomal arrays, the ratio of the Re value obtained in E buffer containing 2 mM $MgCl_2$ to that of the value obtained in E buffer alone would be expected to be greater than that of control nucleosomal arrays.

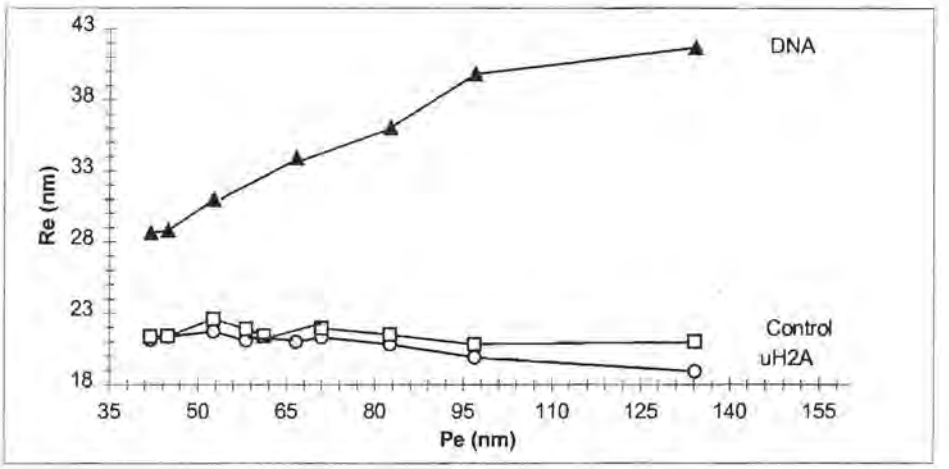

Figure 4.11.The pore size dependence of the Re of 208-12 template DNA and saturated control and uH2A nucleosomal arrays in E buffer containing 2mM $MgCl_2$. Results were obtained from overlapping multigels ranging from 0.9 to 3 % (w/v) agarose. Bacteriophage T3 was included as an internal standard for pore size in all gels.

In 2 mM $MgCl_2$, the average Re values of saturated control and uH2A hybrid nucleosomal arrays at pore size ≥ 200 nm were 22.4 ± 0.5 nm and 22 ± 0.3 nm respectively. These values represent the mean ± standard error of 8 determinations. As expected, both Re values remained constant at higher agarose concentrations. Previously, Re values of saturated 208-12 nucleosomal arrays in 2 mM $MgCl_2$ were determined at 20.5 to 22 nm (Fletcher *et al.*, 1994b; Fletcher and Hansen, 1995; Tse *et al.*, 1998). The ratio of Re^{Mg2+}: Re was 0.85 ± 0.14 for control nucleosomal arrays and 0.88 ± 0.1 for uH2A hybrid nucleosomal arrays. The standard error was calculated according to the equation: % standard error (SE) = $[(\%\ SE\ Re\ Mg^{2+})^2 + (\%\ SE\ Re)^2]^{½}$ (Fletcher *et al.*, 1994b). These results suggest that ubiquitination of histone H2A does not significantly inhibit chromatin compaction and that uH2A hybrid nucleosomal arrays have a similar hydrodynamic shape and conformational flexibility to control nucleosomal arrays.

Under the experimental conditions employed above, saturated 208-12 nucleosomal arrays have been found to exist in equilibrium between a structure that sediments at 40 S and a structure that sediments at 55 S (Schwarz & Hansen, 1994). The extent of compaction of the 40 S structure has been proposed to correspond to an intermediate state of chromatin folding analogous to a zig-zag conformation (Schwarz & Hansen, 1994). Again it is possible that in 2 mM $MgCl_2$, the ubiquitin moiety is found within the array's diameter. This could be feasible if one imagines that the ubiquitin molecules lie on opposite faces of the octamer and that chromatin compaction is brought about by an "accordion-like" mode of compaction of an irregular three-dimensional zig-zag arrangement of nucleosomes. In this model, compaction occurs as a result of reduction of the angle between entering and exiting linker DNA of peripherally arranged nucleosomes (Woodcock *et al.*, 1993; van Holde and Zlatanova, 1996; Bednar *et al.*, 1998). In the zig-zag model, nucleosomes n, n + 1 and n – 1, remain separate at this level of compaction and are not involved in close face to face contacts (Woodcock *et al.*, 1993; Bednar *et al.*, 1998).

4.2.3 Mg^{2+} Dependent nucleosomal array oligomerisation

Chromatin containing linker histones has been shown to form oligomers in solutions containing both monovalent and divalent salts (Ausió *et al.*, 1984; Borochov *et al.*, 1984; Jin & Cole, 1986). In the absence of linker histones, however, nucleosomal arrays only oligomerise in solutions containing divalent salts (Ausió *et al.*, 1986; Schwarz *et al.*, 1996). Some evidence suggests that the results obtained from *in vitro* oligomerisation of relatively short chromatin fragments may be significant regarding the *in vivo* interaction of chromatin fibres during chromosomal condensation (Fletcher & Hansen, 1996; Schwarz *et al.*, 1996). The oligomerisation of nucleosomal arrays in Mg^{2+} solutions occurs rapidly (< 1 min) and is reversible upon removal of the Mg^{2+} by extensive dialysis (Schwarz *et al.*, 1996). Binding of divalent cations to nucleosomal array DNA is believed to be the driving force behind the association process since the addition of monovalent salts reduces the extent of oligomerisation at any concentration of divalent cations (Widom, 1986; Clark & Kimura, 1990; Schwarz *et al.*, 1996).

Oligomerisation is inhibited in the absence of either the tail domains of H3 and H4 or H2A and H2B but is abolished in the absence of all core histone N-termini (Moore & Ausió, 1997; Tse & Hansen, 1997). The extent of oligomerisation is also sensitive to the degree of nucleosome saturation (Schwarz *et al.*, 1996), the extent of histone acetylation (Tse *et al.*, 1998) and the presence of linker histones (Ausió *et al.*, 1986; Howe *et al.*, 1998b). These results suggest that oligomerisation is not completely mediated by an electrostatic mechanism (Clark & Kimura, 1990), but that histone tails also play an important role (Schwarz *et al.*, 1996).

Oligomerisation of nucleosomal arrays results in the co-operative formation of large aggregates that can be removed from solution by centrifugation. The extent of oligomerisation of saturated control and uH2A hybrid nucleosomal arrays in increasing concentrations of $MgCl_2$ was determined using a differential centrifugation assay. The extent of oligomerisation was found to be concentration dependent (not shown). Comparative experiments were performed at the same A_{260} values. The final A_{260} were ~0.8 in order to be able to compare the results obtained with those of other researchers. Nucleosomal arrays were incubated in increasing concentrations of $MgCl_2$ and aggregates were removed by centrifugation. The extent of oligomerisation was quantitated after measuring the A_{260} of the supernatant as described in (section 8). As shown in Fig. 4.12, saturated uH2A hybrid nucleosomal arrays oligomerised at lower Mg^{2+} concentrations than saturated control nucleosomal arrays. Control nucleosomal arrays are 50 % oligomerised at approximately 4 mM $MgCl_2$ in close agreement with the results of Moore & Ausió (1997), whilst uH2A hybrid nucleosomal arrays are almost completely oligomerised at this concentration. Oligomerisation of control nucleosomal arrays was almost complete in 6 mM $MgCl_2$.

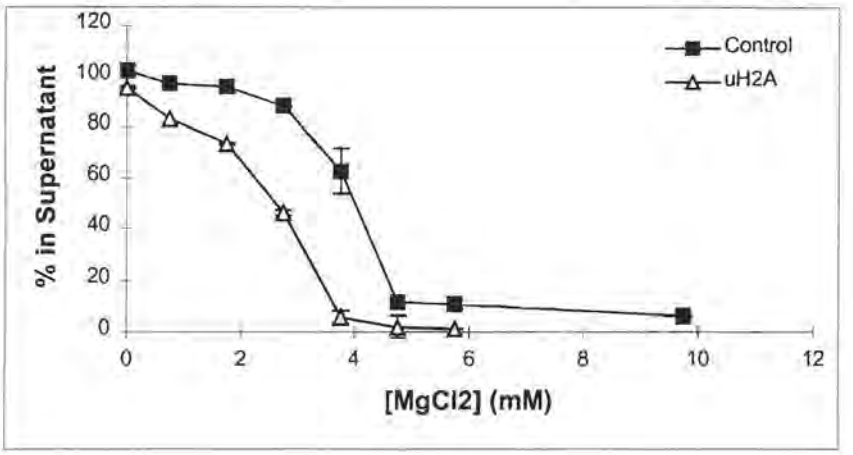

Figure 4.12. Mg^{2+} dependent oligomerisation of saturated control (■) and uH2A hybrid (△) nucleosomal arrays. Unaggregated arrays remain soluble in the supernatant. Each point represents the average of 2 to 3 determinations.

When this experiment was performed with subsaturated uH2A hybrid nucleosomal arrays containing approximately 10 nucleosomes, the results paralleled those of saturated control arrays (not shown). The presence of uH2A therefore does not interfere with chromatin compaction in the absence of linker histones, and appears to promote inter-array contacts. It is possible that the ubiquitin molecules provide domains that can either interact favourably with one another or with other chromatin components.

From the quantitative agarose gel electrophoresis results discussed previously, it is likely that the relative decrease in the gel–free mobility (μ_0) of uH2A hybrid nucleosomal arrays compared to control nucleosomal arrays involves some shielding of negative charges. If the electrostatic free energy of the array is reduced, less Mg^{2+} would be required to bind to the arrays and screen the negative charge of the DNA backbone, thereby allowing aggregation to occur at lower Mg^{2+} concentrations. This property could be of significance in stabilising interactions between certain regions of interphase chromatin fibres.

What are some of the possible *in vivo* implications for the data presented above? In the *in vitro* system used here, ubiquitination of histone H2A neither inhibited the Mg^{2+} induced folding of an array of physiologically spaced nucleosomes in the

absence of linker histones nor was linker histone binding inhibited at the nucleosomal level (sections 2 and 3). It is therefore unlikely that ubiquitination of H2A alone serves to "open up" the chromatin and increase its accessibility to nuclear proteins or facilitate transcription.

It has not yet been investigated if the disappearance of ubiquitinated histones concomitant with chromatin condensation events during the cell cycle (Matsui *et al.*, 1979; Mueller *et al.*, 1985) is a result of ubiquitinated histones acting as a nuclear reserve of ubiquitin. It would be interesting to determine if the ubiquitin released from ubiquitinated histones by isopeptidase activity at metaphase (Matsui *et al.*, 1982) is ligated to proteins, such as the mitotic cyclins, that are to be degraded by the ubiquitin-dependent 26 S proteasome pathway.

A possible role of uH2A is to tag nucleosomes in transcriptionally poised chromatin regions such as the *hsp 70* genes in *Drosophila* (Levinger & Varshavsky, 1982). Transcriptionally active chromatin has been reported to be depleted in H2A-H2B dimers (Baer & Rhodes, 1983; Gonzalez *et al.*, 1987; Gonzalez *et al.*, 1989). The lability of the H2A-H2B dimer associated with nucleosomes of chromatin enriched in transcriptionally active chromatin was found to be increased by the simultaneous ubiquitination of H2A and H2B (Li *et al.*, 1993). However, uH2A alone does not appear to destabilise nucleosomes, since as shown in section 2, the thermal denaturation profiles of uH2A hybrid nucleosomes do not differ significantly from those of control nucleosomes. Removal of H2A-H2B dimers prevents nucleosomal arrays from folding at physiological salt concentrations (Hansen & Wolffe, 1994). Another possibility is that nucleosomes containing uH2A may be recognised by chromatin remodeling complexes (such as SWI/SNF, NURF, CHRAC, RSC (see Workman & Kingston, 1998 for review), RSF or FACT (LeRoy *et al.*, 1998)) that could preferentially remove the uH2A-H2B dimers or alter their molecular contacts, thus increasing the accessibility of a particular chromatin region.

5 Reconstitution of the linker histone H5 onto long stripped chromatin using CM Sephadex C-25.

5.1 Introduction

Reconstitution of linker histones onto mononucleosomes is relatively facile compared to reconstitution onto longer oligonucleosomes, mainly due to the problems of aggregation and nucleosome sliding that occur in the latter.

Linker histones have been reconstituted onto nucleosomal templates by direct addition to the substrate at a "low salt" concentration (less than 100 mM NaCl) (e.g. Allan *et al.*, 1980b; Graziano *et al.*, 1988) or at a "high salt" concentration similar to that required to dissociate the linker histone from native chromatin (~500 mM NaCl) (e.g. Nelson *et al.*, 1979; Biard-Roche *et al.*, 1982; Kaplan *et al.*, 1984; Meersseman *et al.*, 1991) followed by dialysis to reduce the salt concentration.

Carriers such as tRNA (Klingholz & Strätling, 1982) or polyglutamic acid (Künzler & Stein, 1983, Jeong *et al.*, 1991) have also been used. Removal of tRNA after reconstitution using RNase is problematic if the reconstituted material is to be used for transcriptional investigations. Assembly factors such as these allow reconstitution of linker histones at low salt concentrations without causing aggregation. Assembly at low salt has advantages over methods requiring "high" salt concentrations since the mobility of nucleosomes is greatly increased at elevated salt concentrations and can lead to close packing of linker histone free nucleosomes and the formation of tight dimers (Spadafora *et al.*, 1979).

Another method of assembly used involves exchange of histone octamers from an excess of donor chromatin to a recipient (Schlissel & Brown, 1984; Drew & McCall, 1987). Lastly a more heterogeneous system uses extracts from *Xenopus* oocytes (e.g. Rodriguez-Campos *et al.*, 1989) or *Drosophila* embryos (Becker & Wu, 1992; Bulger *et al.*, 1995) to aid linker histone reconstitution. Leuba & Zlatanova (1997) have recently reviewed protocols for linker histone reconstitution.

Linker histones can increase nucleosomal spacing when added to close-packed or irregular arrays in the presence of an artificial histone carrier such as polyglutamic acid (Künzler & Stein, 1983, Jeong *et al.*, 1991) or cell free extracts (Rodriguez-Campos *et al.*, 1989; Becker & Wu, 1992). The use of artificial histone carriers has a

major limitation, however, in that such factors remain in solution together with the reconstituted chromatin after assembly (Retief *et al.*, 1984). The use of an alternative histone carrier that would successfully mediate linker histone reassociation to stripped chromatin but that could also easily be removed from the reconstitution system was therefore investigated. The ultimate goal of this investigation was to develop a rapid, reliable method that could eventually be used to successfully reassociate linker histones with defined nucleosomal arrays containing modified histones. This would be of great benefit to studies investigating the role of post-translational histone modifications on chromatin higher-order structure.

5.2 Results and Discussion

Anionic histone carriers such as polyglutamic acid and polygalacturonic acid (pectin) have been used to reconstitute histone octamers onto DNA (Lindsey *et al.*, 1985; Sobolewski *et al.*, 1993) and polyglutamic acid has also been used to mediate linker histone reassociation to chromatin (Künzler & Stein, 1983, Jeong *et al.*, 1991). Polyglutamic acid cannot be removed from the reconstitution system successfully (Retief *et al.*, 1984) whilst it was reported that the pectin used to assemble core particles could be removed by sucrose gradient centrifugation after treatment with pectinase (Sobolewski *et al.*, 1993). Another advantage of pectin is that it is readily available and inexpensive. Pectin was therefore initially used to reconstitute linker histones onto stripped polynucleosomes.

5.2.1 Pectin as a linker histone carrier

In order to analyse linker histone binding to stripped polynucleosomes, reconstitutions were carried out at fixed pectin and polynucleosome concentrations. A 30 fold weight excess of pectin dissolved in 20 mM NaCl, 0.1 mM EDTA and 10 mM Tris-HCl (pH 7.4) was mixed with stripped polynucleosomes (4-5 nucleosomes) with increasing amounts of either histone H1 or H5 the same buffer. After incubation for one hour at 4 °C, the reconstitution products were purified on linear 5-20 % (w/v) isokinetic sucrose gradients in the same buffer. The gradients were fractionated whilst measuring the absorbance at 260 nm and the protein content of the polynucleosome peak was examined by SDS-PAGE. The relative linker histone content of the reconstitution products was determined by densitometric analysis. Results for the reconstitution of histone H5 are shown in Fig. 5.1. Competition of pectin and polynucleosomes for histone H5 necessitated high input ratios of histone H5 per nucleosome to achieve physiological levels of bound histone H5. The yield of the reconstitution products decreased at and above an input ratio of 10 histone H5 molecules per nucleosome, when the amount of histone H5 present in the reconstitutes was almost twice that of the standard. This is presumably as a result of saturation of the pectin and polynucleosomes with H5 and concomitant aggregation. Below this

ratio, the presence of pectin allowed H5 to reach levels higher than those found in a total acid extract of chicken erythrocyte nuclei. It has been reported that more than one linker histone binding site may exists although the putative secondary site has a much lower affinity for linker histones (Nelson *et al.*, 1979). It is therefore possible that the high levels of incorporation observed are the result of histone H5 binding to a secondary position. The ratio of the core histones was unaffected in the reconstituted samples indicating that pectin did not remove core histones under the reconstitution conditions used (not shown).

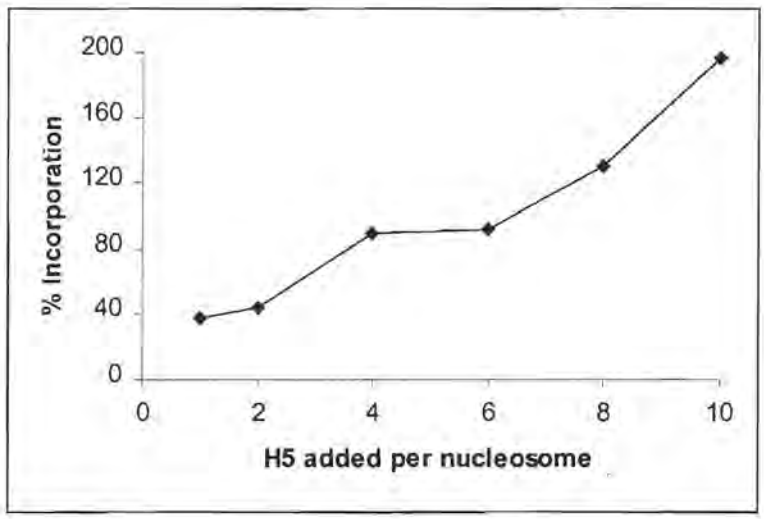

Figure 5.1. Analysis of the relationship between input ratio of histone H5 per nucleosome and the amount of histone H5 bound to polynucleosomes after reconstitution with pectin. The reconstitution mixtures were purified on 5-20 % (w/v) isokinetic sucrose gradients and the histone content of the polynucleosome peak was analysed by SDS-PAGE. The gels were scanned and the percentage incorporation of histone H5 was determined by comparing the ratio of the area found under the histone H5 peak to the area found under the core histone peaks in each sample to that of a total acid extract of chicken erythrocyte nuclei of similar staining intensity run on the same gel.

5.2.1.1 MNase digestion of reconstituted polynucleosomes

One feature that differentiates native from stripped chromatin is that the presence of the linker histone in the former results in a more marked protection of 167 bp DNA during MNase digestion (Noll & Kornberg, 1977; Bakayev *et al.*, 1977) than that afforded by the nucleosome core alone (Weischet *et al.*, 1979; Lindsey & Thompson, 1989; Pruss & Wolffe, 1993). A commonly used parameter to determine the successful reconstitution or presence of linker histones is therefore the production of 167 bp digestion pauses in the course of an MNase limit digest (e.g. Allan *et al.*, 1980b; Biard-Roche *et al.*, 1982; Klingholz & Strätling, 1982; Meersseman *et al.*, 1991). Polynucleosomes were reconstituted with histone H5 as described above using an input ratio of 6 H5 per nucleosome such that the amount of histone H5 bound would be similar to that found in chicken erythrocyte chromatin. The reconstitution mixture was purified through a sucrose gradient, digested with MNase and the digestion products were analysed on a 6 % (w/v) acrylamide gel (Fig. 5.2).

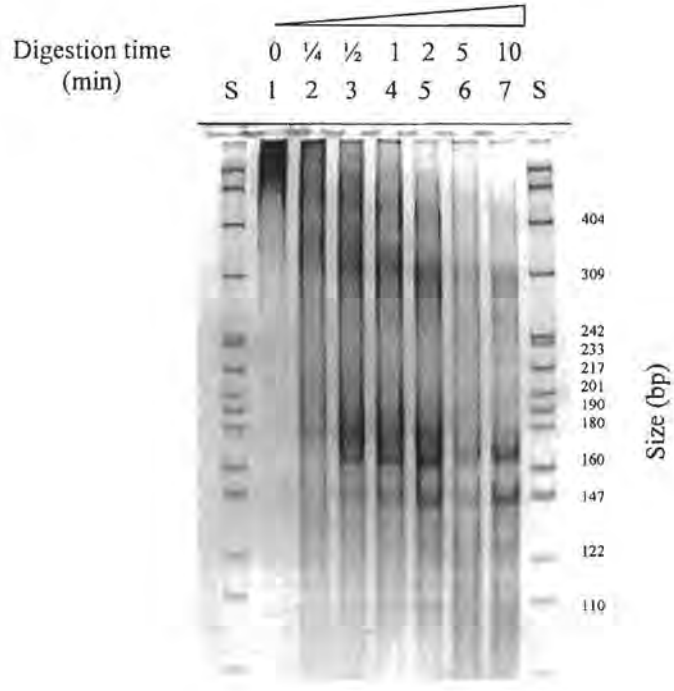

Figure 5.2. Six percent non-denaturing PAGE of the MNase digestion products of 4-6 mer polynucleosomes reconstituted with one histone H5 per nucleosome using pectin as a linker histone carrier. The purified reconstitution mixture (25 µg DNA) was digested with 14 units MNase at 20 °C for 0, 0.25, 0.5, 1, 2, 5 and 10 min (lanes 1-7). The standard used (S) was a *Hpa* II digest of pBR322.

Clear protection of 180, 167 and 146 bp intermediates are visible in Fig. 5.2. This result suggests that histone H5 was bound to the chromatin, since protection of a 180 bp intermediate is not observed in chromatin lacking linker histones (Lindsey & Thompson, 1989).

It was not possible to compare the digestion kinetics of the reconstituted sample and native 4-6 mer polynucleosomes directly since the reconstituted sample required 3 times more MNase to achieve similar extents of digestion as the same amount of native polynucleosomes (not shown). Since pectin is anionic and can therefore bind the Ca^{2+} cofactor required by MNase and perhaps MNase as well, residual pectin was the likely cause of the observed MNase inhibition in the reconstituted sample.

5.2.1.2 Pectinase treatment of reconstituted samples

The same reconstitution mixture as described above was prepared and centrifuged in parallel with the same amount of pectin used in the reconstitution through 5-20 % (w/v) sucrose gradients. The position of polynucleosomes in the gradient was determined from A_{260} measurements and the presence of pectin in gradient fractions was determined using a colourimetric assay for uronic acid (Davidson, 1966). As can be seen in Fig. 5.3, pectin was clearly present in the polynucleosome fraction. Some interaction between pectin and the components of the reconstitution mixture was evident in that the position of pectin in the gradient was shifted in the presence of polynucleosomes and histone H5. Control experiments in the absence of pectin showed that the polynucleosomes were not responsible for the increased A_{660} readings observed.

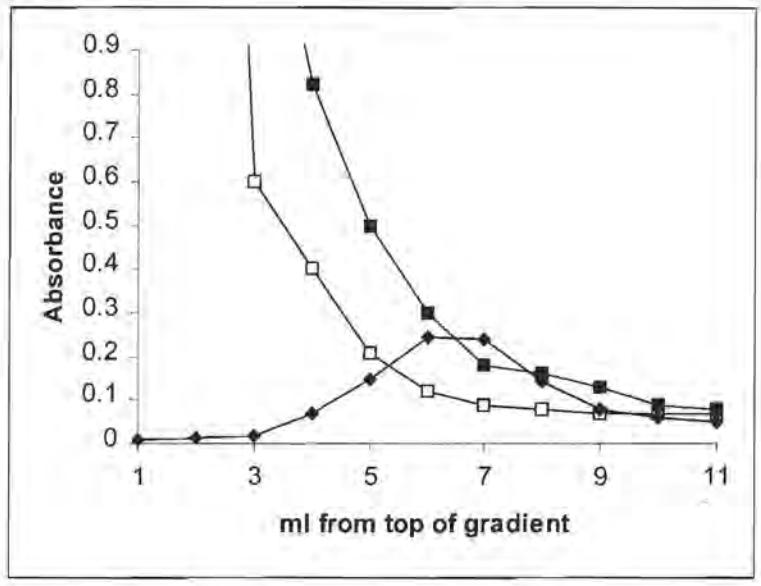

Figure 5.3. Isokinetic sucrose gradient centrifugation of 4-6 mer polynucleosomes reconstituted with one H5 per nucleosome using pectin as a linker histone carrier. The position of polynucleosomes was determined from A_{260} measurements (♦). Pectin measurements were determined from A_{660} measurements of gradient fractions following orcinol treatment. Pectin measurements were carried out for pectin associated with the reconstitution mixture (■) and the same amount of pectin used for reconstitution centrifuged in parallel (□).

In order to remove the pectin, reconstituted samples were digested with pectinase in 20 mM NaCl, 0.1 mM EDTA and 10 mM Tris-HCl (pH 7.4) as described previously (Sobolewski *et al.*, 1993). Agarose gel electrophoretic analysis of the products of MNase digested samples showed a smear in those samples treated with pectinase (not shown) suggesting that the pectinase was contaminated with nucleolytic and/or proteolytic enzymes. To test for contaminating proteolytic activity, a solution of total acid extracted chicken erythrocyte histones was treated with pectinase. The samples were analysed by SDS-PAGE (Fig. 5.4) and clearly indicated that pectinase was responsible for proteolytic degradation of histones. The pectinase used was the same as that used by Sobolewski *et al.* (1993) and a different batch of pectinase gave the same results. A heat stable bacterial amylase was also found to be unsuitable to break down polygalacturonic acid as contaminating proteolytic activity was still present even after 80 °C treatment (Fig.5.4).

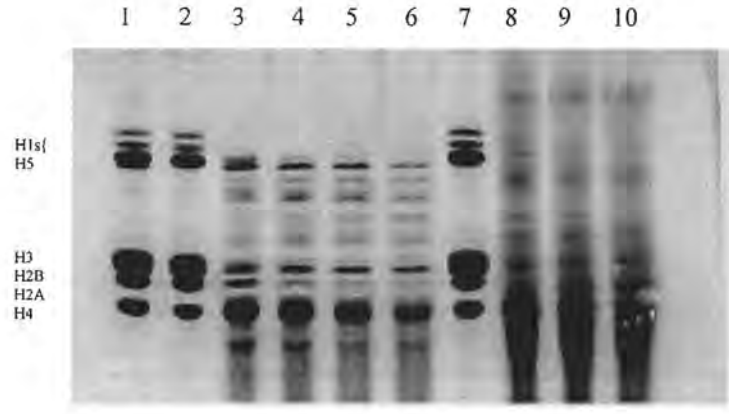

Figure 5.4. SDS-PAGE analysis of total acid extracted chicken erythrocyte histones treated with pectinase and heat treated amylase. Chicken erythrocyte histones (100 μg) were incubated at 37 °C in 20 mM NaCl, 0.1 mM EDTA and 10 mM Tris-HCl (pH 7.4) with 0.5 units of 80 °C treated amylase for 5, 10, 20 and 40 min (lanes 3-6) or 7 units of pectinase for 5, 10, and 20 min (lanes 8-10). Chicken erythrocyte histones were incubated under the same conditions without pectinase or amylase for 10 and 20 min (lanes 2 and 7). Lane 1 is a total acid extract of chicken erythrocyte nuclei.

CM Sephadex C-25 is an insoluble anionic resin that has been used to remove linker histones from chromatin at low and high salt concentrations (Libertini & Small, 1980; Garcia-Ramirez *et al.*, 1990). Since pectin removal was problematic, the use of this resin as an artificial histone carrier was investigated

5.2.2 CM Sephadex C-25 as a linker histone carrier

The use of CM Sephadex C-25 as a linker histone deposition carrier was investigated for the reconstitution of histone H5 onto stripped chicken erythrocyte chromatin of two sizes, namely pentanucleosomes and long chromatin containing 7 to 12 nucleosomes.

Long chromatin of this size should be suitable for folding studies since it has been reported that at least 6 nucleosomes are necessary for linker-histone containing chromatin to assume a physiologically relevant higher order structure upon exposure to increasing salt concentrations (Bates *et al.*, 1981; McGhee *et al.*, 1983a).

In order to determine the input ratio of histone H5 required to obtain reconstituted long chromatin or pentanucleosomes with a histone H5 level akin to that found in native soluble chicken erythrocyte chromatin, reconstitution was performed at fixed CM Sephadex C-25 and stripped chromatin concentrations with increasing amounts of purified histone H5 (Fig. 5.5). Reconstituted samples were centrifuged to pellet the ion exchange resin and then applied to 5-20 % (w/v) sucrose gradients. The histone H5 content of samples recovered from the gradients was compared with that of the same samples not purified by sucrose gradient centrifugation (Fig. 5.5 A). Of the histone H5 present in the reconstituted chromatin prior to sucrose gradient centrifugation (lanes 2-7), 80 % was recovered in the purified samples (lanes 8-13). This loss upon centrifugation may reflect the loss of histone H5 weakly bound to secondary sites on the chromatin. Some histone H5 was found bound to the resin and was analysed quantitatively after washing the resin with reconstitution buffer. The amount of histone H5 bound to the resin (shown only for a histone H5: nucleosome input ratio of 1.5: 1, lane 14), increased with increased histone H5: nucleosome input ratios. This increase was most marked above an input ratio of 1: 1. No core histones were found bound to the resin. Additionally, when stripped chromatin was mock-reconstituted in the absence of histone H5, the ratio of the area of core histone H2A and H4 densitometric peaks remained equivalent to that of native chromatin.

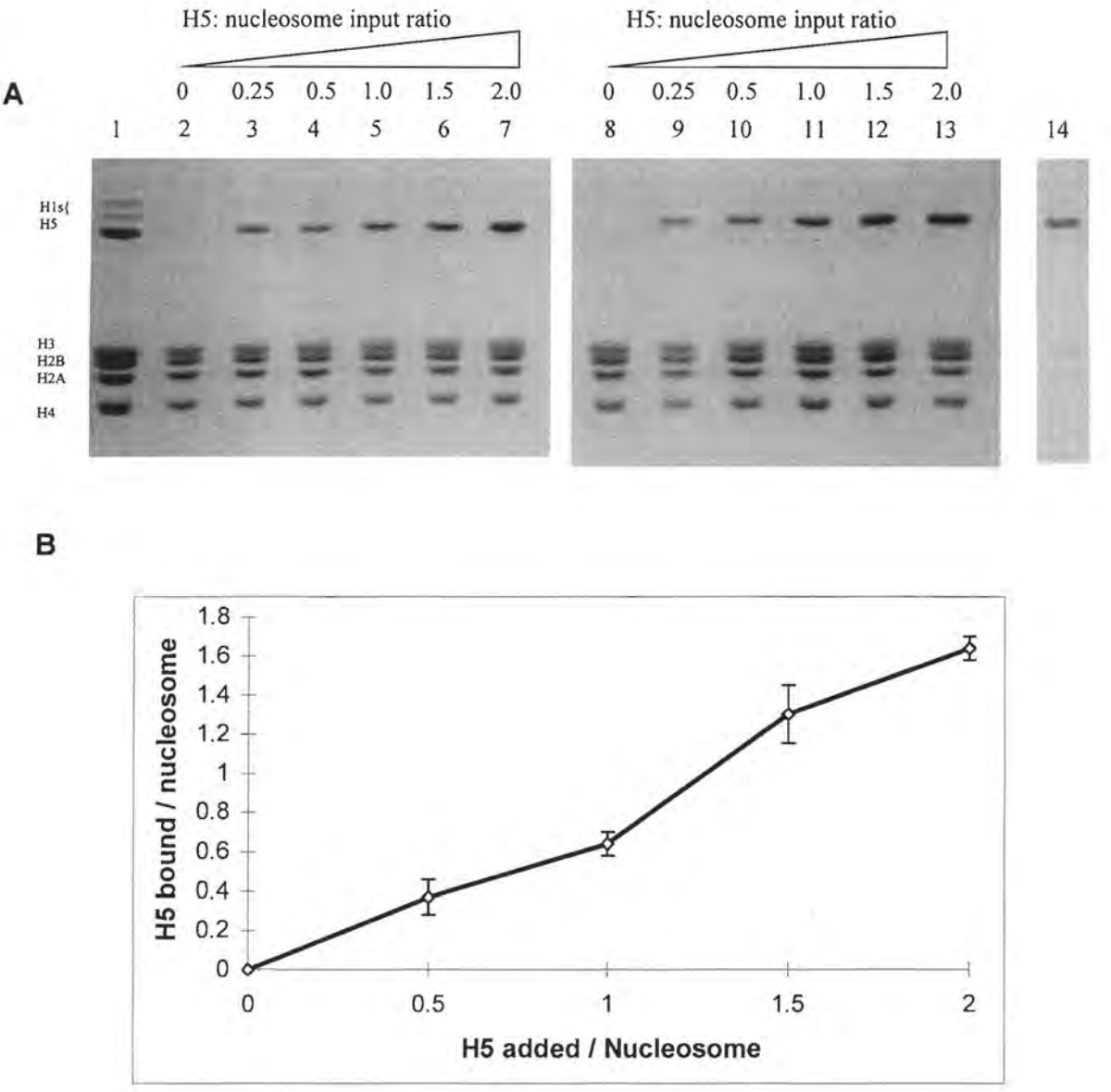

Figure 5.5. Analysis of the relationship between input ratio of histone H5 per nucleosome and that found in reconstituted chromatin. (**A**) SDS-PAGE of long stripped chromatin reconstituted at a histone of 0, 0.25, 0.5, 1, 1.5 and 2 before (lanes 2-7) and after (lanes 8-13) centrifugation on 5-20 % sucrose gradients. Lane 1: total histones from native soluble chicken erythrocyte chromatin. Lane 14: histones associated with the CM Sephadex C-25 resin. The resin was washed twice with reconstitution buffer after removal of the reconstituted sample and histones bound to the resin were removed by acid extraction. The result shown was using an input ratio of 1.5. (**B**) Gels were densitometrically scanned and the ratio of the histone H5 bound per nucleosome was plotted against the input ratio. The data shown represent the average of 10 experiments.

An approximately linear relationship between the input histone H5 and the amount incorporated per nucleosome was observed (Fig. 5.5 B). The yield of chromatin was in the range of 70 to 80 %, provided that the input histone H5: nucleosome ratio did not exceed 2:1. Increasing the input histone H5: nucleosome ratio above this value resulted in significant precipitation of material. Similar results were obtained for histone H5 reconstitution onto stripped pentanucleosomes. In order to achieve reconstitution of one histone H5 per nucleosome using this reconstitution system, an input ratio of 1.28 and 1.4 H5 molecules per nucleosome was required for reconstitution onto stripped pentanucleosomes and stripped long chromatin respectively.

The fidelity of histone H5 reconstitution was assayed by MNase digestion, thermal denaturation and determination of the orientation of neighbouring H5 molecules in extended chromatin.

5.2.2.1 MNase digestion of long chromatin and pentanucleosomes

It has been reported that MNase digestion of chromatin depleted of linker histones leads to nucleosome sliding (Weischet & van Holde, 1980) resulting in a decrease in the observed repeat length. Native, reconstituted and stripped long chromatin were therefore digested with MNase and the digestion products analysed on 1 % (w/v) agarose gels. The repeat lengths were determined from densitometric scans of the digestion products (Fig. 5.6). The repeat lengths of native, reconstituted and stripped chromatin were calculated to be 197 ± 4 bp, 200 ± 3 bp and 185 ± 6 bp respectively. Moreover, the digestion rates of native (Fig. 5.6 A) and reconstituted (Fig. 5.6 B) were found to be very similar and markedly slower than that of stripped chromatin (Fig. 5.6 C) in accordance with previous reports (Noll & Kornberg, 1977, Allan *et al.*, 1980b; Graziano *et al.*, 1988). During this study, repeat length determinations of native chromatin at equivalent extents of digestion were found to be significantly influenced by the concentration of MNase used (see section 6). The relationship between the observed repeat length and the rate of MNase digestion was therefore investigated using different temperatures and different MNase concentrations to modulate the rate of MNase digestion (section 6).

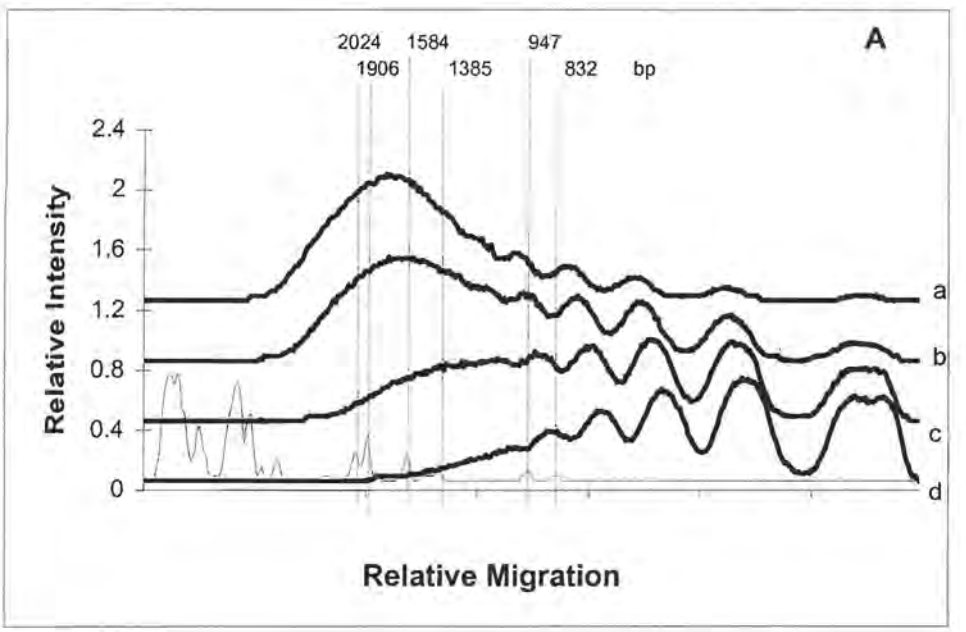
A
2024
1906
1584
1385
947
832
bp
2.4
2
1.6
1.2
0.8
0.4
0
Relative Intensity
a
b
c
d
Relative Migration

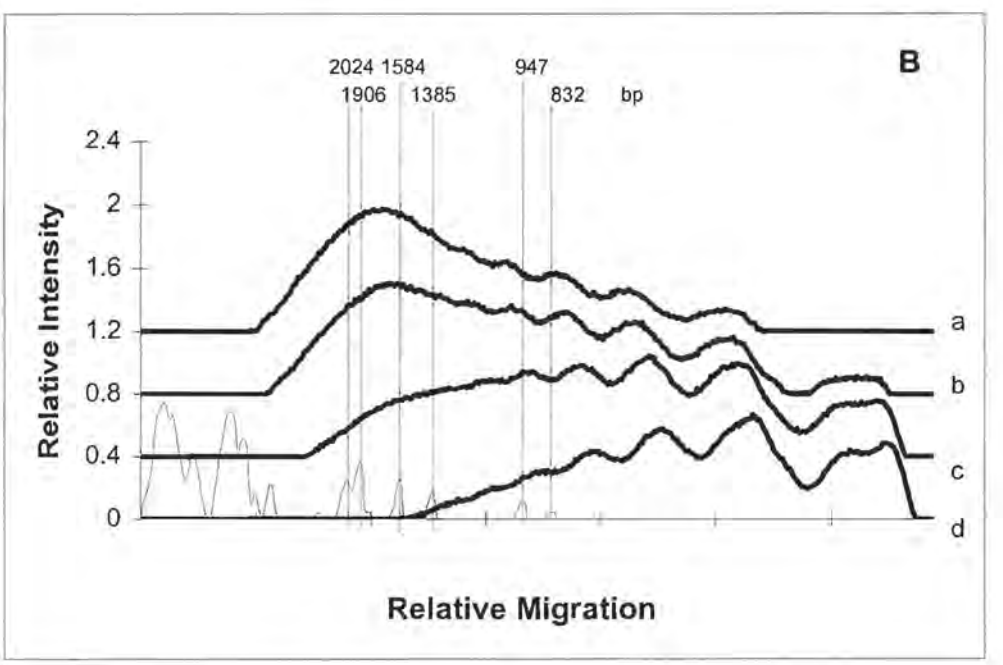
B
2024
1906
1584
1385
947
832
bp
2.4
2
1.6
1.2
0.8
0.4
0
Relative Intensity
a
b
c
d
Relative Migration

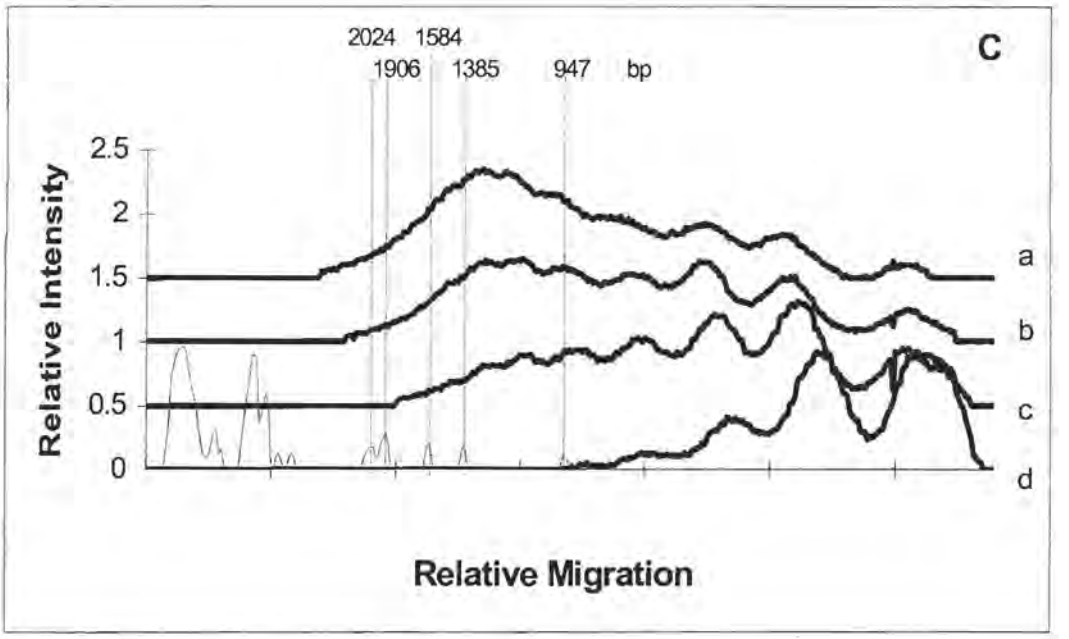

Figure 5.6. Densitometric scans of MNase digestion products from long chromatin samples. Eighty micrograms of (**A**) native, (**B**) reconstituted and (**C**) stripped long chromatin was digested at 20 °C with 1 unit MNase for 1, 2, 5 and 10 min (traces a-d, respectively) and analysed on 1 % (w/v) agarose gels. An input ratio of 1.4 histone H5 per nucleosome was used in (**B**). The trace of the standard, an *Eco* RI/*Hind* III digest of λ phage is also shown.

MNase digestion products were next examined at the core particle level. Pentanucleosomes were reconstituted with histone H5 such that the linker histone content would be akin to that found in native pentanucleosomes. Native, reconstituted and stripped pentanucleosomes were digested with MNase and the digestion products analysed on 6 % non-denaturing acrylamide gels (Fig. 5.7). Digestion of both native (Fig. 5.7 A) and reconstituted (Fig. 5.7 B) pentanucleosomes resulted in marked protection of 167 bp DNA after 2 min digestion; this protection was still evident after further digestion to 5 min. In addition, protection of DNA outside of the chromatosome, namely a band at ~ 181 bp, was observed for both native and reconstituted pentanucleosomes. Digestion of stripped pentanucleosomes (Fig. 5.7 C), however, showed a less prominent pause at 167 bp which was barely visible after 5 min digestion when the chief digestion product was the core particle. No protection of DNA of lengths longer than 167 bp could be observed for stripped pentanucleosomes.

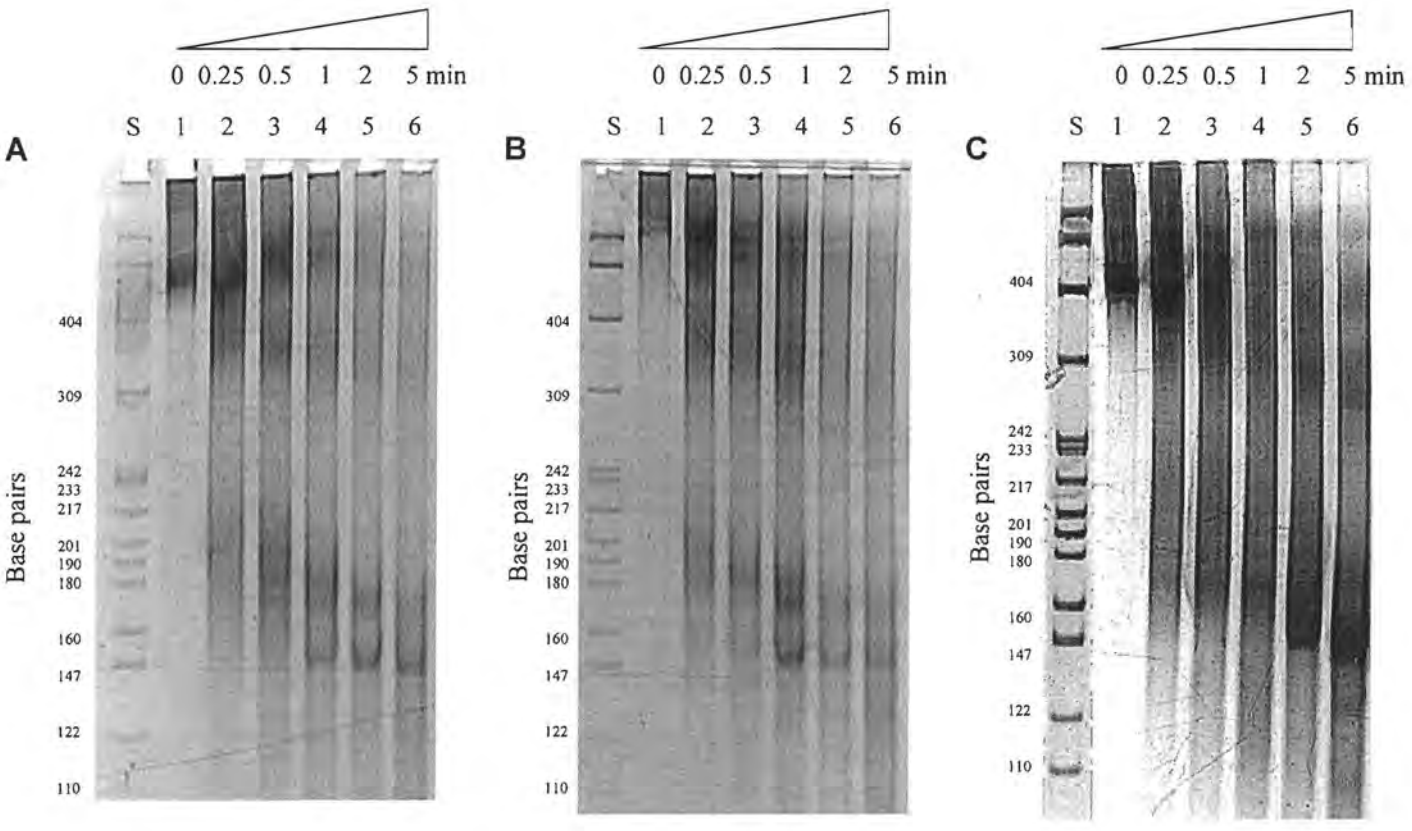

Figure 5.7. MNase limit digest of pentanucleosomes. Fifty micrograms of (**A**) native, (**B**) reconstituted and (**C**) stripped pentanucleosomes was digested at 20 °C with 9 units MNase for 0, 0.25, 0.5, 1, 2 and 5 min (lanes 1-6) and analysed on 6 % (w/v) acrylamide gels. An input ratio of 1.28 histone H5 per nucleosome was used in (**B**). The standard (S) was a *Hpa* II digest of pBR322.

5.2.2.2 Thermal denaturation

The thermal denaturation of native long chromatin has been shown to be a triphasic process (Allan *et al.*, 1980b; Kaplan *et al.*, 1984). The first and second transitions are believed to be associated with the melting of linker DNA and the DNA at the ends of the nucleosome respectively. The third and largest transition is thought to represent the denaturation of the central 10 helical turns of nucleosomal DNA (van Holde, 1989). Thermal denaturation of core particles is a biphasic process similar to the second and third transitions observed with chromatin. The first transition in this case is shifted to a higher temperature in the presence of bound linker histones (Simpson, 1978, McCleary & Fasman, 1980, Cowman & Fasman, 1980).

Stripped pentanucleosomes were reconstituted with increasing amounts of histone H5 using CM Sephadex C-25 or salt dialysis (Nelson *et al.*, 1979) and analysed by thermal denaturation (Fig. 5.8). The thermal denaturation profiles were more similar to core particles or chromatosomes than to long chromatin in that there was no distinct separation of the first and second transitions. The T_m of the first transition increased progressively as the linker histone input ratio increased. The profiles of pentanucleosomes reconstituted with histone H5 using CM Sephadex C-25 became increasingly monophasic upon incorporation of increasing amounts of linker histone whilst those of salt reconstituted pentanucleosomes remained biphasic for all linker histone to nucleosome ratios used in this study.

Stripped pentanucleosomes were next reconstituted with histone H5 using CM Sephadex C-25 at an input ratio of 1.28 H5 molecules per nucleosome so as to analyse the thermal denaturation profile of reconstituted nucleosomes with a similar histone H5 content as native chromatin. Figure 5.9 displays the first derivative of the melting profiles of native, reconstituted and stripped pentanucleosomes. The profiles were numerically deconvoluted assuming a biphasic denaturation by fitting a sum of Gaussian curves using a Marquardt-Levenberg algorithm. In native chromatin, the first transition occurred at 78.8 °C and the second transition at 86.2 °C. The first transition of stripped chromatin, however, occurred at a substantially lower temperature (74.8 °C) whilst that of the second transition (86.5 °C) was essentially unchanged. Reconstituted chromatin displayed very similar first and second transitions to native chromatin with T_ms of 78 °C and 86.5 °C for the first and second transitions respectively.

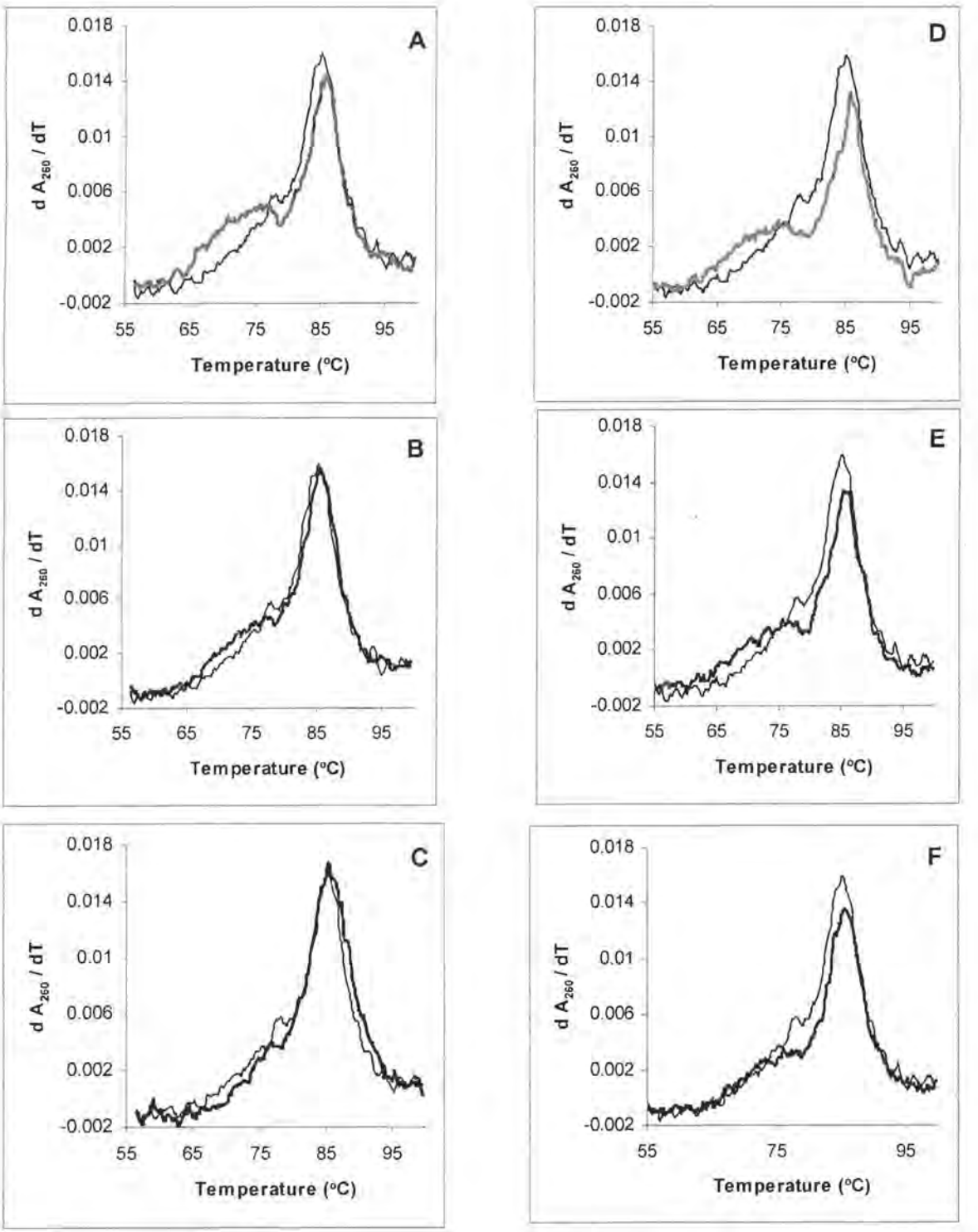

Figure 5.8. Thermal denaturation of pentanucleosomes. Stripped pentanucleosomes were reconstituted with histone H5 using CM Sephadex C-25 (**A** to **C**) or salt dialysis (**D** to **F**) at a histone H5: nucleosome input ratio of 0.5:1 (**A** and **D**), 1:1 (**B** and **E**) and 1.5:1 (**C** and **F**). The first derivatives of the A_{260} versus temperature profiles of the reconstituted sample (heavy line) and native pentanucleosomes (thin line) are shown. Denaturation was carried out in 10 mM NaCl, 0.1 mM EDTA and 10 mM Tris-HCl (pH 7.4).

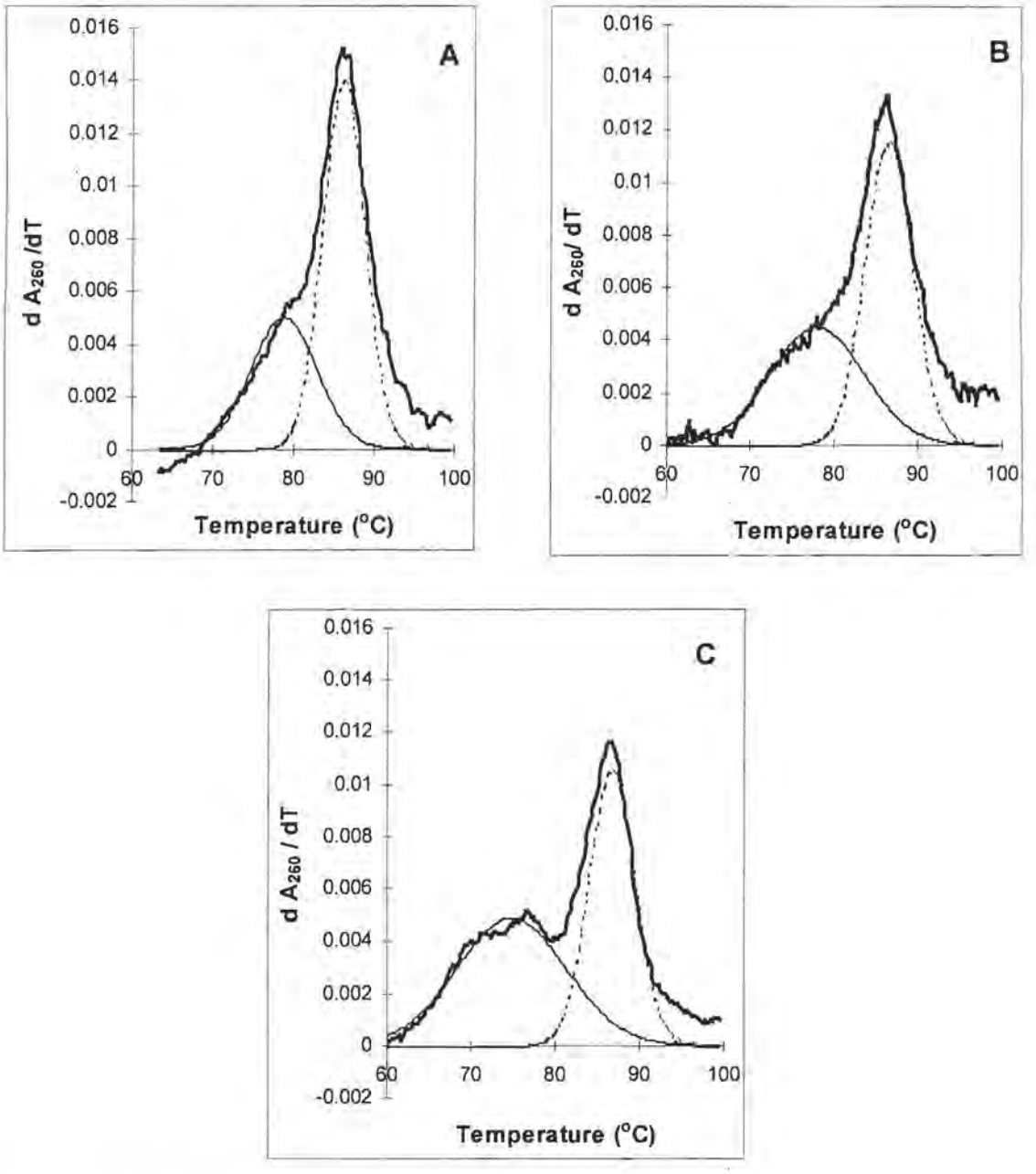

Figure 5.9. Thermal denaturation of native (A) reconstituted (B) and stripped (C) pentanucleosomes. Denaturation was carried out in 10 mM NaCl, 0.1 mM EDTA and 10 mM Tris-HCl (pH 7.4). Reconstitution was performed using CM Sephadex C-25 using a histone H5 to nucleosome ratio of 1.28:1. The first derivative of the A_{260} versus temperature profile is shown (heavy solid line). The first derivative data were numerically deconvoluted into two Gaussian distributions representing the first (thin solid line) and second (thin dashed line) transitions.

5.2.2.3 Determination of the relative orientation of neighbouring linker histones in long chromatin

It has previously been shown that linker histones are predominantly arranged in a head to tail fashion in extended long chromatin (Lennard & Thomas, 1985) although all possible orientations of linker histones (head to head, head to tail, tail to head and tail to tail) have been reported (Nikolaev *et al.*, 1981, 1983; Ring & Cole, 1983; Lennard & Thomas, 1985). The method of Lennard and Thomas (1985) was used to investigate linker histone orientation in chromatin (illustrated in Fig. 5.11). Briefly, reconstituted chromatin was cross-linked with dithiobis(propionic acid N-hydroxysuccinimide ester) under conditions that maximised linker histone cross-linking but limited linker histone to core histone cross-linking. The cross-linked products were extracted from the chromatin with perchloric acid and separated from monomeric histones by gel filtration (Fig. 5.10).

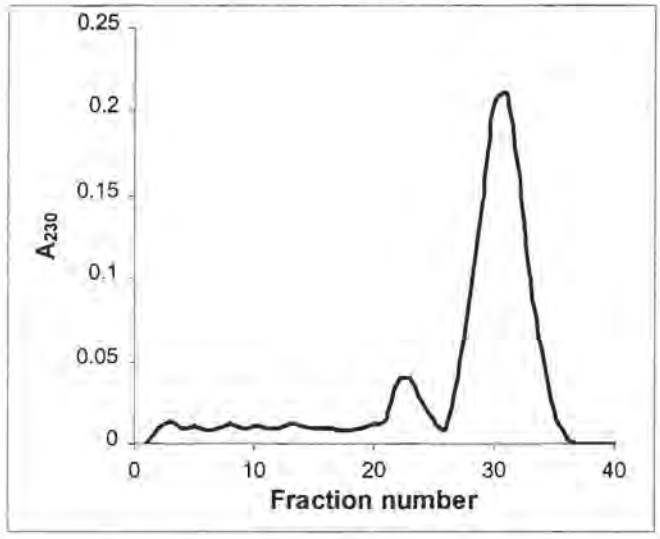

Figure 5.10. BioGel P-60 chromatography of histone H5 cross-linked with dithiobis (propionic acid N-hydroxysuccinimide ester). The column buffer was 20 mM HCl and the flow rate was 6 ml per hour. Dimers eluted with the first peak and monomers eluted with the second peak.

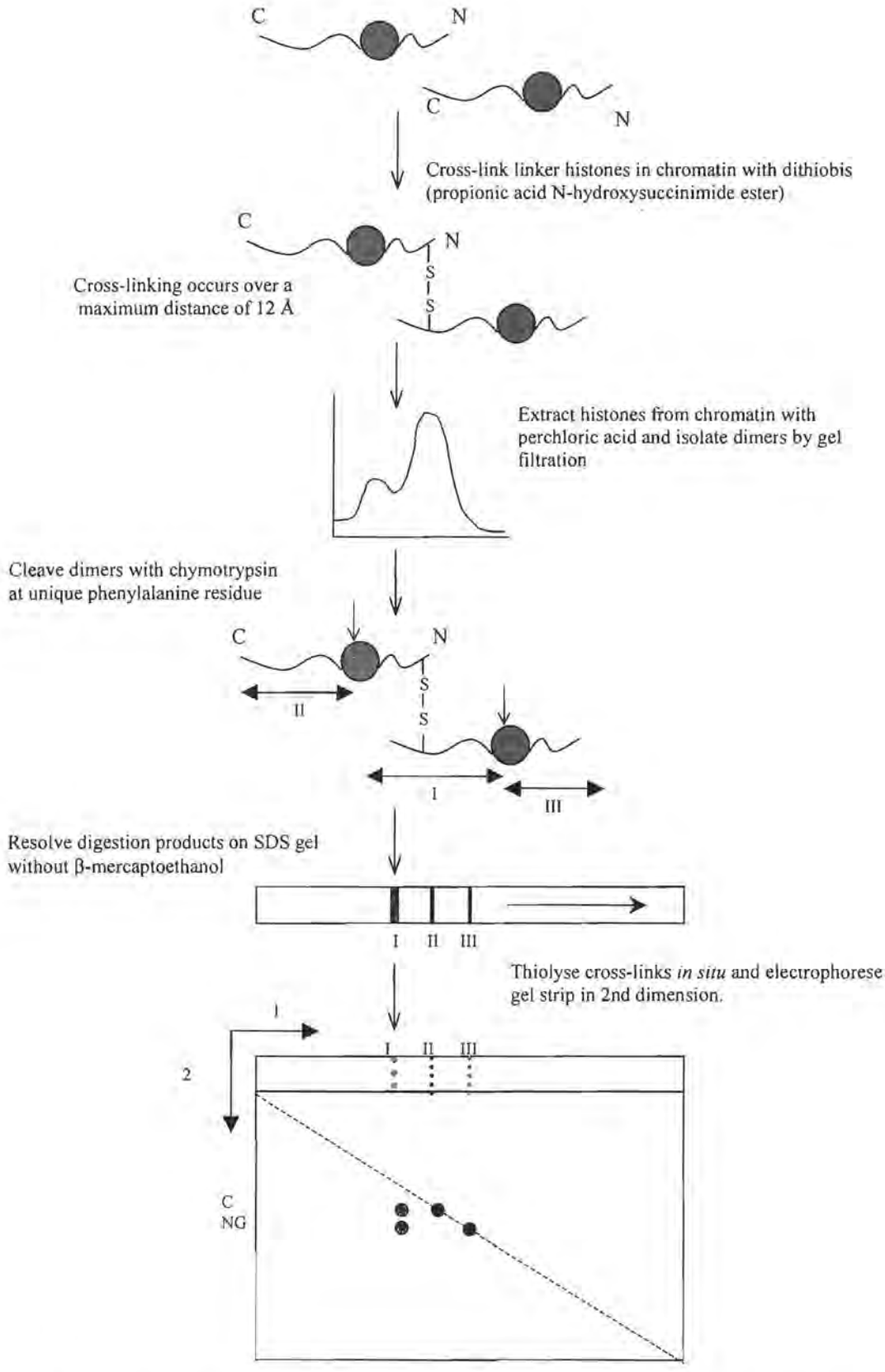

Figure 5.11. Illustration outlining the protocol used to determine the relative disposition of linker histones in long chromatin. Only one possible cross-link is shown. (Adapted from Lennard & Thomas, 1985).

Histone H5 can, under controlled conditions, be preferentially digested by chymotrypsin at phenylalanine 93 (Böhm & Crane-Robinson, 1984). This cleavage results in two fragments of similar size, namely a NG fragment containing the amino terminal domain with most of the globular domain and a C fragment consisting mainly of the carboxyl terminal tail (Fig. 5.12). Although the NG fragment and the C fragment are of similar size, the latter fragment is of relatively slower mobility due to its high positive charge content (Lennard & Thomas, 1985).

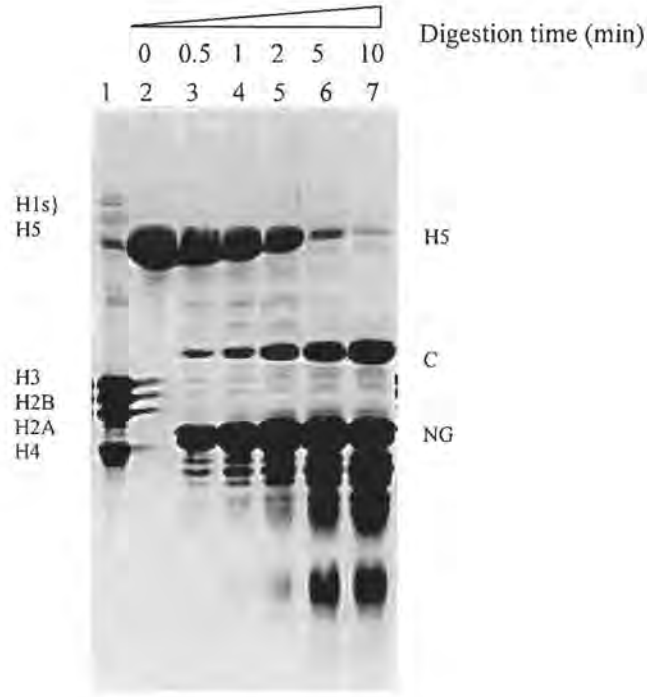

Figure 5.12. Chymotrypsin digestion of chicken erythrocyte histone H5. Three hundred micrograms of chicken erythrocyte histone H5 was digested at room temperature with 0.15 μg α-chymotrypsin. Digestion was stopped after 0, 0.5, 1, 2, 5, and 10 min (lanes 2-7) and the digestion products analysed by SDS-PAGE. The gel was silver stained. The positions of the histone H5 chymotryptic C fragment and NG fragment (the N-terminal domain with most of the globular domain) are shown. The standard in lane 1 is a total acid extract of chicken erythrocyte nuclei.

Histone H5 was digested with chymotrypsin under conditions favouring cleavage at this single site and the identity of the digestion products used as a standard in Fig. 5.13, was confirmed by gas phase sequencing of blots of SDS gels containing these fragments. The first five amino acids obtained for each fragment are shown below.

NG: T-E-S-L-V

C: R-L-A-K-S

Cross-linked material from chromatin samples was purified and digested with chymotrypsin under conditions determined to maximise cleavage without leading to further cleavage of the more labile NG fragment. The digestion products were electrophoresed in the first dimension on a 20 % (w/v) SDS polyacrylamide gel in the absence of β-mercaptoethanol. Following electrophoresis, the gel strip containing the sample was excised and cross-links were broken by thiolysis *in situ*. After electrophoresis in the second dimension, all the protein spots found on the diagonal represent proteins whose mobilities were not affected by the cleavage of the cross-links. The spots removed from the diagonal represent proteins or domains that were initially cross-linked, where vertically aligned spots represent peptides that were cross-linked to each other.

This method was initially applied to extended native chromatin as a control (Fig. 5.13 A). In accordance with the results of Lennard and Thomas (1985), the major cross-linking product (line b) was between the NG and C fragments demonstrating that the predominant arrangement of neighbouring linker histones was head to tail. Additionally some cross-linking between NG fragments (line a) and C-fragments (line c) was also observed (compare with Fig. 5b of Lennard & Thomas, 1985). Lines d and e represent H5 cross-linked to NG and C fragments respectively. Some histone H2B was also found to be cross-linked to linker histones under more extensive cross-linking conditions as previously reported by Dashkevich *et al.* (1983). This was brought about by histone H2B having an increased solubility in perchloric acid compared to the other core histones (not shown).

The head to tail arrangement of linker histones found in native chromatin was also found in reconstituted chromatin (Fig. 5.13 B). Little cross-linking was observed between NG fragments; no C/C cross-linking was found to occur. It is unlikely that the observed cross-links were due to intramolecular cross-linking since cross-linked products were separated from monomeric histones by gel filtration. It was equally unlikely that the cross-links were formed between unbound linker histones in solution since the predominant cross-link under these conditions was found to be C/C (Kotthaus & Strätling, 1984).

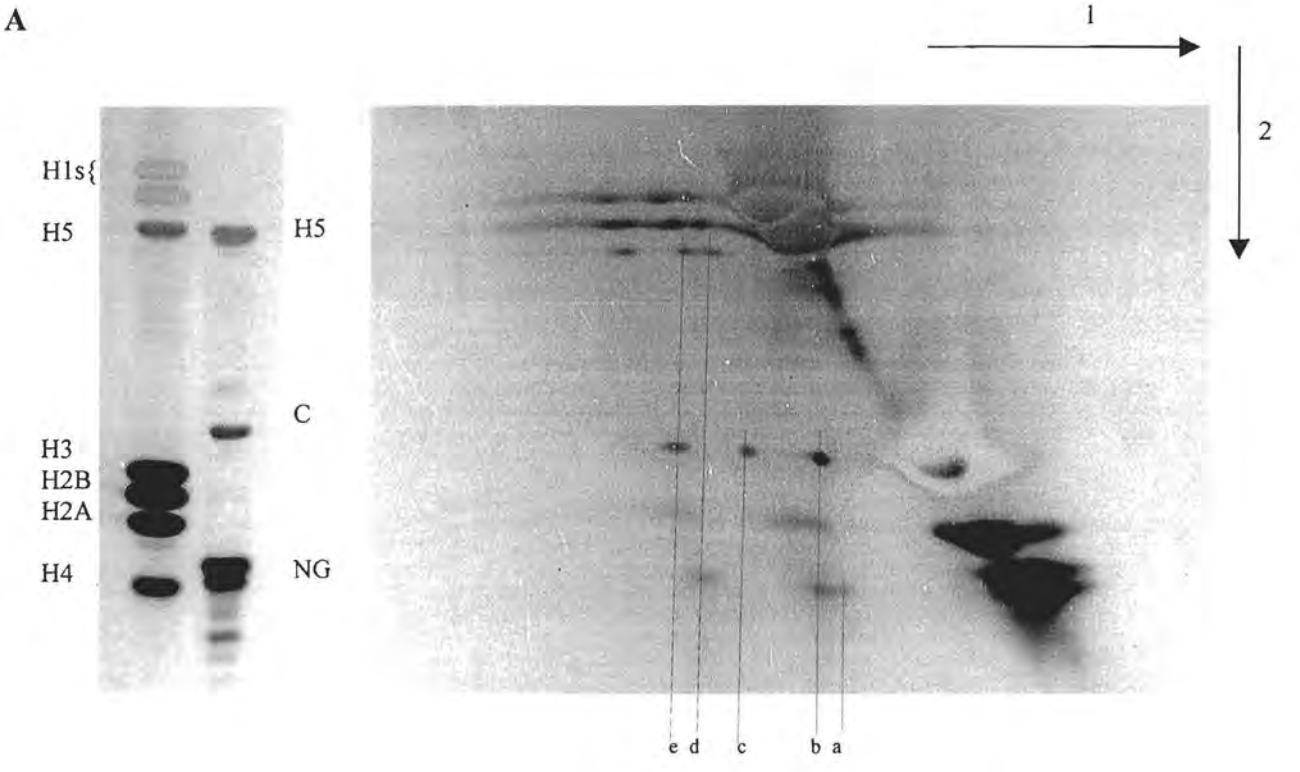

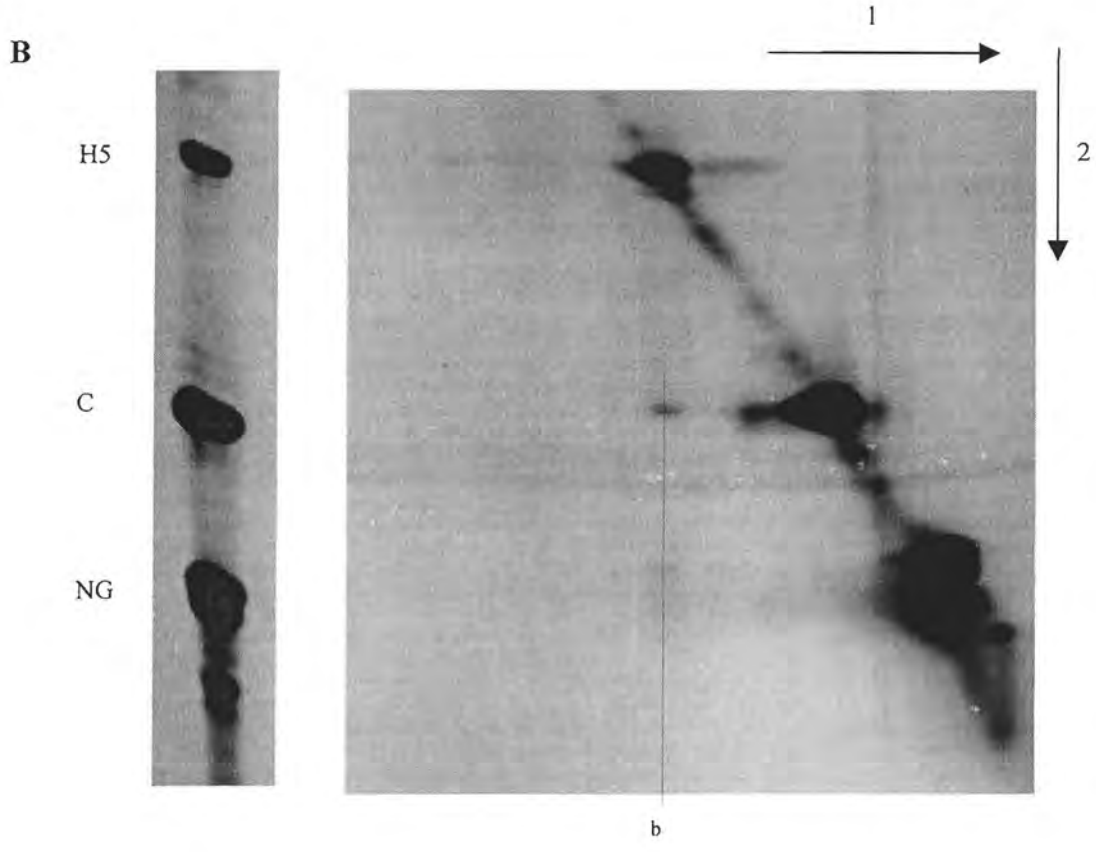

Figure 5.13. Two-dimensional SDS-PAGE analysis of the arrangement of neighbouring linker histones in extended native (A) and reconstituted (B) chromatin. Chromatin samples in 0.1 mM EDTA and 10 mM borate (pH 8.0) were cross-linked with 0.2 mg/ml dithiobis (propionic acid N-hydroxysuccinimide ester). Perchloric acid soluble cross-linked polymers were purified by gel filtration, digested with α-chymotrypsin and electrophoresed in the first dimension without β-mercaptoethanol. Cross-links were thiolysed *in situ* before electrophoresis in the second dimension. Gels were silver stained. A chymotryptic digest of pure histone H5 was used as the standard. The NG and C fragments do not silver stain equivalently. Lines a to e correspond to NG/NG, NG/C, C/C, H5/NG and H5/C cross-links respectively. A total acid extract of chicken erythrocyte nuclei is included in A.

Since the linker histone has no known enzymatic properties, the fidelity of reconstitution must be assessed using physicochemical techniques. These, by their nature, assess average structure. Although it is known that chicken erythrocyte chromatin has 1.3 moles linker histone per mole nucleosome (Bates & Thomas, 1981), direct addition of linker histone to stripped chromatin at low salt has been shown to result in precipitation once the input ratio of histone H5 per nucleosome exceeded 1.2 (Graziano *et al.*, 1988) whereas in other reports precipitation did not occur even at a ratio of 4:1 (Allan *et al.*, 1980b; Kaplan *et al.*, 1984). In contrast, ratios of 2.3 have been reported using addition at high salt and subsequent dialysis (Nelson *et al.*, 1979). These seemingly conflicting results may, however, be a reflection of the various methods used to determine linker histone concentration and incorporation. In the reconstitution system described here, an input ratio of 1.28 and 1.4 histone H5 per nucleosome for stripped pentanucleosomes and stripped long chromatin respectively led to the incorporation of H5 to levels akin to those of native chromatin. CM Sephadex C-25 is likely to act as an electrostatic sink and prevent the aggregation caused by binding of excess linker histone to low affinity sites on chromatin since polyanions have been reported to prevent the aggregation observed when linker histones were added to close-packed chromatin (Künzler & Stein, 1983).

The success of linker histone reconstitution using CM Sephadex C-25 as a linker histone deposition carrier was determined by comparison of the results obtained after MNase digestion, thermal denaturation and analysis of the orientation of neighbouring linker histones of reconstituted and native chromatin. In all cases, the reconstituted chromatin exhibited very similar properties to native chromatin, whilst the results obtained using stripped chromatin were significantly different. At the same time as this work was performed (Jason & Lindsey, 1997), long chromatin reconstituted with histone H5 using CM Sephadex C-25 was analysed by scanning force microscopy. At low ionic strength, the reconstituted chromatin displayed a native-like irregular, three-dimensional arrangement of nucleosomes whilst stripped chromatin exhibited a flat beads-on-a-string structure (Leuba, 1997).

The results presented above demonstrate that CM Sephadex C-25 is a readily available, cost effective and rapid method for the reassociation of histone H5 with

stripped chicken erythrocyte chromatin. Moreover it has the advantage of being autoclavable and can easily be separated non-enzymatically from the reconstituted chromatin by centrifugation or filtration. The linker histone reconstitution method of choice will depend on the nature of work being carried out. Reconstitution by salt dialysis (Nelson *et al.*, 1979; Biard-Roche *et al.*, 1982; Kaplan *et al.*, 1984; Meersseman *et al.*, 1991) is lengthy and can lead of nucleosome sliding and resultant close packing of nucleosomes at these elevated salt concentrations (Spadafora *et al.*, 1979; Allan *et al.*, 1980b). This method would therefore be unsuitable for reconstitution of linker histones onto nucleosomal arrays lacking strong nucleosome positioning sites. Cell extracts would not be used as an assembly method if one intends performing work on a defined system. Soluble histone carriers that cannot be removed from the reconstitution system could, due to their ionic nature, prevent unequivocal interpretation of the results obtained from subsequent experiments. To study linker histone binding to nucleosomal arrays containing core histone variants or post-translationally modified core histones, a useful strategy would be to generate spaced nucleosomes by reconstituting octamers onto a tandem array of a nucleosome positioning sequence such as the 208-n repeats of 5S rDNA (Simpson *et al.*, 1985) and to then use an insoluble histone carrier as described here to reconstitute the linker histone of choice onto this array. This method would be rapid, overcome problems resulting from close packing of nucleosomes and be free of interference from the linker histone carrier, which can easily be removed. Additionally, the effect of linker histone addition at various salt concentrations could easily be investigated since CM Sephadex C-25 can preferentially bind linker histones over core histones at and below 0.6 M NaCl (Libertini & Small, 1980).

6 An investigation into the effect of the rate of micrococcal nuclease digestion on the observed repeat length

6.1 Introduction

During repeat length determinations (see section 5), the repeat length of the chromatin was found to decrease in accordance with the concentration of MNase used (not shown). Since the amount of enzyme used influences the reaction rate, the relationship between the rate of MNase digestion and the observed repeat length was investigated for a variety of chromatins.

The arrangement of the components of chromatin at the simplest level are remarkably conserved over the wide range of species and cell types thus far examined (for reviews see van Holde, 1989 and Wolffe, 1995). The four core histones, especially H3 and H4, are amongst the most highly conserved proteins thus far described. The interaction between core histones has also been conserved in evolution as the reconstitution of hybrid histone octamers with histones from heterologous organisms has been reported (e.g. Richmond *et al.*, 1988; Lindsey & Thompson, 1990, Lindsey *et al.*, 1991; Lindsey & Thompson, 1992). The binding of DNA by the histone octamer is equally conserved in that digestion of chromatin with nucleases such as micrococcal nuclease (MNase) invariably yields the core particle as the fundamental unit of chromatin organisation (van Holde, 1989). Despite this high degree of conservation in the basic structure of chromatin, the arrangement of nucleosomes along the DNA varies widely not only between species, cell types from the same species but also for different genes within the same cell type (van Holde, 1989). Thus the repeat length, the average length of DNA between equivalent points on adjacent nucleosomes, has been reported to vary from 154 bp to over 240 bp for different chromatins. Additionally the nucleosomal repeat length has been reported to vary within the same cell type during differentiation and development (Weintraub, 1978; Savic *et al.*, 1981; Jaeger & Kuenzle, 1982). These variations are likely to reflect altered states of the underlying chromatin, but the possibility of any additional involvement of micrococcal nuclease in the generation of this heterogeneity has often been overlooked.

Despite this variance in repeat lengths, no correlation has been found between the chromatin fibre diameter and the repeat length in frozen hydrated specimens (Woodcock, 1994). This has serious repercussions for models of higher order chromatin structure.

The histone octamer alone has been shown to support the binding of 167 bp DNA with transient protection against MNase digestion extended to 188 bp if the linker histone is present (Weischet *et al.*, 1979; Lindsey & Thompson, 1989). Whereas repeat lengths longer than 188 bp such as reported for repressed chromatin from sea urchin sperm and chicken erythrocytes can easily be explained, it is difficult to understand, without invoking nucleosomal sliding, how repeat lengths less than 188 bp might be generated if the protection of 20 bp of linker DNA by linker histones is ubiquitous. An explanation is even more difficult for repeat lengths shorter than 167 bp, as reported for *Aspergillus nidulans* (Morris, 1978) and *Schizosaccharomyces pombe* (Godde & Widom, 1992) unless a different form of DNA packaging is invoked.

The number of base pairs associated with any particular n-meric chromatin fragment is known to decrease as MNase digestion proceeds (Lohr *et al.*, 1977; Allan *et al.*, 1984; Godde & Widom, 1992). Although it has been postulated that this reduction in length is due to the exonucleolytic activity of MNase, the reduction in length observed was greater than could be explained by this mechanism alone. Thus a chicken erythrocyte tetrameric chromatin fragment should only be reduced to approximately 790 bp by exonucleolytic activity rather than the 750 bp observed (Lohr *et al.*, 1977). Octamers have, however, been shown to be relatively mobile on DNA, with several rotationally conserved positions being adopted even on DNA containing strong positioning sequences such as the 5S rRNA gene (Pennings *et al.*, 1991; Meersseman *et al.*, 1992). This mobility is restricted in the presence of linker histones (Pennings *et al.*, 1994). Although the core histones are highly conserved in evolution, the linker histone shows far higher sequence diversity (for reviews see van Holde, 1989; Zlatanova & van Holde, 1996). Not only does the ratio of linker histone to core histones vary between cell types but the tightness of binding of different linker histone variants to DNA also varies (Clark & Thomas, 1988).

Since the linker histone has been shown to migrate from shorter to longer chromatin fragments (Thomas & Rees, 1983), one possible explanation for repeat lengths less than 188 bp is that these are brought about by digestion conditions that result in nucleosome sliding to observed repeat lengths shorter than the native one. Despite evidence that nucleosome sliding is accentuated under conditions of increased temperature and salt (Spadafora *et al.*, 1979), many determinations of the repeat length have been carried out at 37 °C (van Holde, 1989).

Temperature and enzyme concentration were used to modulate the activity of MNase to determine if the rate of MNase digestion influences the observed repeat length of chromatin at equivalent extents of digestion.

6.2 Results and Discussion

6.2.1 Micrococcal nuclease digestion of chicken erythrocyte chromatin

Chicken erythrocyte chromatin was digested at 20 °C in 20 mM NaCl and 10 mM Tris-HCl (pH 7.4) with 16 units MNase (Sigma) per 20 A_{260} units (Fig. 6.1 A). Using these conditions, the repeat length of the chromatin after one min digestion was 203 ± 4 bp and decreased with increased digestion time to 191 ± 2 bp after 2 min digestion and to 185 bp ± 2 bp after 5 min digestion. The data shown in Fig. 6.1 B reflects the average of 5 such determinations. Continued digestion to 10 min resulted in no further decrease in the repeat length. Extrapolation of the data to zero time resulted in an initial repeat length of 214 bp, in the range of 207 to 216 bp reported previously by several authors for chicken erythrocyte chromatin (van Holde, 1989). To analyse the possible contribution of exonucleolytic trimming to the decreased repeat length observed, the nucleosomal fragment sizes after 1 min digestion were replotted (Fig. 6.1 C) after subtracting 36 bp from each fragment. This value represents the average number of base pairs that would be removed exonucleolytically from a polynucleosomal fragment with a 203 bp repeat length to yield 167 bp chromatosomes at either end. This assumes that the polynucleosomal fragment represents the weight average of all such n-meric fragments having linker DNA lengths between 0 and 36 bp at each end. Figure 6.1 C indicates that exonucleolytic trimming of 203 bp repeat length chromatin could not be solely responsible for the observed 185 bp repeat length as the manipulated data does not correlate with the latter. The manipulated data also displays a negative intercept with the ordinate, characteristic of systematic trimming by MNase (Villeponteau *et al.*, 1992), whereas all repeat length determinations (and those determined later in this study) displayed positive intercepts with the ordinate. Moreover, digestion at 4 °C, which has been reported to suppress the exonucleolytic activity of MNase (Noll & Kornberg, 1977) also resulted in the eventual production of a ± 185 bp repeat length, albeit at a slower rate (see below).

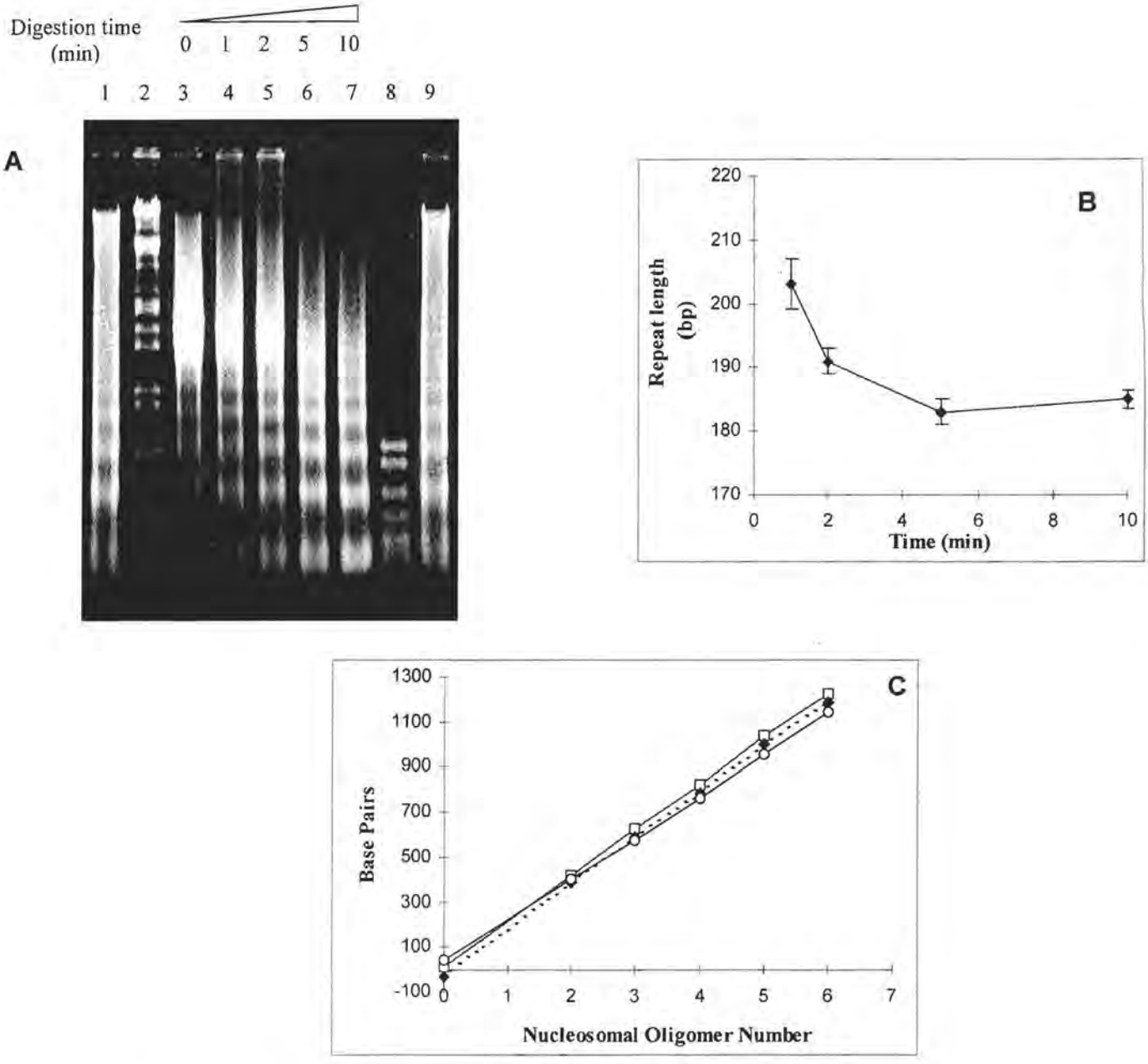

Figure 6.1. MNase digestion of long chicken erythrocyte chromatin. Digestion was performed in 20 mM NaCl, 0.6 mM $Ca^{2+}$and 10 mM Tris-HCl (pH 7.4) using 16 units MNase per 20 A_{260} units at 20 °C. (**A**) Agarose gel electrophoresis of the digestion products after 0, 1, 2, 5 and 10 min digestion (lanes 3-7). Lanes 1 and 9 are the same partial digest of chicken erythrocyte nuclei run to ensure that the gel lanes were parallel. Lane 2 is an *Eco* RI/*Hind* III digest of λ phage; lane 8 is a *Hpa* II digest of pBR322. (**B**) Plot of the repeat length versus digestion time for the average of 5 digests as shown in A. (**C**) Plot of the base pairs associated with each n-meric nucleosome band after 1 min (□) and 10 min (○) digestion with MNase. The data associated with the 1 min digest were replotted after subtracting 36 bp from each fragment (♦).

6.2.2 The effect of the rate of micrococcal nuclease digestion on the observed repeat length

6.2.2.1 Digestion of chicken erythrocyte chromatin at different temperatures

In order to investigate the effect of the rate of MNase digestion on the observed repeat length, chicken erythrocyte chromatin was initially digested with the same amount of MNase but at different temperatures (Fig. 6.2). Chromatin preparations were incubated at the desired digestion temperature for 10 min prior to the addition of MNase. Digestion at 20 °C was taken as the standard digestion rate. In order to compare the apparent repeat length after an equivalent extent of digestion, the frequency of time points at the other temperatures was adjusted as described in section 8. Sample times for digestion at 4 °C were extended by a factor of 15 as the activity of MNase towards chicken erythrocyte chromatin was determined to be 15 times slower at 4 °C compared with that at 20 °C. Decreasing the digestion rate by performing the digest at 4 °C yielded an initial repeat length of 210 ± 2 bp. Continued digestion resulted in the repeat length decreasing to 183 bp via a 198 bp intermediate.

The same starting chromatin preparation was next digested at 37 °C. This resulted in an initial repeat length of 185 ± 1 bp which did not change as digestion proceeded. The frequency of the time points for the 37 °C digests was decreased to compensate for the 2.5 fold increase in the rate of digestion at this temperature. Digestion of the same starting chromatin sample at 20 °C after exposure to 37 °C for four hours (Fig. 6.2) was very similar to digestion without prior exposure (Fig. 6.1).

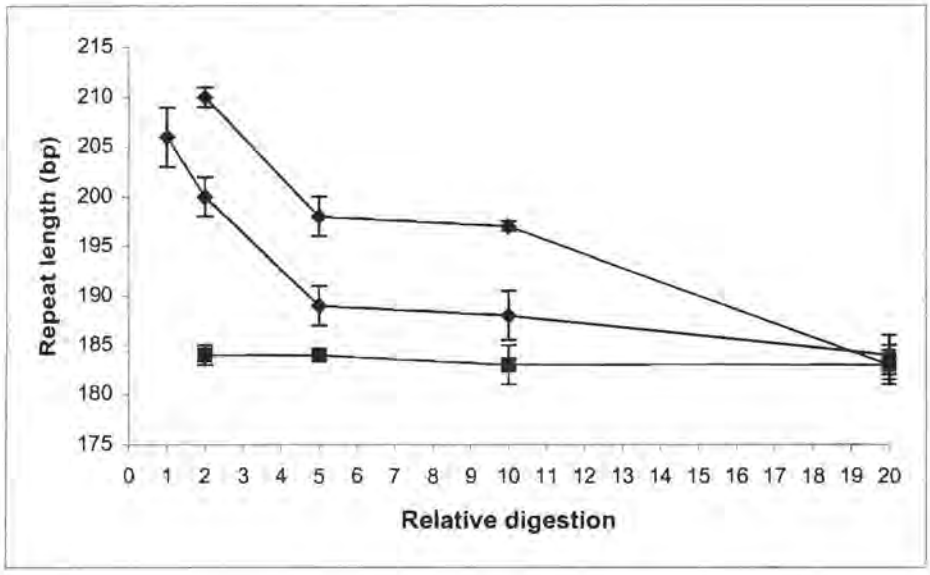

Figure 6.2. The rate of MNase digestion affects the rate of decrease of the observed repeat length. Plot of repeat length versus relative digestion for chicken erythrocyte chromatin digested with MNase in 10 mM NaCl, 0.6 mM Ca^{2+}, 10 mM Tris-HCl pH 7.4 at 4 °C (♦), 37 °C (■) and at 20 °C after exposure to 37 °C for four hours (•).

These results indicated that the decreased repeat length is not brought about by rearrangements of chromatin at the higher temperature but rather by performing the digestion at a faster rate at 37 °C. Similar observations by other authors that the observed repeat length decreased with increasing digestion time have been attributed to preferential digestion of different populations of chromatin (Allan *et al.*, 1984). This explanation is unlikely for the results shown here since the same starting chromatin preparation was digested to the same extent, albeit at different temperatures. A possible cause for the decreased repeat lengths observed could be an increased nucleosomal mobility caused by higher temperature (Pennings *et al.*, 1991) or an increased digestion rate.

6.2.2.2 Digestion of chicken erythrocyte chromatin using different concentrations of MNase

To further investigate the effects of an increased digestion rate, chicken erythrocyte chromatin was digested at 20 °C in 10 mM NaCl buffer using increasing amounts of MNase per 20 A_{260} units. The intermediate digestion conditions (dashed line, Fig. 6.3 A) were identical to that used in 20 mM NaCl buffer at 20 °C (Fig. 6.1). Samples were taken at different time points for each digest so that the extent of digestion of each sample was again equivalent at each time point. The extent of digestion, D, was assumed to be proportional to the concentration of MNase (C_o) and the time of digestion (t) over the range of MNase concentrations used. It was found (Fig. 6.3 A) that at the slowest digestion rate the initial repeat length was 214 ± 3 bp, with the repeat length decreasing to 200 ± 1 bp after 5 min relative digestion. At the intermediate digestion rate, the initial repeat length was 211 ± 1 bp; continued digestion resulted in this decreasing to 195 ± 3 bp via a 200 bp intermediate. The most rapid digest showed an initial repeat length of 200 ± 3 bp which decreased to 185 ± 2 bp via a 190 bp intermediate. These results further indicated that an inverse relationship existed between the rate of digestion and the observed repeat length. Histone proteolysis was ruled out as the cause of these observations since no degradation was evident when the histones associated with the chromatin digested with the highest concentration of MNase were analysed by SDS-PAGE after MNase digestion of the chromatin (Fig. 6.3 B).

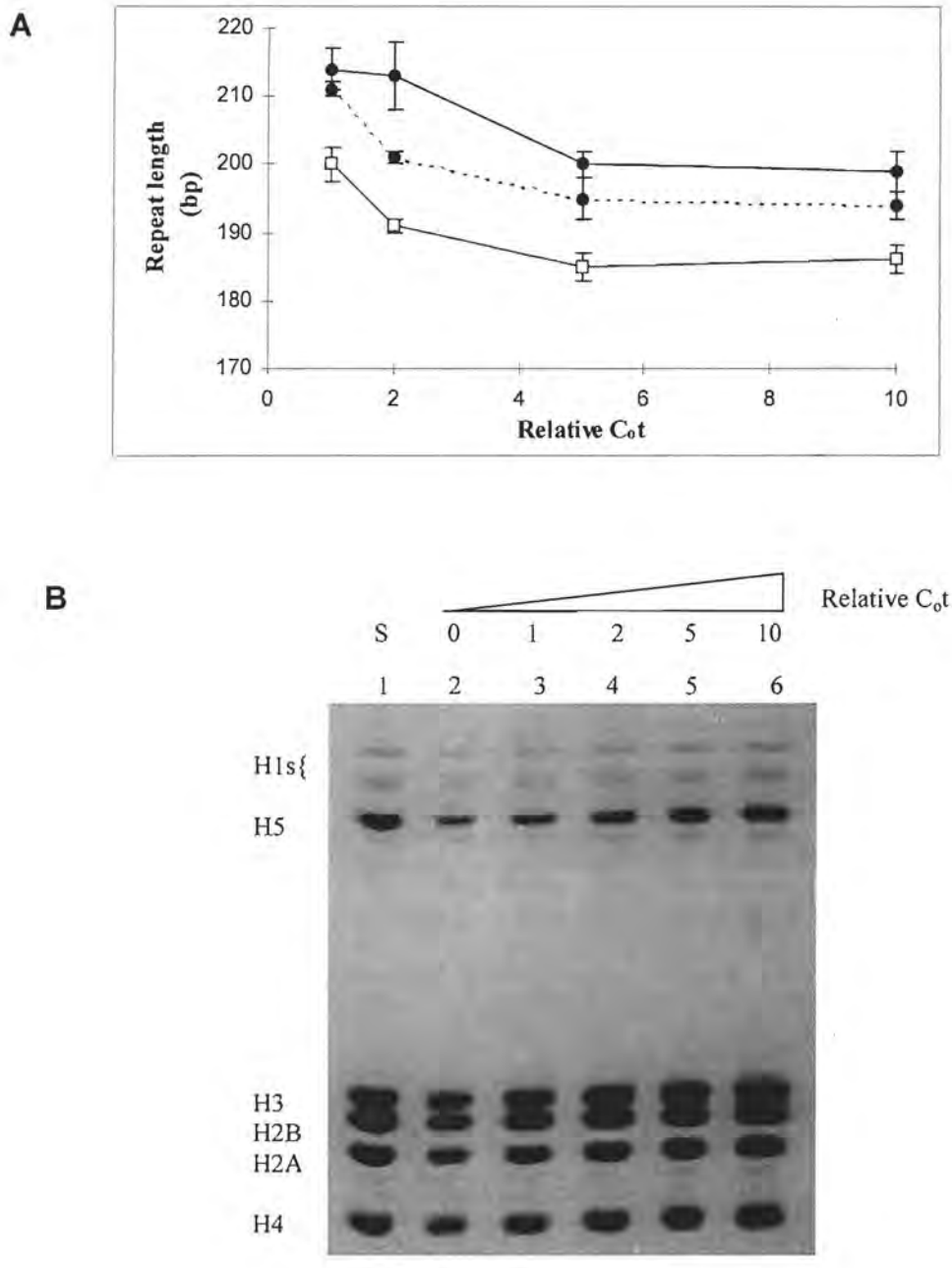

Figure 6.3. MNase digestion of chicken erythrocyte chromatin using increasing concentrations of MNase. (**A**) Plot of repeat length versus relative $C_o t$ for MNase digestion of chicken erythrocyte chromatin carried out at 20 °C in 10 mM NaCl, 0.6 mM Ca^{2+}, 10 mM Tris-HCl (pH 7.4) using 3.2 (♦), 16 (•) and 80 (□) units MNase per 20 A_{260} units. The extent of digestion, $D = C_o t$ where C_o is the units of MNase added and t is the time of digestion, was equivalent at each time point irrespective of the amount of enzyme added. (**B**) SDS-PAGE of the histones present in chicken erythrocyte chromatin samples digested using 80 units MNase per 20 A_{260} units. The standard (S) in lane 1 is a total acid extract of chicken erythrocyte nuclei. The histones associated with the chromatin at the relative extents of digestion shown in A are in lanes 2 to 6.

6.2.3 The effect of the rate of MNase digestion on the observed repeat length of soy bean and calf neuronal chromatins

To investigate whether the observation that a decreased repeat length occurred due to an increased rate of MNase digestion was unique to chicken erythrocyte chromatin, chromatin from two other sources was digested to equivalent extents at different rates. Soybean chromatin has been reported to have a repeat length of 175 ± 8 bp (Leber & Hembelen, 1979), which is significantly less than the 188 bp protection afforded by the linker histone in chicken erythrocytes. Soy nuclei were prepared from soybean hypercotyls and digested in buffer A (Hewish & Burgoyne, 1973) using 2.6 (Fig. 6.4) and 26 units MNase per 20 A_{260} units. Samples were again withdrawn from the digests at different times to compensate for the different rates of digestion, assuming that $D = C_o t$. The initial repeat length for the higher concentration of MNase was 167 ± 4 bp whilst at the lower concentration of MNase the observed repeat length was 188 ± 3 bp.

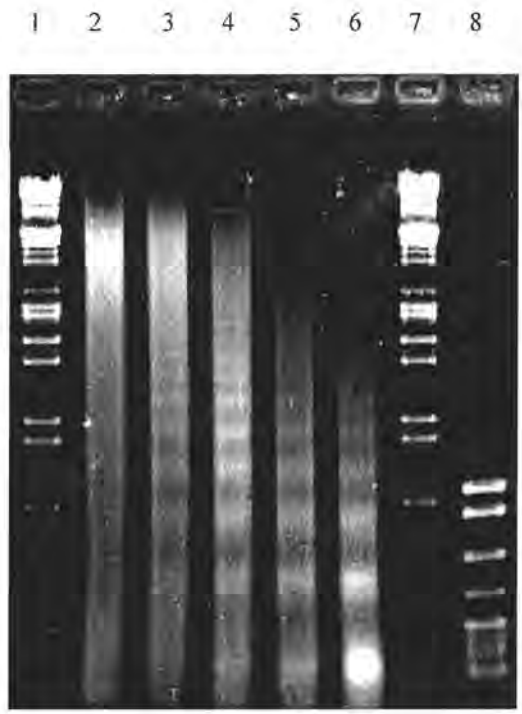

Figure 6.4. MNase digestion of soy bean nuclei at 20 °C using 2.6 units MNase per 20 A_{260} units. Digestion was stopped after 0, 1, 2, 5 and 10 min (lanes 2-7). Lanes 1 and 7 are *Eco* RI/*Hind* III digests of λ phage. Lane 8 is a *Hpa* II digest of pBR322.

Neuronal chromatin has been reported to exhibit a repeat length of between 160 bp and 168 bp (Allan *et al.*, 1984; Pearson *et al.*, 1984; Brown & Sutcliffe, 1987) although considerably longer lengths in the range of 175 bp to 200 bp were also observed by these authors at early times of digestion. These longer repeat lengths were either ignored, attributed to glial cell contamination or to heterogeneity of repeat lengths. Neuronal nuclei were prepared from calf brain by sucrose step gradient centrifugation. Since glial cell nuclei, which have been reported to exhibit a repeat length of 201 bp (Pearson *et al.*, 1984), have been reported to contaminate preparations of neuronal cell nuclei, the neuronal and glial nuclei preparations were examined by light microscopy (not shown). The neuronal fraction was essentially free of glial nuclei and appeared identical to that reported previously (Thompson, 1973). Neuronal nuclei were digested in buffer A (Hewish & Burgoyne, 1973) with either 0.6 or 12 units MNase per 20 A_{260} units. The repeat length observed at the faster rate of digestion was 175 ± 9 bp. At the slower rate of digestion, the repeat length was determined to be 189 ± 4 bp after 80 min digestion and decreased to 184 ± 4 bp after 160 min digestion (Fig. 6.5). Thus the rate of MNase digestion also influenced the observed repeat length of neuronal chromatin.

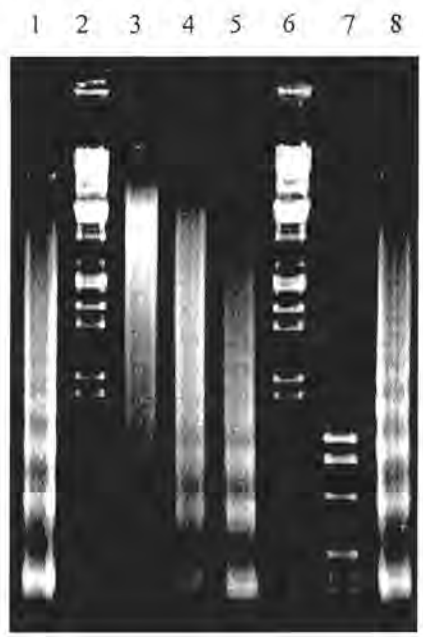

Figure 6.5. MNase digestion of calf brain neuronal nuclei using 0.6 units MNase per 20 A_{260} units at 20 °C. Samples were removed at 40, 80 and 160 min (lanes 3-5). Lanes 1 and 8 are the same partial digest of chicken erythrocyte nuclei as for Fig. 6.1 A. Lanes 2 and 6 are *Eco* RI/*Hind* III digests of λ phage. Lane 7 is a *Hpa* II digest of pBR322.

Neuronal nuclei differ from glial nuclei in that the neuronal nuclei display higher transcriptional activity and decreased linker histone content (Pearson *et al.*, 1984 and references cited therein). One or both of these characteristics are found in most short repeat length chromatins examined (e.g. Godde & Widom, 1992; Villeponteau *et al.*, 1992; Cavalli & Thoma, 1993). It is known that linker histones exhibit a preference for binding to longer chromatin fragments (Thomas & Rees, 1983) and that exchange of linker histones can occur even in low ionic strengths buffers (Louters & Chalkey, 1984). It is therefore possible that exchange of linker histones from shorter chromatin fragments produced by MNase digestion would render them more susceptible to nuclease induced sliding as digestion proceeds, especially when that chromatin contains less than one linker histone per nucleosome.

Although the factors that determine the initial spacing of nucleosomes are still not well understood, charge neutralisation and chromatin topology seem to play an important role (Blank & Becker, 1995; 1996). However the establishment of internucleosomal repeat and the internucleosomal spacing observed after digestion experiments may well be different. In agreement with many other authors (e.g. Lohr *et al.*, 1977; Allan *et al.*, 1984; Watkins & Smerdon, 1985; Godde & Widom, 1992) the observed repeat length of chromatin was also found to decrease as digestion proceeded. Increasing the rate of MNase digestion resulted in a concomitant decrease in the repeat length of chromatins differing in linker histone content, differentiation status and transcriptional activity. The contribution of the rate of MNase digestion to the observed repeat length should not be underestimated since different rates of digestion affected the observed repeat length of the same chromatin digested to the same extent by around 20 bp. This effect was even observed in chicken erythrocyte chromatin where nucleosome mobility might be expected to be restricted by the tightly bound linker histone H5. The mechanism whereby nucleosomal sliding is induced by relatively high rates of MNase digestion is difficult to conceive. Assuming that DNA strand separation is required prior to MNase cleavage, it is possible that this destabilises adjacent nucleosomes with the effect transmitted some distance along the nucleosomal array. Faster rates of digestion are likely to result in multiple cleavage of more accessible chromatin regions and would therefore enhance nuclease induced nucleosomal sliding in these fragments whereas at slower rates of digestion these

effects would be more distributed. It is possible that chromatin samples in which nucleosomes are less restricted in mobility, for example due to alterations in histone and non-histone protein content or binding affinity, are more susceptible to MNase induced nucleosome sliding. In this respect it is interesting to note that in newly replicated DNA where reduced histone-DNA interactions occur, prior cross-linking of histones resulted in a repeat length similar to that of bulk chromatin. Without prior cross-linking, however, this repeat length was significantly shorter indicating involvement of the digestion process in the generation of a short repeat length (Smith *et al.*, 1984).

Analysis of the chromatin repeat lengths observed from many cell types of many species shows that there are distinct groupings of repeat length values at around 165 bp, 185 bp and in excess of 185 bp (van Holde, 1989). The groupings around 165 bp and 185 bp could be attributed to nucleosome sliding to the limit of the core particle and the chromatosome respectively. Several authors have reported repeat lengths shorter than 167 bp (Morris, 1978; Silver, 1979; Pearson *et al.*, 1984; Godde & Widom, 1992). These could presumably arise from nucleosome sliding past the limit of the core particle (Weischet & van Holde, 1980), since it is known that the histone-DNA interactions are weakest near the edges of the core particle.

7 Conclusions

Although octamers containing ubiquitinated histones can be reconstituted successfully, few *in vitro* studies have been used to investigate the role of this modification in chromatin (Kleinschmidt & Martinson, 1981; Davies & Lindsey, 1994). In this study, hybrid octamers containing uH2A were reconstituted onto random sequence 167 bp DNA and a 208 bp fragment of the *Lytechinus variegatus* 5S rDNA (Simpson & Stafford, 1983; Simpson *et al.*, 1985). These nucleosomes behaved very similarly to control nucleosomes in that their thermal denaturation profiles (section 2) and positions on the 208 bp DNA (section 3) were essentially the same. This suggests that, in agreement with previous studies (Kleinschmidt & Martinson, 1981; Davies & Lindsey, 1994), this post-translational modification has little effect on nucleosome structure.

One of the aims of this study was to determine if uH2A influences linker histone binding since some evidence suggests that chromatin enriched in ubiquitinated histones has a reduced linker histone content (Davie & Nickel, 1987). The results discussed in sections 2 and 3 showed that under the conditions used, uH2A did not inhibit linker histone binding to nucleosomes but rather favoured it. This is in agreement with cross-linking studies that have shown that H1 can be cross-linked to uH2A both *in vitro* (Nelson *et al.*, 1979) and *in vivo* (Bonner & Stedman, 1979). This effect was more subtle with 167 bp nucleosome cores than with 208 bp nucleosomes suggesting that the length of DNA associated with the octamer may play a role in determining accessibility to linker histone binding. Ubiquitin does not influence linker histone mediated positioning of nucleosomes as the positions of control and uH2A chromatosomes on the 208 bp DNA were also the same (section 3). Further investigations will be required to determine if linker histone binding to nucleosomal arrays containing uH2A is also unaffected.

It therefore seems that if histone ubiquitination is involved in modulating chromatin structure, it is likely to influence higher order chromatin structures, as cell cycle studies imply (Matsui *et al.*, 1979; Wu *et al.*, 1981; Mueller *et al.*, 1985). As a first step towards investigating this possibility, the folding of control and uH2A hybrid nucleosomal arrays in the absence of linker histones was examined using a quantitative agarose gel electrophoresis assay (Fletcher *et al.*, 1994a,b; Hansen *et al.*, 1997). Whilst the mobility of uH2A arrays in the agarose matrix was consistently lower than that of control arrays, the extent of folding of both arrays in response to 2 mM $MgCl_2$ was similar (section 4). Thus, under the conditions used, ubiquitin did not affect chromatin folding. The flexible carboxyl terminal tail of ubiquitin may allow movement of the ubiquitin moiety such that chromatin compaction is not affected by steric clashes. This model is feasible if chromatin compaction occurs in a three-dimensional zig-zag fashion as proposed by Woodcock and colleagues (Bednar *et al.*, 1998). This is consistent with reports of ubiquitin (Izquierdo, 1994) and uH2A (Baarends *et al.*, 1999) being associated with compact chromatin structures. It must be noted that in the absence of linker histones, a proportion of nucleosomal arrays can exist in a compact structure that sediments at ~55 S whilst most of the arrays exist as a structure of intermediate compaction that sediments at ~40 S (Schwarz & Hansen, 1994). Further studies will be required to determine if ubiquitin influences the extent of compaction of linker histone containing chromatin. Interestingly, ubiquitinated nucleosomal arrays were found to oligomerise at lower $MgCl_2$ concentrations than control arrays (section 4). This property may be of significance for stabilising interactions between uH2A containing chromatin regions. The absence of ubiquitinated histones in metaphase chromosomes (Matsui *et al.*, 1979; Wu *et al.*, 1981; Mueller *et al.*, 1985) may therefore reflect the inaccessibility of histone ubiquitination sites to the ubiquitination machinery rather than the necessary removal of the ubiquitin moiety to allow chromosome condensation. It will also be of interest to determine if the ubiquitin released from histones at metaphase provides a source of free ubiquitin that is used to tag other proteins for degradation by the ubiquitin-proteasome pathway.

A novel methodology was developed to reconstitute H5 onto long chromatin stripped of linker histones (section 5). Polygalacturonic acid (pectin) was initially used as a linker histone carrier but its removal from the reconstitution mixture proved to be problematic. The suitability of the anionic resin, CM Sephadex C-25, as a carrier to reconstitute H5 onto stripped pentanucleosomes and stripped long chromatin was investigated. Comparison of native, reconstituted and stripped chromatins after MNase digestion, thermal denaturation and determination of neighbouring linker histone orientation revealed that the reconstituted chromatin was very similar in all cases to native chromatin but substantially different from stripped chromatin. This technique provides an effective, simple and relatively quick method for linker histone reconstitution that could be used to reconstitute linker histones onto defined sequence nucleosomal arrays.

The observed repeat length of chromatin was found to be inversely correlated to the rate of MNase digestion (section 6) for chromatin from three different sources differing in linker histone content, differentiation status and transcriptional activity. This result supports previous suggestions that MNase may induce nucleosome sliding and result in erroneously low repeat length values (Weischet & van Holde, 1980; Smith *et al.*, 1984). The observed repeat length is therefore likely to depend not only on the original nucleosome spacing but also on the susceptibility of MNase induced sliding of nucleosomes. These results suggest in addition to choosing conditions that limit end-trimming of nucleosomes (Noll & Kornberg, 1977), low rates of MNase digestion should also be used in order to minimise artifacts.

8 Methods

All operations were performed at 4 °C unless stated otherwise.

8.1 Isolation of chicken erythrocyte nuclei

One litre of chicken whole blood was collected from freshly slaughtered chickens at the local abattoir using ACD buffer (12 mM citric acid, 90 mM tri-sodium citrate, 18 mM sodium monophosphate and 13 mM D-glucose) as an anti-coagulant. The blood was filtered through two layers of cheesecloth and all further operations were carried out at 4 °C. The blood was centrifuged at 1000 g for 5 min and the plasma and white blood cells were removed by aspiration. Erythrocytes were washed three times in SSC buffer (10 mM trisodium citrate and 150 mM NaCl) by centrifugation at 5000 g for 5 min. In order to release the nuclei, erythrocyte membranes were lysed by resuspending the pellet obtained after the last washing step into SSC containing 0.1% (v/v) Triton X100. The suspension was centrifuged as before, and this procedure was repeated until the creamy coloured nuclei were free of unlysed erythrocytes. Nuclei were finally washed twice in 5 to 10 volumes of buffer A (15 mM Tris-HCl (pH 7.5), 65 mM NaCl, 60 mM KCl, 0.15 mM spermine, 0.5 mM spermidine, 0.2 mM EGTA, 0.2 mM EDTA, 5 mM β-mercaptoethanol and 10 μM PMSF) (Hewish & Burgoyne, 1973). Nuclei were stored at –20 °C in buffer A containing 50 % (v/v) glycerol.

8.2 Isolation of chicken erythrocyte histones

Stored nuclei were pelleted at 10 000 g for 5 min and washed twice with buffer A to remove the glycerol. The washed nuclei were homogenised with a Kinematica Polytron in 10 volumes of 0.25 M HCl. The homogenate was rolled for 30 min to ensure complete extraction of histones before centrifugation at 10 000 g for 15 min. The supernatant containing the acid soluble histones was dialysed overnight against 20 litres of deionized water with one change. The dialysate was lyophilised and the histones were stored at –20 °C. BioGel P60 (100-200 mesh) chromatography was performed at room temperature in 50 mM NaCl and 20 mM HCl to resolve the

histones into a H2A fraction, a H2B-H3 fraction and a H4 fraction. Column dimensions were 5 × 90 cm and a 42 ml per hour flow rate was used. Fractions were analysed by SDS-PAGE prior to pooling and stored at 4 °C after the addition of sodium azide to 0.01 % (w/v).

8.3 Purification of Chicken H3 and H2B

One quarter of the pooled H2B-H3 fractions from the BioGel P60 chromatographic step was concentrated by ultrafiltration under nitrogen using an Amicon PM-10 membrane to a final volume of approximately 2 ml, and chromatographed on a Sephadex G100 column (1.5 × 100 cm) in 50 mM NaCl and 20 mM HCl at a flow rate of 8 ml per hour. One millilitre fractions were collected and analysed by SDS-PAGE. Fractions containing pure H3 and H2B, respectively, were pooled and stored at 4 °C with after the addition of sodium azide to 0.01 % (w/v).

8.4 Purification of linker histones from chicken erythrocyte nuclei

Extraction of linker histones from chicken erythrocyte nuclei was carried out using CM Sephadex C-25 as described by Garcia-Ramirez and colleagues (Garcia-Ramirez *et al*, 1990), as it has been reported that acid irreversibly alters linker histone structure (Brand *et al.*, 1981). The pooled histone H5 and H1 fractions were dialysed against 10 mM NaCl, 0.1 mM EDTA and 10 mM Tris-HCl (pH 7.4) and concentrated by ultrafiltration at 4 °C under nitrogen using an Amicon PM-10 membrane. Purified linker histones were stored in 50 % (v/v) glycerol at -20 °C and were found to remain stable for up to one year. Storage in glycerol counteracts the problem of histone precipitation that occurs upon repeated freezing and thawing of histone samples as reported by Kaplan *et al.* (1984).

8.5 Isolation of calf ubiquitinated H2A (uH2A)

8.5.1 Isolation of calf thymus histones

Thymus glands were collected on ice from freshly slaughtered calves at the local abattoir. If necessary, thymus glands were stored at –70 °C until required. All manipulations were carried out at 4 °C. Blood vessels, connective tissue and excess fat were removed from the glands using scissors. The thymus was cut up into small pieces and homogenised in a Waring blender for 2 minutes in approximately 5 volumes 140 mM NaCl, 10 mM trisodium citrate and 5 mM sodium bisulphite. The homogenate was filtered through four layers of cheesecloth and centrifuged at 5000 g for 10 min. The nucleoprotein pellet was washed 5 times in the same buffer. The washed pellet was homogenised in approximately 10 volumes of 0.4 M HCl with a Kinematica Polytron. The homogenate was rolled for 30 min to ensure complete extraction of histones before centrifugation at 10 000 g for 15 min. The supernatant containing the acid soluble histones was dialysed overnight against 20 litres of deionized water with one change. The dialysate was lyophilised and the histones stored at –20 °C. To purify individual histones, approximately 250 mg lyophilized histones were dissolved in 5 ml 8 M urea and 4 % (v/v) β-mercaptoethanol, and chromatographed at room temperature on a 4.5 × 100 cm BioGel P60 (100-200 mesh) column. The column buffer was 50 mM NaCl and 20 mM HCl and the flow rate 40 ml per hour. Histones were resolved into a H2A-H3 fraction, a H2B fraction, and a H4 fraction.

8.5.2 Purification of uH2A

H2A fractions from three BioGel P60 column runs were pooled and adjusted to 6 M urea and 50 mM sodium acetate (pH 5.4) and loaded onto a 1.5 × 20 cm Whatman CM 52 column equilibrated in 6 M urea, 50 mM NaCl and 50 mM sodium acetate (pH 5.4). Bound proteins were eluted at room temperature with a linear salt gradient (125–175 mM NaCl) in the same buffer. Fractions were analysed by SDS-PAGE, and

those containing uH2A were pooled, dialysed against 40 litres deionized water, and lyophilised. The final purification step required pooled fractions from three Whatman CM 52 column runs. Lyophilised pools were resuspended in 8 M urea, 2 mM Tris-HCl and 10 % (v/v) β-mercaptoethanol and rolled for 4 hours at 4 °C. The pH was adjusted to 2.2 (Thorne *et al.*, 1987) with HCl and the solution was applied to a 2.5 × 100 cm BioGel P60 (100-200 mesh) column equilibrated in 7 M urea and 2 mM Tris-HCl (pH 2.2). The flow rate used was 4 ml per hour and approximately 0.5 ml fractions were collected. Fractions containing pure uH2A were identified by SDS-PAGE analysis, pooled and dialysed against deionized water. Purified fractions were stored in acid washed counting vials at –20 °C.

8.6 Reconstitution of histone octamers

Stoichiometric amounts of the four individual core histones were mixed to give a final protein mass of 2 mg. Chicken erythrocyte H3, H4 and H2B and calf H2A were used to assemble control hybrid octamers. Calf uH2A replaced H2A when uH2A hybrid octamers were assembled. The histone mixture was dialysed overnight at 4 °C against 2 litres of 2 M NaCl and 10 mM Tris-HCl (pH 7.4). The dialysate was concentrated to approximately 1ml by ultrafiltration under nitrogen using an Amicon PM-10 membrane and chromatographed at 4 °C on a Sepharose 6B column (1.5 × 90 cm) equilibrated in 2 M NaCl and 10 mM Tris-HCl (pH 7.4) at a flow rate of 7 ml per hour. One millilitre fractions were collected and an aliquot of each fraction containing A_{230} absorbing material was precipitated with 15 % (w/v) trichloroacetic acid. The pellets were washed with acetone and 20 mM HCl and finally with acetone, and analysed by SDS-PAGE. Fractions containing equimolar amounts of the histones, as judged by comparison with gel scans of histone standards run on the same gel, were pooled and stored at 4 °C after addition of sodium azide to 0.01 % (w/v).

8.7 Cross-linking of histone octamers

In order to establish that *bona fide* octamers had been isolated, pooled octamers were concentrated by ultrafiltration as before to approximately 5 mg/ml. Concentrated octamers were mixed with an equal volume of 10 mg per ml dimethylsuberimidate in 2 M NaCl and 0.25 M borate (pH 9.8). The cross-linking reaction was terminated at set time intervals by addition of 500 mM glycine (pH 8.0) to a final concentration of 125 mM on ice. Samples were dialysed for at least 4 h against 25 mM glycine (pH 8.0) at 4 °C and analysed by SDS-PAGE using sample application buffer without β-mercaptoethanol.

8.8 Preparation of native long chromatin and pentanucleosomes

Chicken erythrocyte nuclei in buffer A (Hewish & Burgoyne, 1973) at a concentration of 1 mg DNA/ml (equal to an A_{260} of 20 in 1 M NaOH) were digested at a final Ca^{2+} concentration of 0.8 mM at 20 °C with either 6 units MNase per mg DNA for 10 min for long chromatin or 40 units MNase per mg DNA for 10 min for pentanucleosomes. Digestion times could be increased with a concomitant reduction in the concentration of MNase added. The digestion was stopped by addition of EDTA to 5 mM. Nuclei were collected by centrifugation at 4000 rpm in Beckman JA-20 rotor for 5 min and resuspended in and dialysed against 0.2 mM EDTA and 10 mM Tris-HCl (pH 7.4), for 16 hours. Nuclear debris was removed by centrifugation at 12 000 rpm in a Beckman JA-20 rotor. Soluble chromatin fragments were separated on linear 5 to 20 % (w/v) sucrose gradients in 20 mM NaCl, 0.1 mM EDTA and 10 mM Tris-HCl (pH 7.4), and centrifuged at 24 000 rpm for 16 hours in a Beckman SW 28 rotor. Gradients were fractionated with 50 % (w/v) sucrose using an ISCO density gradient fractionator. Absorbance was monitored at 254 nm. Fractions of interest were dialysed against 20 mM NaCl, 0.1 mM EDTA and 10 mM Tris-HCl (pH 7.4) for 16 hours. Aliquots of fractions were deproteinized by extractions with phenol (pH 8.0), 1 % (w/v) SDS and then with diethylether, followed by precipitation with 7 volumes of ethanol. The DNA pellets were washed with 70 % (v/v) ethanol and resuspended in 5 % (v/v) glycerol containing 0.01 % (w/v) bromophenol blue. The length of the

chromatin fragments in each fraction was determined by electrophoresis in 1 % (w/v) agarose gels in TBE (90 mM Tris-Borate (pH 8.3) and 2.5 mM EDTA) by comparison to the restriction fragments generated by digestion of pBR322 DNA with *Hpa* II and digestion of λ DNA with *Hind* III and *Eco* RI. Long chromatin contained 7 to 12 nucleosomes.

8.9 Removal of linker histones from native chromatin and pentanucleosomes

Chromatin to be stripped of linker histones was dialysed for 16 hours against 600 mM NaCl, 0.1 mM EDTA and 10 mM Tris-HCl (pH 7.4) and concentrated by ultrafiltration under nitrogen using an Amicon PM-10 membrane. Chromatin samples (5 mg/ml) were then centrifuged on linear 5 to 20 % (w/v) sucrose gradients in 600 mM NaCl, 0.1 mM EDTA and 10 mM Tris-HCl (pH 7.4) at 24 000 rpm for 16 hours in a Beckman SW 28 rotor. Gradients were fractionated as before and fractions were dialysed against 10 mM NaCl, 0.1 mM EDTA and 10 mM Tris-HCl (pH 7.4) for 16 hours. Aliquots of dialysed fractions were precipitated with 10 % (v/v) trichloroacetic acid for 30 min at 4 °C followed by centrifugation in a Beckman JA-20.1 rotor for 10 min at 15 000 rpm. Pellets were washed first with acetone, 0.02 M HCl and then acetone. The histone content of fractions was determined by SDS polyacrylamide gel electrophoresis to confirm the removal of linker histones.

8.10 Preparation of 167 bp random sequence DNA

Long chicken erythrocyte chromatin stripped of linker histones was digested with MNase at room temperature in 20 mM NaCl, 1 mM $CaCl_2$ and 10 mM Tris-HCl (pH 7.4). Digestion products from trial digests were analysed on 6 % non-denaturing polyacrylamide gels. Conditions for the bulk preparation of 167 bp nucleosome cores were determined by scaling up optimal digestion times from the trial digests. Typical digests required 107 units MNase per 20 A_{260} units per min. Digestion was stopped by addition of 100 mM EDTA to a final concentration of 5 mM. Nucleosome cores were purified by chromatography using a Sepharose CL 6B (1.5 × 100 cm) column in 0.3 M NaCl, 0.1 mM EDTA and 10 mM Tris-HCl (pH 7.4) at a flow rate of 8 ml per hour. The elevated salt concentration assists in the removal of traces of MNase that

may be adhering to the cores. Fractions were analysed by 6 % non-denaturing PAGE and those containing 167 bp nucleosome cores were pooled and concentrated by ultrafiltration. DNA was purified from these nucleosomes by phenol extraction.

8.11 Purification of defined sequence DNA templates

p5S 208-12 plasmid containing 12 tandem repeats of a 208 bp sequence derived from the *Lytechinus* 5S rRNA gene (Simpson *et al.*, 1985), were amplified and extracted by alkaline lysis (Maniatis *et al.*, 1982). The original plasmid was named p5S 207-12 but later results indicated that the length of the tandem repeat fragment was 208 bp and not 207 bp (Dong & van Holde, 1991). The plasmid was purified using Nucleobond (Machery-Nagel) columns. 208-12 DNA and 208 DNA were excised from the plasmid by *Hha* I and *Ava* I digestion respectively according to the manufacturer's instructions (Boehringer Mannheim). DNA fragments of interest were separated from the remainder of the plasmid by centrifugation through a linear 5-12 % (w/v) sucrose gradient in TE (10 mM Tris-HCl (pH 8.0) and 1 mM EDTA) for 16 hours at 4 °C in a Beckman SW 40 Ti rotor at 30 000 rpm. Gradients were fractionated with 50 % (w/v) sucrose using an ISCO gradient fractionator. Aliquots of fractions were analysed by agarose gel electrophoresis in order to identify and pool fractions containing the DNA fragment of interest. DNA fragments were concentrated by ethanol precipitation according to standard protocols.

8.12 Reconstitution of nucleosomes

Nucleosome cores were reconstituted onto purified 167 bp random sequence or defined sequence 208 bp 5S rDNA fragments using the reconstituted hybrid chicken erythrocyte octamers as a histone source, containing either calf H2A (control) or calf uH2A. The final DNA concentration ranged from 20 to 50 μg/ml. The DNA and octamer mixtures were dialysed against TE (pH 7.4) containing 2 M NaCl for 1 hour followed by dialysis periods of 3-4 hours against TE (pH 7.4) buffer containing decreasing salt concentrations (1.2 M, 0.9 M and 0.6 M NaCl). This was followed by overnight dialysis against TE (pH 7.4) with one change of buffer. Trial reconstitutions were carried out in microdialysers with increasing molar ratios of octamer to DNA

ranging from 0.5 to 3, and analysed on 0.7 % (w/v) agarose nucleoprotein gels in 0.5 × TBE (45 mM Tris-borate and 1 mM EDTA). Optimal input ratios thus derived were utilised for bulk reconstitutions. Reconstitutes were stored for up to one week at 4 °C.

8.13 Reconstitution of linker histones onto nucleosome cores

8.13.1 Direct addition

Reconstituted nucleosome cores were incubated with various amounts of chicken erythrocyte linker histones as stated in the text in 50 mM NaCl, 1 mM EDTA and 10 mM Tris-HCl (pH 7.4) for 30 min at room temperature (Hayes & Wolffe, 1993). The average molecular weight of chicken erythrocyte H1 was taken as 21 782 Da (Sugarman *et al.*, 1983).

8.13.2 Salt dialysis

Reconstituted nucleosome cores and linker histones in 550 mM NaCl, 1 mM EDTA and 10 mM Tris-HCl (pH 7.4) were mixed in the ratios stated in the text and dialysed for at least 4 hours against 10 mM NaCl, 1 mM EDTA and 10 mM Tris-HCl (pH 7.4).

8.14 Purification of reconstituted nucleosomes and chromatosomes

Reconstitution products were applied to linear 5-20 % (w/v) sucrose gradients in 10 mM NaCl, 1 mM EDTA and 10 mM Tris-HCl (pH 7.4) and centrifuged in a Beckman SW 40 Ti rotor for 16 hours at 30 000 rpm. Gradients were fractionated as described above and aliquots of fractions were analysed by 0.7 % (w/v) agarose gel electrophoresis in 0.5 × TBE.

8.15 Gel retardation assays

Reconstitution products were adjusted to 5 % (v/v) glycerol and analysed by gel retardation assays on 0.7 % (w/v) agarose gels in 0.5 × TBE. Gels were stained with ethidium bromide and photographed on a UV trans-illuminator.

8.16 Ultraviolet absorbance versus temperature profiles

Samples at a concentration of 50 μg/ml in the buffer specified in the text were heated at 1 °C/min from 30 °C to 100 °C in a 2 mm × 10 mm quartz cuvette (Helma, Mulheim, Germany). Absorbance at 260 nm was recorded every 0.3 °C using a Pye-Unicam SP 1800 spectrophotometer equipped with a custom made temperature controller interfaced to an analog to digital device (Oasis/4; 3 D Digital Design and Development Ltd, London) and an IBM 386 computer. Where indicated, the first derivatives of A_{260} versus temperature profiles were numerically deconvoluted by fitting a sum of Gaussian curves using a Marquardt-Levenberg algorithm (software provided by Dr P. Hüsler, unpublished).

8.17 Determination of nucleosome and chromatosome positioning

Nucleosomes and chromatosomes reconstituted onto 208 bp *Lytechinus* 5S rDNA were digested with 0.3 units of MNase per 10 μg DNA at a final $CaCl_2$ concentration of 0.8 mM. Naked DNA was digested with 0.06 units of MNase per 10 μg DNA. Optimal digestion times required for production of 146 bp and 167 bp intermediates respectively were determined from trial digests. Ten micrograms of DNA was used for bulk digestions. Digestion products were phenol extracted and analysed by 6 % (w/v) non-denaturing PAGE. Gel slices containing the bands of interest were cut out using a sterile scalpel blade and crushed. The DNA was eluted in 0.3 ml TE overnight on a rotator in the dark at 4 °C. The DNA was purified from the gel pieces by filtration through siliconised glass wool and concentrated by ethanol precipitation. The pellet was washed with 70 % (v/v) ethanol, resuspended in TE and digested with the specified restriction enzyme according to standard procedures. Digestion products were analysed by 8 % (w/v) non-denaturing PAGE. Gels were stained with SYBR gold (Molecular probes).

8.18 Reconstitution of nucleosomal arrays

Nucleosomal arrays were reconstituted by salt dialysis from purified 208-12 DNA fragments and reconstituted hybrid chicken erythrocyte octamers containing either calf H2A (control) or calf uH2A by salt dialysis as described previously for the reconstitution of nucleosomes. The number of nucleosomes per DNA template was estimated by overnight digestion of an aliquot of the reconstituted material with *Ava* I (20 units per μg DNA) and analysis of the digestion products on 0.7 % (w/v) agarose nucleoprotein gels in 0.5 × TBE (45 mM Tris-borate and 1 mM EDTA). Gels were stained with ethidium bromide and photographed on a UV trans-illuminator. Negatives were scanned using a Nikon LS-4500 AF film scanner and analysed using ImageQuant software. This method has previously been shown to be a sensitive assay for nucleosome loading (Tse & Hansen, 1997). The results from trial reconstitutions were used to adjust input ratios of octamers to DNA template to yield saturated nucleosomal arrays (> 50 % of templates containing 12 nucleosomes). Reconstitutes were stored for up to one week at 4 °C.

8.19 Intermolecular Association Assay

Reconstituted nucleosomal arrays were concentrated by ultrafiltration under nitrogen using an Amicon PM-10 membrane. The A_{260} of the reconstituted nucleosomal arrays was determined and adjusted to 1.6 with 10 mM Tris-HCl (pH 7.4) and 5 mM EDTA. Fifteen microlitres each of nucleosomal array sample and $MgCl_2$ solutions were mixed to yield the final $MgCl_2$ concentrations reported in the text and incubated for 10 min at 22 °C. Samples were centrifuged at 16 000 in a Beckman JA 20.1 rotor for 10 min at 20 °C. The A_{260} of the supernatants was determined following centrifugation, and the proportion of unaggregated nucleosomal array was expressed as (A_{260} of supernatant after centrifugation / A_{260} in TE) × 100.

8.20 Quantitative agarose gel electrophoresis

8.20.1 Materials

Low EEO agarose from four different manufacturers (Hispanagar, Biometra, Promega and Seaplaque) was tested and all samples were found to be unsuitable for quantitative agarose gel electrophoresis. Either nucleosome core disruption was evident as judged from smearing and lack of histone staining following Coomassie staining or the agarose gel matrix was too fragile. Sigma type II agarose was found to be suitable for nucleoprotein gels although it has slightly higher EEO than that of agarose used in previous reports. Seakem Gold agarose, which is assumed to be electroendo-osmosis free (Hansen *et al.*, 1997), was used in the μ_E determinations. Bacteriophage T3, which was used as an internal standard, was obtained from ATCC, amplified and purified according to the protocol of Serwer and colleagues (Serwer *et al.*, 1983).

8.20.2 Determination of μ and μ'_o

A nine lane multigel system as described by Hansen and co-workers (Fletcher *et al.*, 1994a,b; Hansen *et al.*, 1997) was utilised to determine the electrophoretic mobilities of reconstituted nucleosomal arrays in 0.2 to 3.0 % (w/v) agarose. Running gels were prepared in 40 mM Tris-HCl (pH 7.8) and 0.25 mM EDTA (E buffer) containing a final concentration of 0 or 2 mM $MgCl_2$. Samples containing 0.6 μg of bacteriophage T3 and approximately 0.5 μg either nucleosomal arrays or DNA were electrophoresed at 2.65 $V.cm^{-1}$ at 20 ± 2 °C for 8 hours with buffer recirculation. Buffer recirculation was started 6 min after the start of electrophoresis. Gels were stained with ethidium bromide and photographed on a UV trans-illuminator. Negatives were scanned (Nikon LS-4500 AF film scanner) and values of μ (distance of migration from the well in cm) were calculated from the distance of the middle of the bands to the well. Values were determined using either ProImage software (Prolab Tech Co., ltd) or by measuring the distances from an enlarged A4 size printout of the gel. Values were calibrated using a ruler that was included in the photograph alongside the gel. The gel free migration was calculated by the extrapolation of the line fitted by linear regression to a plot of migration distance (≤ 1 % (w/v) agarose) *versus* percentage agarose concentration. The gel free migration was then converted to μ'_o, the gel free mobility ($cm^2V^{-1}s^{-1}$).

The μ of electro-osmotically driven buffer in Sigma agarose, μ_E, was determined by subtracting the $\mu'_o{}^{T3}$ in Seakem gold agarose from the $\mu'_o{}^{T3}$ in Sigma agarose. The value of μ_E was $-2.68 \times 10^{-5} cm^2V^{-1}s^{-1}$ in E buffer and -1.91×10^{-5} $cm^2V^{-1}s^{-1}$ in E buffer containing 2 mM $MgCl_2$.

8.21 Reconstitution of linker histones onto stripped chromatin

8.21.1 Pectin reconstitution protocol

A thirty fold weight excess of pectin (10 mg/ml in 20 mM NaCl, 0.1 mM EDTA and 10 mM Tris-HCl (pH 7.4)) with respect to the DNA content of chromatin to be reconstituted was mixed with the amount of histone H5 specified in the text. The molar input ratio of H5 in reconstitution mixtures was determined by assuming that 1 mole of H5 weighs 20 580 g, and 1 mole nucleosomal DNA (200 bp) weighs 132,000 g. The extinction coefficient of H5 was determined spectrophotometrically at 230 nm based on an $A_{230} = 3.2$ for 1 mg/ml H5 for a lyophilised sample of histone H5 that had been exhaustively dialysed against double distilled water and subjected to amino acid analysis. Densitometric scans of SDS polyacrylamide gels of known amounts of native chromatin (from 3 to 15μg) were used to generate a calibration curve from which the amount of histone H5 present in 0.1 mg native chromatin was determined. The corresponding amount of stock H5 was determined from densitometric analysis of known amounts of stock H5 (from 3 to 15μg) electrophoresed in parallel to the native chromatin. The two methods of determination of input molar ratio of H5 correlated to within 6 %, corresponding to 0.16 mg H5/mg DNA. Polynucleosomes (4-5 nucleosomes) stripped of linker histones, in the same buffer were then added to a final concentration of 0.1 mg/ml. Reconstitution mixtures were incubated at 4 °C for one hour on a rotator prior to purification on linear 5-20 % (w/v) sucrose gradients in 20 mM NaCl, 0.1 mM EDTA and 10 mM Tris-HCl (pH 7.4). Centrifugation was performed using a Beckman SW 40Ti rotor for 16 hours at 4 °C at 24 000 rpm. Gradients were fractionated with 50 % (w/v) sucrose using an ISCO density gradient fractionator (model 640).

8.21.2 CM Sephadex C-25 linker histone reconstitution protocol

A ten fold weight excess of CM Sephadex C-25, (20 mg/ml in 20 mM NaCl, 0.1 mM EDTA and 10 mM Tris-HCl (pH 7.4)) with respect to the DNA content of chromatin to be reconstituted was mixed with histone H5. The amount of histone H5 used depended on the experiment. Stripped chromatin in 20 mM NaCl, 0.1 mM EDTA and 10 mM Tris-HCl (pH 7.4) was then added to a final concentration of 0.1 mg/ml. Reconstitution mixtures were rolled in polypropylene tubes at 4 °C for 4 hours with both rocking and rolling motions since it is important that thorough gentle mixing occurs. Following centrifugation at 4000 g for 10 min, the supernatant was carefully withdrawn avoiding contamination with CM Sephadex C-25. The percentage of chromatin recovered after reconstitution was determined by comparison of the A_{260} of the sample with a mock reconstitution containing only stripped chromatin. In the case of bulk reconstitutions, the supernatant was filtered through a Whatman #1 filter. Where necessary, the reconstitution mixture was concentrated by ultrafiltration as before. Any H5 not bound tightly to nucleosomes was separated from the reconstituted sample by centrifugation through linear 5-20 % (w/v) sucrose gradients in 0.1 mM EDTA and 10 mM Tris-HCl (pH 7.4) at 16 000 rpm in a Beckman SW 40 rotor for 16 hours. Following fractionation as before, samples were dialysed into the appropriate buffer.

8.21.3 Salt dialysis linker histone reconstitution protocol

Linker histone and chromatin stripped of linker histones, both in 550 mM NaCl, 1 mM EDTA and 10 mM Tris-HCl (pH 7.4), were mixed in the ratios specified in the text and dialysed against this buffer for one hour. Reconstitution mixtures were then dialysed against 250 mM NaCl, 1 mM EDTA and 10 mM Tris-HCl (pH 7.4) for 3 hours and finally against 10 mM NaCl, 1 mM EDTA and 10 mM Tris-HCl (pH 7.4) for at least 4 hours.

8.22 Determination of pectin concentration

Pectin concentration was determined using a colourimetric assay for uronic acid (Davidson, 1966). Briefly, 1 ml of sample was incubated with 3 ml orcinol reagent for 40 min at 100 °C. The orcinol reagent consists of 400 mg orcinol, 155 ml 10 M HCl and 10 ml of 1.5 % (w/v) ferric chloride dissolved in 0.01 M HCl. Samples were cooled to room temperature and the absorbance was measured at 660 nm. The pectin concentration of a sample was determined by comparison with a standard curve ranging from 50 to 700 µg pectin per ml.

8.23 Pectinase digestion

Reconstituted samples in 20 mM NaCl, 0.1 mM EDTA and 10 mM Tris-HCl (pH 7.4) were digested with pectinase (14 units pectinase/ mg pectin) for 10 min at 37 °C and dialysed against the same buffer at 4 °C for four hours.

8.24 Micrococcal nuclease digestion of pentanucleosomes and long chromatin

Native, stripped and reconstituted pentanucleosomal chromatin samples (50 µg in 1 ml 20 mM NaCl, 0.1 mM EDTA and 10 mM Tris-HCl (pH 7.4)), were digested at 20 °C with 9 units MNase at a final Ca^{2+} concentration of 0.33 mM. Native, stripped and reconstituted long chromatin samples (80 µg in 1 ml 20 mM NaCl, 0.1 mM EDTA and 10 mM Tris-HCl (pH 7.4)), were digested at 20 °C with 1 unit MNase at a final calcium concentration of 0.6 mM. Aliquots were taken at different times and the reactions terminated by addition of phenol (pH 8.0) and SDS to a final concentration of 1 % (w/v). The samples were deproteinated by phenol extraction followed by diethylether extraction. The DNA was precipitated from the aqueous phase with 7 volumes of ethanol. The DNA pellets were washed with 70 % (v/v) ethanol and resuspended in 5 % (v/v) glycerol containing 0.01 % (w/v) bromophenol blue. Digests of pentanucleosomes were analysed by electrophoresis in 6 % (w/v) acrylamide gels containing 30 mM Tris-HCl (pH 7.5), 36 mM NaH_2PO_4 and 0.1 mM EDTA. Digests of long chromatin were analysed by electrophoresis in 1 % (w/v) agarose gels in TBE.

Following electrophoresis, gels were stained with ethidium bromide and photographed on a UV trans-illuminator using Ilford Pan F plus film. DNA fragments were sized by comparison with the restriction fragments generated by digestion of pBR322 with *Hpa* II and digestion of λ DNA with *Hind* III and *Eco* RI. Film negatives of long chromatin digests were converted to bitmap images using a Nikon LS-4500 AF film scanner and Adobe photoshop 3.0. Densitometric analysis of gel scans was performed using Geltrak software (written by Dr. D. Maeder) which is obtainable at http://www.uct.ac.za/depts/biochem/service.htm#software.

8.25 Determination of the arrangement of histone H5 molecules in native and reconstituted chromatin.

This was carried out essentially as described by Thomas and co-workers (Lennard & Thomas, 1985). Chromatin samples were dialysed against 10 mM borate (pH 8.0) and 0.1 mM EDTA, and adjusted to 0.25 mg DNA/ml. Dithiobis (succinimidyl propionate) was added from a stock solution (10 mg/ml in dry dimethylformamide) to 30 ml of chromatin to a final concentration of 0.2 mg/ml. The cross-linking reaction was terminated after 6 min at 25 °C by placing the reaction on ice and by the addition of 500 mM glycine (pH 8.0) to a final concentration of 25 mM. Longer cross-linking times led to the formation of extensive cross-links with core histones. Linker histones were extracted with 7.5 % (v/v) perchloric acid for 30 min at 4 °C. Perchloric acid soluble material was recovered by centrifugation at 15 000 rpm for 15 min in a Beckman JA-20 rotor and was precipitated with 10 % (v/v) trichloroacetic acid for 30 min at 4 °C followed by centrifugation as above. The histone pellet was washed with acetone and 0.02 M HCl, and then with acetone. The dried pellet was resuspended in 600 µl 6 M urea and 50 mM NaCl (pH 1.7) and applied to a BioGel P60 (9 mm x 1 m) column in 50 mM NaCl (pH 1.7) at a flow rate of 4 ml/h. The elution profile was monitored at 230 nm and fractions were analysed by SDS-polyacrylamide gel electrophoresis. β-mercaptoethanol was omitted from the sample application buffer. Cross-linked products eluted in the first peak. Fractions containing cross-linked products were pooled, precipitated with trichloroacetic acid as above, resuspended in 50 mM Tris-HCl (pH 7.4) and digested with α-chymotrypsin for 5 min at 37 °C at an enzyme:histone ratio of 1:600 (w/w). The digestion was stopped with

0.2 mM PMSF and samples were again trichloroacetic acid precipitated before being subjected to two-dimensional SDS polyacrylamide gel electrophoresis to determine the composition of the cross-linked products.

8.26 SDS-Polyacrylamide Gel Electrophoresis

SDS polyacrylamide gel electrophoresis was performed essentially as described by Laemmli (1970). Resolving gels contained 20 % (w/v) acrylamide, 0.1 % (w/v) N,N'-methylenebis(acrylamide), 375 mM Tris-HCl (pH 8.8), 0.1 % (w/v) SDS, 0.1 % (w/v) ammonium persulfate and 0.05 % (v/v) N,N,N',N'-tetramethylethylenediamine (TEMED). Stacking gels contained 6.67 % (w/v) acrylamide, 0.03 % (w/v) N,N'-methylenebis(acrylamide), 125 mM Tris-HCl (pH 6.8), 0.1 % (w/v) SDS, 0.25 % (w/v) ammonium persulfate and 0.05 % (v/v) TEMED. Sample application buffer contained 1 % (w/v) SDS, 37.5 mM Tris-HCl (pH 6.8), 10 % (v/v) glycerol, 360 mM β-mercaptoethanol and 0.01 % (w/v) bromophenol blue. Electrophoresis was performed at 20 °C in running buffer (25 mM Tris-base, 200 mM glycine and 0.1 % (w/v) SDS) at a constant voltage of 150 V until the dye front reached the bottom of the resolving gel. Gels were stained either with 0.1 % (w/v) Amido Black in 7 % (v/v) acetic acid and destained in 7 % (v/v) acetic acid or with 0.2 % (w/v) Coomassie blue in 25 % (v/v) methanol, 7 % (v/v) acetic acid and destained in 7 % (v/v) acetic acid unless otherwise mentioned.

For two dimensional electrophoresis, chromatographically purified cross-linked samples (50 µg) were resuspended in sample application buffer without β-mercaptoethanol and electrophoresed in the first dimension on a 0.5 mm thick gel with 0.8 cm wide wells (stacking gel 1.5 cm, resolving gel 12 cm). Following electrophoresis, the gel strip containing the sample was carefully excised and soaked for 10 min in 100 ml 280 mM β-mercaptoethanol, 375 mM Tris-HCl (pH 8.8) and 0.1 % (w/v) SDS in a sealed container under gentle agitation. This was followed by two 5 min washes in 50 ml 125 mM Tris-HCl (pH 6.8) and 0.1 % (w/v) SDS. It was found that increasing the length of these washes resulted in loss of protein material. The gel strip was then bonded lengthwise to the top of a 0.9 mm thick second dimension gel (stacking gel 1.5 cm, resolving gel 18 cm) with 1 % (w/v) agarose in

125 mM Tris-HCl (pH 6.8) and 0.1 % (w/v) SDS. Following electrophoresis, the gel was soaked in 50 % (v/v) methanol and silver stained according to the method of Wray *et al.* (1981). A partial chymotryptic digest of histone H5 or linker histones was included as an internal standard for the determination of the arrangement of neighbouring linker histones in extended reconstituted and native chromatin respectively.

8.27 SDS-PAGE densitometric scanning

Gels were destained to remove all traces of dye from the background and scanned using a Hoefer GS 300 scanning densitometer. Data were processed using associated Hoefer GS 365 W software in order to determine areas of densitometric peaks. There was a linear relationship between the area under the Amido black or Coomassie blue stained peak of each histone, except H2B, and the input of histone when total acid extracted histones in the range 3 to 20 μg were electrophoresed. To determine the percentage of linker histone incorporated in reconstituted samples, the ratio of linker histone to histone H4 or core histones in the reconstituted samples was divided by that of a native chromatin sample of similar densitometric intensity run on the same gel. The ratio of H5 to H4 was calculated as H4 is well resolved from the other core histones. As an internal control, the ratio of H2A to H4 was also determined and found to vary by 5 to 10 % (not shown).

8.28 Chromatin repeat length determination

Chromatin was digested in with MNase (Sigma) using the specified conditions after the addition of 100 mM $CaCl_2$ to a final Ca^{2+} concentration of 0.6 mM. Where the effect of MNase digestion was investigated using different enzyme concentrations, samples were withdrawn from the digest at different times to compensate for the different enzyme concentration. Thus, assuming a linear relationship for the range of MNase concentrations used, the extent of digestion $D = C_0t$, where C_0 is the units of MNase added and t is the time of digestion, was equivalent at each time point irrespective of the amount of enzyme added. In order to maintain equivalent extents of

digestion when carrying out the digest at different temperatures, the rate of digestion at the stated temperature relative to that at 20 °C was determined.

The rate of digestion carried out in 20 mM NaCl and 10 mM Tris-HCl (pH 7.4) at 20 °C, using 16 units MNase per 20 A_{260} units, was taken as the standard digestion rate. This corresponds to a molar ratio of MNase: DNA base pair of approximately 1: 320, using a molecular weight of 16 807 g/mol for MNase (Taniuchi *et al.*, 1967) and 660 g/mol for a base pair. This assumes that the average activity of Sigma MNase is 200 units per mg protein (Sigma catalogue). Relative rates were determined from trial digests by comparing the extent of digestion as a function of time using the same chromatin sample and an identical amount of MNase. The extent of digestion was determined by measuring the relative mononucleosome and dinucleosome content. These results were used to determine the frequency of time points for the digestions at the various temperatures such that equivalent extents of digestion were compared. DNA was prepared by phenol extraction and ethanol precipitation from samples after digestion. Samples were electrophoresed on 1 % (w/v) agarose gels. Gels were stained with ethidium bromide and photographed on a UV trans-illuminator. Each gel had molecular size standards from 200 bp to 21 kbp as well as identical samples of a chicken erythrocyte nuclei partial MNase digest applied to the outer lanes to verify that electrophoresis was parallel across the gel. The sizes of the DNA fragments were calculated from the standard curve generated from the concurrent electrophoresis of a *Hpa* II digest of plasmid pBR322 and an *Eco* RI/*Hind* III digest of λ bacteriophage. The number of base pairs associated with a particular nucleosomal band was plotted versus the n-meric fragment for $2 = n \geq 6$. The nucleosomal repeat length was calculated from the slope of the line generated by linear regression analysis of the digestion data at each time point (Noll & Kornberg, 1977). Only linear plots with a correlation coefficient ≥0.9983 were used.

8.29 Preparation of soybean nuclei

Hypercotyls from germinating soybeans were excised and homogenised in 10 mM NaCl, 10 mM $MgCl_2$, 0.4 M sucrose and 50 mM Tris-HCl (pH 7.8). The homogenate was filtered through cheesecloth and the nuclei collected after centrifugation of the filtrate at 800 g for 5 min. The nuclei were washed in buffer A (Hewish & Burgoyne, 1973) and digested with MNase as described in the text at 20 °C. Digestion products were analysed and extracted as before.

8.30 Preparation of calf neuronal nuclei

Neuronal and glial cell nuclei were prepared from calf brains freshly collected from the local abattoir as described by Pearson *et al.* (1984). The nuclei were examined by phase contrast microscopy to confirm their authenticity. The nuclei were washed in buffer A (Hewish & Burgoyne, 1973) and digested with MNase at 20 °C. Digestion products were analysed and extracted as before.

9 Literature Cited

Agell, N., Chiva, M. & Mezquita, C. (1983) *FEBS Lett.* **155**, 209-212.

Albright, S.C., Nelson, P.P. & Garrard, W.T. (1979) *J. Biol. Chem.* **255**, 1065-1073.

Allan, J., Cowling, G.J., Harborne, N., Cattini, P., Craigie, R. & Gould, H. (1981) *J. Cell. Biol.* **90**, 279-288.

Allan, J., Harborne, N., Rau, D.C.& Gould, H. (1982) *J. Cell Biol.* **93**, 285-297.

Allan, J., Hartman, P.G., Crane-Robinson, C. & Aviles, F.X. (1980a) *Nature* **288**, 675-679.

Allan, J., Rau, D.C., Harborne, N. & Gould, H. (1984) *J. Cell Biol.* **98**, 1320-1327.

Allan, J., Staynov, D.Z. & Gould, H. (1980b) *Proc. Natl. Acad. Sci. USA* **77**, 885-889.

An, W., van Holde, K. & Zlatanova, J. (1998) *Nucleic Acids Res.* **26**, 4042-4046.

Andersen, M.W., Goldknopf, I.L. & Busch, H. (1981) *FEBS Lett.* **132**, 210-214.

Ausió, J., Borochov, N., Seger, D. & Eisenberg, H. (1984) *J. Mol. Biol.* **177**, 373-398.

Ausió, J., Sasi, R. & Fasman, G.D. (1986) *Biochemistry* **25**, 1981-1988.

Ausió, J. & van Holde, K.E. (1986) *Biochemistry* **25**, 1421-1428.

Baarends, W.M., Hoogerbrugge, J.W., Roest, H.P., Vreeburg, J., Hoeijmakers, J.H. & Grootegoed, J.A. (1999) *Dev. Biol.* **207**, 322-333.

Baer B.W. & Rhodes, D. (1983) *Nature* **301**, 482-488.

Bakayev, V.V., Bakayeva, T.G. & Varshavsky, A.J. (1977) *Cell* **11**, 619-629.

Ballal, N.R., Goldknopf, I.L., Goldberg, D.A. & Busch, H. (1974) *Life Sci.* **14**, 1835-1845.

Ballal, N.R., Kang, Y., Olson, M.O.J. & Busch, H. (1975) *J. Biol. Chem.* **250**, 5921-5925.

Barsoum, J. & Varshavsky, A. (1985) *J. Biol. Chem.* **260**, 7688-7697.

Bates, D.L. & Thomas, J.O. (1981) *Nucleic Acids Res.* **9**, 5883-5894.

Bates, D.L., Butler, P.J.G., Pearson, E.C. & Thomas, J.O. (1981) *Eur. J. Biochem.* **119**, 469-476.

Becker, P.B. & Wu, C. (1992) *Mol. Cell Biol.* **12**, 2241-2249.

Bednar, J., Horowitz, R.A., Dubochet, J. & Woodcock, C.L. (1995) *J. Cell Biol.* **131**, 1365-1376.

Bednar, J., Horowitz, R.A., Grigoryev, S.A., Carruthers, L.M., Hansen, J.C., Koster, A.J. & Woodcock, C.L. (1998) *Proc. Natl. Acad. Sci. USA* **95**, 14173-14178.

Bellard, M., Kuo, M.T., Dretzen, G. & Chambon, P. (1980) *Nucleic Acids Res.* **8**, 2737-2750.

Biard-Roche, J., Gorka, C. & Lawrence, J.J. (1982) *EMBO J.* **12**, 1487-1492.

Blank, T.A. & Becker, P.B. (1995) *J. Mol. Biol.* **252**, 305-313.

Blank, T.A. & Becker, P.B. (1996) *J. Mol. Biol.* **260**, 1-8.

Bloom, K.S. & Anderson, J.N. (1978) *Cell* **15**, 141-150.

Böhm, L., Briand, G., Sautière, P. & Crane-Robinson, C. (1982) *Eur. J. Biochem.* **123**, 299-303.

Böhm, L. & Crane-Robinson, C. (1984) *Biosci. Rep.* **4**, 365-386.

Böhm, L., Crane-Robinson, C. & Sautière, P. (1980) *Eur. J. Biochem.* **106**, 525-530.

Bond, U., Agell, N., Haas, A.L., Redman, K. & Schlesinger, M.J. (1988) *J. Biol. Chem.* **263**, 2384-2388.

Bond, U. & Schlesinger, M.J. (1985) *Mol. Cell. Biol.* **5**, 949-956.

Bonner, W.M. & Stedman, J.D. (1979) *Proc. Natl. Acad. Sci. USA* **76**, 2190-2194.

Borochov, N., Ausió, J. & Eisenberg, H. (1984) *Nucleic Acids Res.* **12**, 3089-3096.

Boulikas, T., Wiseman, J.M. & Garrard, W.T. (1980) *Proc. Natl. Acad. Sci. USA* **77**,127-131.

Bradbury, E.M. (1992) *Bioessays* **14**, 9-16.

Bradbury, E.M., Chapman, G.E., Danby, S.E., Hartman, P.G. & Riches, P.L. (1975) *Eur. J. Biochem.* **57**, 521-528.

Brand, S.H., Kumar, N.M. & Walker, I.O. (1981) *FEBS Lett.* **133**, 63-66.

Brown, I.R. & Sutcliffe, J.G. (1987) *Nucleic Acids Res.* **15**, 3563-3571.

Bulger, M., Takashi, I., Kamakaka, R.T. & Kadanonga, J.T. (1995) *Proc. Natl. Acad. Sci. USA* **92**, 11726-11730.

Busch, H. & Goldknopf, I.L. (1981) *Mol. Cell. Biochem.* **40**, 173-187.

Carruthers, L.M., Bednar, J., Woodcock, C.L. & Hansen J.C. (1998) *Biochemistry* **37**, 14776-14787.

Cary, P.D., King, D.S., Crane-Robinson, C., Bradbury, E.M., Rabbani, A., Goodwin, G.H. & Johns, E.W. (1980) *Eur. J. Biochem.* **112**, 577-580.

Cavalli, G. & Thoma, F. (1993) *EMBO J.* **12**, 4603-4613.

Cerf, C., Lippens, G., Muyldermans, S., Segers, A., Ramakrishnan, V., Wodak, S.J., Hallenga, K. & Wyns, L. (1993) *Biochemistry* **32**, 11345-11351.

Cerf, C., Lippens, G., Ramakrishnan, V., Muyldermans, S., Segers, A., Wyns, L., Wodak, S.J. & Hallenga, K. (1994) *Biochemistry* **33**, 11079-11086.

Chau, V., Tobias, J.W., Bachmair, A., Mariott, D., Ecker, D.J., Gonda, D.K. & Varshavsky, A. (1989) *Science* **243**, 1576-1583.

Chen, H., Li, B. & Workman, J.L. (1994) *EMBO J.* **13**, 380-390.

Chen, H.Y, Sun, J-M., Zhang, Y., Davie, J.R. & Meistrich, M.L. (1998) *J. Biol. Chem.* **273**, 13165-13169.

Ciechanover, A., Finley, D. & Varshavsky, A. (1984) *Cell* **37**, 57-66.

Ciechanover, A., Shkedy, D., Oren, M. & Bercovich, B. (1994) *J. Biol. Chem.* **269**, 9582-9589.

Clark, D.J. & Thomas, J.O. (1988) *Eur. J. Biochem.* **178**, 225-233.

Clark, D.J. & Kimura, T. (1990) *J. Mol. Biol.* **211**, 883-896.

Clark, K.L., Halay, E.D., Lai, E. & Burkley S.K. (1993) Nature **364**, 412-420.

Clore, G.M., Gronenborn, A.M., Nilges, M., Sukumaran, D.K. & Zarbock, J. (1987) *EMBO J.* **6**, 1833-1842.

Cook, J. & Chock, P.B. (1991a) *Biochem. Biophys. Res. Commun.* **174**, 564-571.

Cook, J. & Chock, P.B. (1991b) *Proc. Natl. Acad. Sci. USA* **88**, 11388-11392.

Cook, J. & Chock, P.B. (1988) *Biofactors* **1**, 133-146.

Cowman, M.K. & Fasman, G.D. (1980) *Biochemistry* **19**, 532-541.

Crane-Robinson, C. (1997) *Trends Biochem. Sci.* **22**, 75-77.

Dashkevich, V.K., Nikolaev, L.G., Zlatanova, J.S., Glotov, B.O. & Severin, E.S. (1983) *FEBS Lett.* **158**, 276-279.

Davidson, E.A. (1966) *Methods Enzymol.* **8**, 52-60.

Davie, J.R. (1998) *Curr. Opin. Genet. Dev.* **8**, 173-178.

Davie, J.R., Delcuve, G.P., Nickel, B.E., Moirier, R. & Bailey, G. (1987) *Cancer Res.* **47**, 5407-5410.

Davie, J.R. & Nickel, B.E. (1987) *Biochim. Biophys. Acta* **909**, 183-189.

Davie, J.R. & Murphy, L.C. (1990) *Biochemistry* **29**, 4752-4757.

Davies, N. & Lindsey, G.G. (1991) *Biochim Biophys Acta* **1129**, 57-63.

Davies, N. & Lindsey, G.G. (1994) *Biochim. Biophys. Acta* **1218**, 187-193.

Dawson, B.A., Herman, T., Haas, A.L. & Lough, J. (1991) *J. Cell. Biochem.* **46**, 166-173.

Deveraux, Q., Ustrell, V., Pickart, C. & Rechsteiner, M. (1994) *J. Biol. Chem.* **269**, 7059-7061.

Deveraux, Q., Wells, R. & Rechsteiner, M. (1990) *J. Biol. Chem.* **265**, 6323-6329.

Dimitrov, S., Makarov, V., Apostolova, T. & Pashev, I. (1986) *FEBS Lett.* **197**, 217-220.

Dong, F., Hansen, J.C. & van Holde, K.E. (1990) *Proc. Natl. Acad. Sci. USA* **87**, 5724-5728.

Dong, F. & van Holde, K.E. (1991) *Proc. Natl. Acad. Sci. USA* **88**, 10596-10600.

Drew, H.R. & McCall, M.J. (1987) *J. Mol. Biol.* **197**, 485-511.

Elgin, S.C. (1988) *J. Biol. Chem.* **263**, 19259-19262.

Ericsson, C., Goldknopf, I.L. & Daneholt, B. (1986) *Exp. Cell. Res.* **167**, 127-134.

Finch, J.T. & Klug, A. (1976) *Proc. Natl. Acad. Sci. USA* **73**,1897-1901.

Finley, D. & Chau, V. (1991) *Annu. Rev. Cell Biol.* **7**, 25-69.

Finley, D., Ciechanover, A. & Varshavsky, A. (1984) *Cell* **37**, 43-55.

Finley, D., Sadis, S., Monia, B.P., Boucher, P., Ecker, D.J., Crooke, S.T. & Chau, V. (1994) *Mol. Cell. Biol.* **14**, 5501-5509.

FitzGerald, P.C. & Simpson, R.T. (1985) *J. Biol. Chem.* **260**, 15318-15324.

Fletcher, T.M. & Hansen, J.C. (1995) *J.Biol.Chem.* **270**, 25359-25362.

Fletcher, T.M. & Hansen, J.C. (1996) *Crit. Rev. Eukaryotic Gene Expression* **6**, 149-188.

Fletcher, T.M., Krishnan, U., Serwer, P. & Hansen, J.C. (1994a) *Biochemistry* **33**, 2226-2233.

Fletcher, T.M., Serwer, P. & Hansen, J.C. (1994b) *Biochemistry* **33**, 10859-10863.

Franke, W.W., Scheer, U., Trendelenburg, M.F., Spring, H. & Zentgraf, H. (1976) *Cytobiologie* **13**, 401-434.

Fujimuro, M., Sawada, H. & Yokosawa, H. (1997) *Eur. J. Biochem.* **249**, 427-433.

Garcia-Ramirez, M., Dong, F. & Ausió, J. (1992) *J.Biol.Chem* **267**, 19587-19595.

Garcia-Ramirez, M., Leuba, S.H. & Ausió, J. (1990) *Prot. Expres. Pur.* **1**, 40-44.

Garcia-Ramirez, M., Rocchini, C. & Ausió, J. (1995) *J.Biol.Chem* **270**, 17923-17928.

Gavilanes, J.G., de Buitrago, G.G., Perez-Castells, R. & Rodriguez R. (1982) *J. Biol. Chem.* **257**, 10267-10270.

Glotzer, M., Murray, A.W. & Kirschner, M.W. (1991) *Nature* **349**, 132-138.

Godde, J.S. & Widom, J. (1992) *J. Mol. Biol.* **226**, 1009-1025.

Goldknopf, I.L., & Busch, H. (1975) *Biochem. Biophys. Res. Commun.* **65**, 951-960.

Goldknopf, I.L., & Busch, H. (1977) *Proc. Natl. Acad. Sci. USA* **74**, 864-868.

Goldknopf, I.L., Taylor, C.M., Baum, R.M., Yeoman, L.C., Olson, M.O.J., Prestayko, A.W. & Busch, H. (1975) *J.Biol.Chem.* **250**, 7182-7187.

Goldknopf, I.L., Wilson, G., Ballal, N.R. & Busch, H. (1980) *J.Biol.Chem.* **255**, 10555-10558.

Gonzalez, J.P. & Palacián, E. (1989) *J.Biol.Chem.* **264**, 18457-18462.

Gonzalez, J.P., Martinez, C. & Palacián, E. (1987) *J.Biol.Chem.* **262**, 11280-11283.

Graziano, V., Gerchman, S.E. & Ramakrishnan, V. (1988) *J. Mol. Biol.* **203**, 997-1007.

Griess, G.A., Moreno, E.T., Easom, R. & Serwer, P. (1989) *Biopolymers* **28**, 1475-1484.

Griess, G.A., Moreno, E.T., Herrmann, R. & Serwer, P. (1990) *Biopolymers* **29**, 1277-1287.

Guschin, D., Chandler, S. & Wolffe, A.P. (1998) *Biochemistry* **37**, 8629-8636.

Haas, A.L. & Bright, P.M. (1985) *J. Biol. Chem.* **260**, 12464-12473.

Haas, A.L. & Bright, P.M (1988) *J. Biol. Chem.* **263**, 13258-13267.

Haas, A.L., Bright, P.M. & Jackson, V.E. (1988) *J. Biol. Chem.* **263**, 13268-13275.

Haas, A.L., Reback, P.B. & Chau, V. (1991) *J. Biol. Chem.* **266**, 5104-5112.

Haas, A., Reback, P.M., Pratt, G. & Rechsteiner, M. (1990) *J. Biol. Chem.* **265**, 21664-21669.

Hamiche, A., Schultz, P., Ramakrishnan, V., Oudet, P. & Prunell, A. (1996) *J. Mol. Biol.* **257**, 30-42.

Hansen, J.C. & Wolffe, A.P. (1992) *Biochemistry* **31**, 7977-7988.

Hansen, J.C. & Wolffe, A.P. (1994) *Proc. Natl. Acad. Sci. USA* **91**, 2339-2343.

Hansen, J.C., Ausió, J., Stanik, V.H. & van Holde, K.E. (1989) *Biochemistry* **28**, 9129-9136.

Hansen, J.C., Kreider, I., Demeler, B. & Fletcher, T.M. (1997) *Methods* **12**, 62-72.

Hartman, P.G., Chapman, G.E., Moss, T. & Bradbury, E.M. (1977) *Eur. J. Biochem.* **77**, 45-51.

Hayes, J.J. (1996) *Biochemistry* **35**, 11931-11937.

Hayes, J.J. & Wolffe, A.P. (1993) *Proc. Natl. Acad. Sci. USA* **90**, 6415-6419.

Hayes, J.J., Pruss, D. & Wolffe, A.P. (1994) *Proc. Natl. Acad. Sci. USA* **91**, 7817-7821.

Hershko, A., Ganoth, D., Sudakin, V., Dahan, A., Cohen, L.H., Luca, F.C., Ruderman, J.V. & Eytan, E. (1994) *J. Biol. Chem.* **269**, 4940-4946.

Hershko, A., Heller, H., Eytan, E. & Reiss, Y. (1986) *J. Biol. Chem.* **261**, 11992-11999.

Hewish, D.R. & Burgoyne, L.A. (1973) *Biochem. Biophys. Res. Commun.* **52**, 475-481.

Hofmann, R.M. & Pickart, C. (1999) *Cell* **96**, 645-653.

Hough, R., Pratt, G. & Rechsteiner, M. (1987) *J. Biol. Chem.* **262**, 8303-8313.

Howe, L., Iskandar, M. & Ausió, J. (1998a) *J. Biol. Chem.* **273**, 11625-11629.

Howe, L., Itoh, T., Katagiri, C. & Ausió, J. (1998b) *Biochemistry* **37**, 1174-1177.

Huang, S., Barnard, M.B., Xu, M., Matsui, S., Rose, S.M. & Garrard, W.T. (1986) *Proc. Natl. Acad. Sci. USA* **83**, 3738-3742.

Hunt, L.T. & Dayhoff, M.O. (1977) *Biochem. Biophys. Res. Commun.* **74**, 650-655.

Hunt, T. (1991) *Nature* **349**, 100-101.

Izban, M.G. & Luse, D.S. (1991) *Genes Dev.* **5**, 683-696.

Izquierdo, M. (1994) *Chromosoma* **103**, 193-197.

Jaeger, A.W. & Kuenzle, C.C. (1982) *EMBO J.* **1**, 811-816.

Jason, L.J.M. & Lindsey, G.G. (1997) *Methods Mol. Cell. Biol.* **6**, 134-150.

Jennissen, H.P. (1995) *Eur. J. Biochem.* **231**, 1-30.

Jentsch, S., McGrath, J.P., Varshavsky, A. (1987) *Nature* **329**, 131-134.

Jeong, S.W., Lauderdale, J.D. & Stein, A. (1991) *J. Mol. Biol.* **222**, 1131-1147.

Jin, Y.-J. & Cole, R.D. (1986) *J. Biol. Chem.* **261**, 15805-15812.

Kamakaka, R.T. & Thomas, J.O. (1990) *EMBO J.* **9**, 3997-4006.

Kaplan, L.J., Bauer, R., Morrison, E., Langan, T.A. & Fasman, G.D. (1984) *J. Biol. Chem.* **259**, 8777-8785.

Kong, S.K. & Chock, P.B. (1992) *J. Biol. Chem.* **267**, 14189-14192.

Kiryanov, G.I., Manamshjan, T.A., Polyakov, V.Y., Fais, D. & Chentsov, J.S. (1976) *FEBS Lett.* **67**, 323-327.

Klapper, D.G. (1982) *Methods in protein sequence analysis.* Elzinga, M. ed. (Humana Press, New Jersey) 509-515.

Klebe, C., Bischoff, F.R., Ponstingl, H. & Wittinghofer, A. (1995) *Biochemistry* **34**, 639-647.

Kleinschmidt, A.M. & Martinson, H.G. (1981) *Nucleic Acids Res.* **9**, 2423-2431.

Klingholz, R. & Strätling, W.H. (1982) *J. Biol. Chem.* **257**, 13101-13107.

Koken, M.H., Hoogerbrugge, J.W., Jasper-Dekker, I., de Wit, J., Willemsen, R., Roest, H.P., Grootegoed, J.A. & Hoeijmakers, J.H. (1996) *Dev. Biol.* **173**, 119-32.

Kotthaus, E. & Strätling, W.H. (1984) *J. Biol. Chem.* **259**, 13640-13643.

Künzler, P. & Stein, A. (1983) *Biochemistry* **22**, 1783-1789.

Laemmli, U.K. (1970) *Nature* **227**, 680-685.

Leber, B. & Hembelen, V. (1979) *Pl. Syst. Evol. Suppl.* **2**, 187-199.

Lee, K.M. & Hayes, J.J. (1998) *Biochemistry* **37**, 8622-8628.

Lenkinski, R.E., Chen, D.M., Glickson, J.D. & Goldstein, G. (1977) *Biochim. Biophys. Acta* **494**, 126-130.

Lennard, A.C. & Thomas, J.O. (1985) *EMBO J.* **4**, 3455-3462.

LeRoy, G., Orphanides, G., Lane, W.S. & Reinberg, D. (1998) *Science* **282**, 1900-1904.

Leuba, S.H. & Zlatanova, J. (1997) *Methods Mol. Cell. Biol.* **6**, 116-124.

Leuba, S.H. (1997) *Methods Mol. Cell. Biol.* **6**,125-133.

Leuba, S.H., Yang, G., Robert, C., Samori, B., van Holde, K.E., Zlatanova, J. & Bustamante, C. (1994) *Proc. Natl. Acad. Sci. USA* **91**, 11621-11625.

Levinger, L. (1985) *J. Biol. Chem.* **260**, 11799-11804.

Levinger, L. & Varshavsky, A. (1980) *Proc. Natl. Acad. Sci. USA* **77**, 3244-3248.

Levinger, L. & Varshavsky, A. (1982) *Cell* **28**, 375-385.

Levinger, L., Barsoum J. & Varshavsky, A. (1981) *J. Mol. Biol.* **146**, 287-304.

Li, W., Nagajara, S., Delcuve, G.P., Hendzel, M.J. & Davie J.R. (1993) *Biochem J.* **296**, 737-744.

Libertini, L.J. & Small, E.W. (1980) *Nucleic Acids Res.* **8**, 3517-3534.

Lindsey, G.G., Orgeig, S., Thompson, P., Davies, N. & Maeder, D. (1991) *J. Mol. Biol.* **218**, 805-813.

Lindsey, G.G. & Thompson, P. (1989) *Biochim. Biophys. Acta* **1009**, 257-263.

Lindsey, G.G. & Thompson, P. (1990) *Biochim. Biophys. Acta.* **1049**, 9-14.

Lindsey, G.G. & Thompson, P. (1992) *J. Biol. Chem.* **267**, 14622-14628.

Lindsey, G.G., Thompson, P., Pretorius, L. & von Holt, C. (1985) *FEBS Lett.* **192**, 230-234.

Lindsey, G.G., Thompson, P., Pretorius, L., Purves, L.R. & von Holt, C. (1983) *FEBS Lett.* **155**, 301-305.

Lohr, D., Cohen, J., Tatchell, K., Kovacic, R.T. & van Holde, K.E. (1977) *Proc. Natl. Acad. Sci. USA* **74**, 79-83.

Louters, L. & Chalkey, R. (1984) *Biochemistry* **23**, 547-552.

Low, T.L.K., Thurman, G.B., McAdoo, M., McClure, J., Rossio, J.L., Naylor, P.H. & Goldstein, A.L. (1979) *J.Biol.Chem.* **254**, 981-986.

Luger, K., Mäder, A.W., Richmond, R.K., Sargent, D.F. & Richmond, T.J. (1997) *Nature* **389**, 251-260.

Luger, K. & Richmond, T.J. (1998) *Curr. Opin. Gen. Dev.* **8**, 140-146.

Maniatis, T., Fritsch, E.F. & Sambrook, J. (1982) *Molecular cloning – A laboratory manual*, Cold Spring Harbor, New York.

Matsui, S., Sandberg, A.A., Negoro, S., Seon, B.K. & Goldstein, G. (1982) *Proc. Natl. Acad. Sci. USA* **79**, 1535-1539.

Matsui, S., Seon, B.K. & Sandberg, A.A. (1979) *Proc. Natl. Acad. Sci. USA* **76**, 6386-6390.

Matsumoto, Y., Yasuda, H., Marunouchi, T. & Yamada, M. (1983) *FEBS Lett.* **151**, 139-142.

Mayer, A., Siegel, N.R., Schwartz, A.L. & Ciechanover, A. (1989) *Science* **244**, 1480-1483.

McCleary, A.R. & Fasman, G.D. (1980) *Arch. Biochem. Biophys.* **201**, 603-614.

McGhee, J.D., Nickol, J.M., Felsenfeld, G. & Rau, D.C. (1983a) *Cell* **33**, 831-841.

McGhee, J.D., Nickol, J.M., Felsenfeld, G. & Rau, D.C. (1983b) *Nucleic Acids Res.* **11**, 4065-4075.

McMurray, C.T. & van Holde, K.E. (1986) *Proc. Natl. Acad. Sci. USA* **83**, 8472-8476.

Meersseman,G., Pennings, S. & Bradbury, E.M. (1991) *J. Mol. Biol.* **220**, 89-100.

Meersseman,G., Pennings, S. & Bradbury, E.M. (1992) *EMBO J.* **11**, 2951-2959.

Mimnaugh, E.G., Chen, H.Y., Davie, J.R., Celis, J.E. & Neckers, L. (1997) *Biochemistry* **36**, 14418-14429.

Moore, S.C. & Ausió, J. (1997) *Biochem. Biophys. Res. Commun.* **230**, 136-139.

Moreau, N., Angelier, N., Bonnanfant-Jais, M.L., Gounon, P. & Kubisz, P.(1986) *J. Cell Biol.* **103**, 683-690.

Morris, N.R. (1978) *Cell* **8**, 357-363.

Mueller, R.D., Yasuda, H., Hatch, C.L., Bonner, W.M. & Bradbury, E.M. (1985) *J.Biol.Chem.* **260**, 5147-5153.

Mutskov, V., Gerber, D., Angelov, D., Ausió, J., Workman, J. & Dimitrov, S. (1998) *Mol. Cell. Biol.* **18**, 6293-6304.

Nacheva, G.A., Guschin, D.Y., Preobrazhenskaya, O.V., Karpov, V.L., Ebralidze,K.K. & Mirzabekov, A.D. (1989) *Cell* **58**, 27-36.

Nelson, P.P., Albright, S.C., Wiseman, J.M. & Garrard, W.T. (1979) *J. Biol.Chem.* **254**, 11751-11760.

Nickel, B.E., Allis, C.D. & Davie, J.R. (1989) *Biochemistry* **28**, 958-963.

Nickel, B.E. & Davie, J.R. (1989) *Biochemistry* **28**, 964-968.

Nickel, B.E., Roth, S.Y., Cook, R.G., Allis, C.D. & Davie, J.R. (1987) *Biochemistry* **26**, 4417-4421.

Nikolaev, L.G., Glotov, B.O., Dashkevic, V.K., Barbashov, S.F. & Severin, E.S. (1983) *FEBS Lett.* **163**, 66-68.

Nikolaev, L.G., Glotov, B.O., Itkes, A.V. & Severin, E.S. (1981) *FEBS Lett.* **125**, 20-24.

Noll, M. & Kornberg, R.D. (1977) *J. Mol. Biol.* **109**, 393-404.

Norton, V.G., Imai, B.S., Yau, P. & Bradbury, E.M. (1989) *Cell* **57**, 449-457.

Ohtsubo, M., Okazaki, H. & Nishimoto, T. (1989) *J. Cell. Biol.* **109**, 1389-1397.

Oliva, R. & Dixon, G.H. (1991) *Prog. Nucleic Acid Res. Mol. Biol.* **40**, 25-94.

Olson, M.O.J., Goldknopf, I.L., Guetzow, K.A., James, G.T., Hawkins, T.C., Mays-Rothberg, C.J. & Busch, H. (1976) *J.Biol.Chem.* **251**, 5901-5903.

Orrick, L.R., Olson, M.O. & Busch, H. (1973) *Proc. Natl. Acad. Sci. USA* **70**, 1316-1320.

Parag, H.A., Raboy, B. & Kulka, R.G. (1987) *EMBO J.* **6**, 55-61.

Parlow, M.H., Haas, A.L. & Lough, J. (1990) *J. Biol. Chem.* **265**, 7507-7512.

Pearson, E.C., Bates, D.L., Prospero, .D. & Thomas, J.O. (1984) *Eur. J. Biochem.* **144**, 353-360.

Pehrson, J.R. (1989) *Proc. Natl. Acad. Sci. U. S. A.* **86**, 9149-9153.

Pennings, S., Meersseman, G. & Bradbury, E.M. (1991) *J. Mol. Biol.* **220**, 101-110.

Pennings, S., Meersseman, G. & Bradbury, E.M. (1994) *Proc. Natl. Acad. Sci. USA* **91**, 10275-10279.

Pickart, C.M. & Rose, I.A. (1985) *J. Biol. Chem.* **260**, 1573-1581.

Pollard, K.J. & Peterson, C.L. (1997) *Mol. Cell. Biol.* **17**, 6212-6222.

Postnikov, Y.V., Shick, V.V., Belyavsky, A.V., Khrapko, K.R., Brodolin, K.L., Nikolskaya, T.A. & Mirzabekov, A.D. (1991) *Nucleic Acids Res.* **19**, 717-725.

Pruss, D. & Wolffe, A. (1993) *Biochemistry* **32**, 6810-6814.

Pruss, D., Bartholomew, B., Persinger, J., Hayes, J., Arents, G., Moudrianakis, E.N. & Wolffe, A.P. (1996) *Science* **274**, 614-617.

Raboy, B., Parag, H.A. & Kulka, R.G. (1986) *EMBO J.* **5**, 863-869.

Ramakrishnan, V. (1997) *Crit. Rev. Eukaryot. Gene Express.* **7**, 215-230.

Ramakrishnan, V., Finch, J.T., Graziano, V., Lee, P.L. & Sweet, R.M. (1993) *Nature* **362**, 219-223.

Razin, A. (1998) *EMBO J.* **17**, 4905-4908.

Rechsteiner, M. (ed.) (1988) *Ubiquitin* Plenum Press, London.

Recht, J. & Osley, M.A. (1999) *EMBO J.* **18**, 229-240.

Renault, L., Nassar, N., Vetter, I., Becker, J., Klebe, C., Roth, M. & Wittinghofer, A. (1998) *Nature* **392**, 97-101.

Retief, J.D., Sewell, B.T., Greyling, H.G., Schwager, S. & von Holt, C. (1984) *FEBS Lett.* **167**, 170-175.

Richmond, T.J., Searles, M.A. & Simpson, R.T. (1988) *J. Mol. Biol.* **199**, 161-170.

Ridsdale, J.A.& Davie, J.R. (1987) *Nucleic Acids Res.* **15**,1081-1096.

Ring, D. & Cole, R.D. (1983) *J. Biol. Chem.* **258**, 15631-15634.

Rodriguez-Campos, A., Shimamura, A. & Worcel, A. (1989) *J. Mol. Biol.* **209**, 135-150.

Roest, H.P., van Klaveren, J., de Wit, J., van Gurp, C.G., Koken, M.H.M., Vermey, M., van Roijen, J.H., Hoogerbrugge, J.W., Vreeburg, J.T.M., Baarends, W.M., Bootsma, D., Grootegoed, J.A. & Hoeijmakers, J.H.J. (1996) *Cell* **86**, 799-810.

Russo, I., Barboro, P., Albertini, I., Parodi, S. & Balbi, C. (1995) *Biochemistry* **34**, 301-311.

Savic, A., Richman, P., Williamson, P. & Poccia, D. (1981) *Proc. Natl. Acad. Sci. USA* **78**, 3706-3710.

Scheffner, M., Werness, B.A., Huibregtse, J.M., Levine, A.J. & Howley, P.M. (1990) *Cell* **63**, 1129-1136.

Schlesinger, D.H.& Goldstein, G. (1975) *Nature* **255**, 423-424.

Schlesinger, D.H., Goldstein, G. & Niall, H.D. (1975) *Biochemistry* **14**, 2214-2218.

Schlissel, M.S. & Brown, D.D. (1984) *Cell* **37**, 903-913.

Schwartz, A.L., Trausch, J.S., Ciechanover, A., Slot, J.W. & Geuze, H. (1992) *Proc. Natl. Acad. Sci. USA* **89**, 5542-5546.

Schwarz, P.M. & Hansen, J.C. (1994) *J. Biol. Chem* **269**, 16284-16289.

Schwarz, P.M., Felthauser,A., Fletcher, T.M. & Hansen, J.C. (1996) *Biochemistry* **35**, 4009-4015.

Seale, R.L. (1981) *Nucleic Acids Res.* **9**, 3151-3158.

Sera, T. & Wolffe, A.P. (1998) *Mol. Cell. Biol.* **18**, 3668-3680.

Serwer, P., Watson, R.H., Hayes, S.J. and Allen, J.L. (1983) *J. Mol. Biol.* **170**, 447-469.

Shimada, T., Okihama, Y., Murata, C. & Shukuya, R. (1981) *J. Biol. Chem.* **256**, 10577-10582.

Silver, J.C. (1979) *Biochim. Biophys. Acta* **561**, 261-264.

Simpson, R.T. (1978) *Biochemistry* **17**, 5524-5531.

Simpson, R.T. (1991) *Prog. Nucleic Acid Res. Mol. Biol.* **40**, 143-84.

Simpson, R.T. & Stafford, D.W. (1983) *Proc. Natl. Acad. Sci. U. S. A.* **80**, 51-55.

Simpson, R.T., Thoma, F. & Brubaker, J.M. (1985) *Cell* **42**, 799-808.

Smith, P.A., Jackson, V. & Chalkey, R. (1984) *Biochemistry* **23**, 1576-1581.

Smith, R.D., Seale, R.L. & Yu, J. (1983) *Proc. Natl. Acad. Sci. USA* **80**, 5505-5509.

Sobolewski, C.H.M., Klump, H.H. & Lindsey, G.G. (1993) *FEBS Lett.* **318**, 27-29.

Spadafora, C., Oudet, P. & Chambon, P. (1979) *Eur. J. Biochem.* **100**, 225-235.

Staynov, D. (1983) *Int. J. Biol. Macromol.* **5**, 3-9.

Staynov, D.Z. & Crane-Robinson, C. (1988) *EMBO J.* **7**, 3685-3691.

Stein, A & Künzler, P. (1983) *Nature* **302**, 548-550.

Struhl, K. (1998) *Genes Dev.* **12**, 599-606.

Studitsky, V.M., Clark, D.J. & Felsenfeld, G. (1996) *Methods Enzymol.* **274**, 246-256.

Subirana, J.A., Muñoz-Guerra, S., Aymamí, J., Radermacher, M. & Frank, J. (1985) *Chromosoma* **91**, 377-390.

Sugarman, B.J., Dodgson, J.B. & Engel, J.D. (1983) *J. Biol. Chem.* **258**, 9005-9016.

Swerdlow, P.S., Schuster, T. & Finley, D. (1990) *Mol. Cell. Biol.* **10**, 4905-4911.

Taniuchi, H., Anfinsen, C. & Sodja, A. (1967) *J. Biol. Chem.* **242**, 4752- 4758.

Tatchell, K. & van Holde, K.E. (1977) *Biochemistry* **16**, 5295-5303.

Thoma, F. (1992) *Biochim. Biophys. Acta* **1130**, 1-19.

Thoma, F., Koller, T. & Klug, A. (1979) *J. Cell Biol.* **83**, 403-427.

Thomas, J.O. & Rees, C. (1983) *Eur. J. Biochem.* **134**, 109-115.

Thompson, R.J. (1973) *J. Neurochem.* **21**, 19-40.

Thorne, A.W., Sautière, P., Briand, G. & Crane-Robinson C. (1987) *EMBO J.* **6**, 1005-1010.

Travers, A. (1999) *Trends Biochem. Sci.* **24**, 4-7.

Travers, A. & Drew, H. (1997) *Biopolymers* **44**, 423-33.

Travers, A.A. & Muyldermans, S.V. (1996) *J. Mol. Biol.* **257**, 486-491.

Tse, C. & Hansen, J.C. (1997) *Biochemistry* **36**, 11381-11388.

Tse, C., Sera, T., Wolffe, A.P. & Hansen, J.C. (1998) *Mol. Cell. Biol.* **18**, 4629-4638.

Ura, K., Wolffe, A.P. & Hayes, J.J. (1994) *J. Biol. Chem.* **269**, 27171-27174.

Ura, K., Hayes, J.J. & Wolffe, A.P. (1995) *EMBO J.* **14**, 3752-3765.

Usachenko, S.I., Bavykin, S.G., Gavin, I.M. & Bradbury, E.M. (1994) *Proc. Natl. Acad. Sci. USA.* **91**, 6845-6849.

van Holde, K.E., Lohr, D.E. & Robert, C. (1992) *J. Biol. Chem.* **267**, 2837-2840.

van Holde K. E. & Zlatanova J. (1995) *J. Biol. Chem.* **270**, 8373-8376.

van Holde K. E. & Zlatanova J. (1996) *Proc. Natl. Acad. Sci. USA* **93**, 10548-10555.

van Holde K. E. (1989) *Chromatin*, Springer-Verlag, New York.

Vijay-Kumar, S., Bugg, C.E. & Cook, W.J. (1987) *J. Mol. Biol.* **194**, 531-544.

Vijay-Kumar, S., Bugg, C.E., Wilkinson, K.D. & Cook, W.J. (1985) *Proc. Natl. Acad. Sci. USA* **82**, 3582-3585.

Villeponteau, B., Brawley, J. & Martinson, H.G. (1992) *Biochemistry* **31**, 1554-1563.

von Holt, C., Brandt, W.F., Greyling, H.J., Lindsey, G.G., Retief, J.D., Rodrigues, J., Schwager, S. & Sewell, B.T. (1989) *Methods Enzymol.* **170**, 431-523.

Watkins, J.F. & Smerdon, M.J. (1985) *Biochemistry* **24**, 7279-7287.

Weber, P., Brown, S. & Mueller, L. (1987) *Biochemistry* **26**, 7282-7290.

Weintraub, H. (1978) *Nucleic Acids Res.* **5**, 1179-1188.

Weintraub, H. & Groudine, M. (1976) *Science* **193**, 848-856.

Weischet, W.O. & van Holde, K.E. (1980) *Nucleic Acids Res.* **8**, 3743-3755.

Weischet, W.O., Allen, J.R., Riedel, G. & van Holde K.E. (1979) *Nucleic Acids Res.* **6**, 1843-1862.

West, M.H. & Bonner, W.M. (1980) *Nucleic Acids Res.* **8**, 4671-4680.

Widom, J. (1986) *J. Mol. Biol.* **190**, 411-424.

Wilkinson, K.D. & Audhya, T.K. (1981) *J. Biol. Chem.* **256**, 9235-9241.

Williams, S.P., Athey, B.D., Muglia, L.J., Schapee, R.S., Gough, A.H. & Langmore, J.P. (1986) *Biophys. J.* **49**, 233-248.

Wolffe, A.P. (1994) *Trends Biochem. Sci.* **19**, 240-244.

Wolffe, A.P. (1995) *Chromatin structure and Function*, 2nd ed., Academic Press, NY.

Wolffe, A.P. (1998) *J. Exp. Zool.* **282**, 239-244.

Wong, J., Li, O., Levi, B.-Z., Shi, Y.-B. & Wolffe, A.P. (1997) *EMBO J.* **23**, 7130-7145.

Woodcock, C.L. (1994) *J. Cell. Biol.* **125**, 11-19.

Woodcock, C.L.F., Frado, L.L. & Rattner, J.B. (1984) *J. Cell. Biol.* **99**, 42-52.

Woodcock, C.L., Grigoryev, S.A., Horowitz, R.A. & Whitaker, N. (1993) *Proc. Natl. Acad. Sci. USA* **90**, 9021-9025.

Workman, J.L. & Kingston, R.E. (1998) *Annu. Rev. Biochem.* **67**, 545-579.

Wray, W., Boulikas, T., Wray, V.P. & Hancock, R. (1981) *Anal. Biochem.* **118**, 197-203.

Wu, R.S., Kohn, K.W. & Bonner, W.M. (1981) *J. Biol. Chem.* **256**, 5916-5920.

Wunsch, A.M., Haas, A.L. & Lough, J. (1987) *Dev. Biol.* **119**, 85-93.

Yao, J., Lowary, P.T. & Widom, J. (1991) *Biochemistry* **30**, 8408-8414.

Yasuda, H., Matsumoto, Y., Mita, S., Marunouchi, T. & Yamada, M. (1981) *Biochemistry* **20**, 4414-4419.

Zhou, Y.B., Gerchman, S.E., Ramakrishnan, V., Travers, A. & Muyldermans, S. (1998) *Nature* **395**, 402-405.

Zlatanova, J. & van Holde, K.E. (1992) *J. Cell Sci.* **103**, 889-895.

Zlatanova, J. & van Holde, K.E. (1996) *Prog. Nucl. Acids Res. Mol. Biol.* **52**, 217-259.